Gravity in our Cosmos:
Einstein and Beyond

Hiu Yan Ip

München 2018

Gravity in our Cosmos:
Einstein and Beyond

Hiu Yan Ip

Dissertation
an der Fakultät für Physik
der Ludwig–Maximilians–Universität
München

vorgelegt von
Hiu Yan Ip
aus Hong Kong

München, den 22.03.2018

Erstgutachter: Prof. Eiichiro Komatsu
Zweitgutachter: Prof. Simon White
Tag der mündlichen Prüfung: 15.06.2018

Zusammenfassung

Der erster Teil dieser Dissertation beschÃďftigt sich mit modifizierten Gravitationstheorien. Das kosmologische Standardmodell, ΛCDM genannt, ist zwar mit allen derzeitigen Messungen auf groÃ§en Skalen kompatibel. Es leidet jedoch an einigen theoretischen Problemen, insbesondere des unnatÃijrlichen Wertes der kosmologischen Konstante Λ. Dies hat die Suche nach alternativen Modellen motiviert, die, anders als die Einsteinsche allgemeine RelativitÃďtstheorie (ART), auf kosmologischen Skalen zu einer beschleunigten Expansion fÃijhren, ohne eine kosmologische Konstante zu benÃűtigen. Andererseits mÃijssen solche modifizierten Gravitationstheorien die sehr engen Grenzwerte erfÃijllen, die Messungen innerhalb des Sonnensystems auf Abweichungen von der ART ergeben haben. Dies wird durch sogenannte Screening-Mechanismen erreicht, die in der EinfÃijhrung beschrieben werden. Der Fokus liegt hier auf sogenannten Skalar-Tensor-Theorien (ST). Zuerst wird gezeigt, dass Modelle, die in jÃijngerer Zeit viel Interesse erfahren haben, nÃďmlich disformal gekoppelte ST-Modelle, tatsÃďchlich durch Messungen im Sonnensystem im Rahmen der âĂIJparametrized post-NewtonianâĂİ (PPN)-Beschreibung sehr stark eingeschrÃďnkt sind. Insbesondere folgt dies aus Effekten, die als bevorzugte Bezugssysteme bezeichnet werden. Es wird demonstriert, dass Modelle dieses Typs, die von diesen EinschrÃďnkungen erlaubt werden, keine interessanten kosmologischen Effekte produzieren kÃűnnen.

Die Auswirkungen von modifizierten Gravitationstheorien mit Screening-Mechanismen werden typischerweise in der sogenannten quasi-statischen NÃďherung behandelt. In dieser NÃďherung wird die Ausbreitung von Wellen des Skalarfeldes vernachlÃďssigt. Vor kurzem wurden in numerischen Simulationen, die die nicht diese NÃďherung benutzen, sondern die volle Wellengleichung lÃűsen, Hinweise auf starke BeeintrÃďchtigungen des Screening-Effekts durch eingehende Skalarfeldwellen gefunden. Diese Simulationen basierten jedoch auf sphÃärischer Symmetrie. In dieser Dissertation wird dieser Effekt analytisch untersucht, indem die Wellengleichung zu erster Ordnung in der Wellenamplitude gelÃűst wird. Wir zeigen, dass die groÃ§en Auswirkungen, die in der numerischen Studie gefunden wurden, eine Folge der sphÃärischen Symmetrie sind, die zu einer Fokussierung der Wellenenergie auf das Sonnensystem fÃijhrt. Eine ebene Welle hingegen, die der physikalischen RealitÃät wesentlich nÃäher ist, fÃijhrt zu wesentlich kleineren Modifikationen des Screening-Effekts. Eine weitere wichtige Frage ist, wie die PPN-Parameter, die im Sonnensystem gemessen werden, insbesondere der sogenannte EddingtonâĂŹsche γ-Parameter, fÃijr modifizierte Gravitationstheorien mit Screening-Mechanismen theoretisch auszurechnen sind. Dies wird hier ebenfalls aufgezeigt.

Der zweite Teil der Dissertation ist der nichtlinearen groÃ§rÃďumigen Strukturbildung (large-scale structure, LSS) im Kosmos gewidmet. Die Anfangsbedingungen, das heisst die ursprÃijnglichen Saatfluktuationen, stammen aus dem frÃijhen Universum (insbesondere der Inflationsepoche). Messungen der groÃ§rÃďumigen Struktur erlauben daher RÃijckschlÃijsse auf die statistische Verteilung der Saatfluktuationen, und kÃűnnen zwischen verschiedenen Inflationsszenarien unterscheiden. DafÃijr braucht man jedoch im allgemeinen eine nichtlineare allgemein-relativistische Beschreibung der LSS, die extrem kompliziert und bisher nicht bekannt ist. Der Einfluss (Kopplung) von langwelligen Fluktuationen auf kleinskalige Strukturen durch die Schwerkraft ist jedoch wesentlich einfacher zu beschreiben, und ist der relevanteste Bereich, um Inflationsmodelle zu testen. Diese Kopplung kann im Rahmen der sogenannten konformalen Fermi-Koordinaten (conformal Fermi coordinates) physikalisch transparent beschrieben werden. Damit wurde bereits gezeigt, dass eine isotrope langwellige Fluktuation lokal exakt einem separaten Universum (einer FRW-Raumzeit) Ãďquivalent ist. Hier wird gezeigt, wie sich dieses Bild zu anisotropen Fluktuationen verallgemeinern lÃďsst. Anders als manchmal in der Literatur angenommen, ist eine anisotrope langwellige Fluktuation nicht lokal Ãďquivalent zu einem anisotrop expandierenden Universum (Bianchi-I Raumzeit).

Abstract

Part I: While the standard cosmological model ΛCDM is the simplest model we have consistent with all current observations, including the accelerated expansion of the Universe, it suffers from a number of theoretical and naturalness problems. This prompts us to look for modified gravity (MG) models that reduce to General Relativity (GR) in the Solar System (SS) to within the very narrow leeway permitted by current bounds, while deviating significantly from GR on cosmological scales so as to self-accelerate naturally. This is often achieved by adopting screening mechanisms. We shall first review these concepts, focusing on Scalar-Tensor (ST) theories. We will show that a model of recently revived interest, disformal ST theory, supposedly with its own novel screening mechanism is actually so tightly constrained by SS constraints at post-Newtonian level, in particular via its preferred frame effects singling out the CMB. This renders the model uninteresting on cosmological scales and highlights the importance of taking the right non-relativistic limit when matching with observations.

The quasi-static approximation (QSA) is often imposed when examining the implications of screening mechanisms in various MG models. This prohibits the propagation of scalar waves from astrophysical and cosmological sources. We investigate the claim that relaxing the QSA would lead to significant disruptions to the screening in the SS, thus tightening the parameter space for viable MG models. We solve the system (linearised in the wave perturbation) analytically, which gives us a clearer understanding of the mechanisms at work. The geometry of the incoming wave (spherical or planar) is found to significantly affect the severity of the disruption, such that for the more physically relevant planar waves, disruption while theoretically possible, is far milder than previously thought. The amplification is purely of geometrical origin and from energy-conservation, thus holds independent of our linearisation. We also elucidate the physical meaning of the PPN framework and consequently the Eddington light bending parameter. Since this is science, only observable disruptions are relevant and we discuss the conditions for this to be so.

Part II: Large Scale Structure (LSS) in the nonlinear regime can tell us a lot about the early Universe. In order to track the evolution of primordial fluctuations into the LSS observed today, we desire a framework that is fully nonlinear and fully relativistic (fNLfR) in which quantities are directly relatable to physical observables. Most physically-relevant setups involve a long wavelength perturbation modulating the dynamics of small scale physics, prompting the generalisation of the Fermi Normal Coordinates into the

Conformal Fermi Coordinates (CFC). A long-wavelength spherically-symmetric adiabatic perturbation on an FLRW spacetime is locally equivalent to a different FLRW solution, a result that holds fNLfR: the separate universe picture. We investigate the case where the long wavelength perturbation is anisotropic, i.e. large-scale tidal fields, by deriving the set of evolutionary equations for the long mode fNLfR. We do however have to impose a natural approximation, dropping certain higher-derivative terms to close the system. The result is a very simple framework (in terms of mathematical complexity and physical relatability) for computing the fully relativistic growth of structure to second order in perturbations. In the process, we elucidate the physical meaning of these large scale tidal fields, to be distinguished from a Bianchi I spacetime.

Contents

List of Figures

List of Tables

For the inimitable Simon...

Notations and Conventions

In this thesis, we shall adopt the **mostly positive metric signature**, such that the Minkowski metric $\eta_{\mu\nu} = \text{diag}(-+++)$. Four-dimensional **Lorentzian indices are Greek** letters, while the three-dimensional **Euclidean indices are Latin** letters. We adopt the **natural units** where $\hbar = c = 1$.

Theory of gravity: Set of field equations obeyed by the rank-2 tensor (not necessarily EinsteinâĂŹs), and any other non-matter fields it interacts with.

General Relativity (GR): A theory that exhibits general covariance, universal couplings to all matter fields and satisfies EinsteinâĂŹs field equations, $G_{\mu\nu} = T_{\mu\nu}/M_{\rm pl}^2$.[1]

To clean up our expressions, we may write for some quantity $\mathbb{X}$, $\boldsymbol{\nabla_\mu}\mathbb{X} \equiv \mathbb{X}_{;\boldsymbol{\mu}}$, $\boldsymbol{\partial_\mu}\mathbb{X} \equiv \mathbb{X}_{,\boldsymbol{\mu}}$ and $\Box\mathbb{X} \equiv \boldsymbol{g^{\mu\nu}}\phi_{;\boldsymbol{\mu\nu}}$.

Gauges

The perturbed FLRW metric with only scalar metric perturbations $(\mathbb{A}, \mathbb{B}, \mathbb{C}, \mathbb{D})$ in a generic gauge takes the following form

$$\mathrm{d}s^2 = a^2(\tau)\left[-(1-2\mathbb{A})\mathrm{d}\tau^2 - 2\boldsymbol{\nabla}_i\mathbb{B}\mathrm{d}\tau\mathrm{d}x^i + [(1+\mathbb{C})q_{ij} + \mathcal{D}_{ij}\mathbb{D}]\mathrm{d}x^i\mathrm{d}x^j\right], \tag{1}$$

where $a(\tau)$ is the scale factor normalised to unity today; q_{ij} is a maximally symmetric 3-metric of Gaussian curvature κ; $\mathcal{D}_{ij} \equiv \boldsymbol{\nabla}_i\boldsymbol{\nabla}_j - (1/3)q_{ij}q^{mn}\boldsymbol{\nabla}_m\boldsymbol{\nabla}_n$ is a traceless spatial derivative operator; $\boldsymbol{\nabla}_i$ is the covariant derivative compatible with spatial metric q_{ij}.

Note that these metric perturbations aren't uniquely defined, instead their values depend on our gauge choice, i.e. we need to choose a specific time-slicing of spacetime and then the spatial coordinates on these time slices. An inconvenient gauge choice can introduce gauge artefacts, not to mention complicate calculations.

Popular gauges, mentioned in this thesis are

- **Conformal Newtonian gauge:** $\mathbb{B} = \mathbb{D} = 0$. In the Newtonian limit, c.f. Section 3, $-\mathbb{A} \to \Phi_{\rm N}$, the Newtonian gravitational potential satisfying the Poisson equation. $\mathbb{B} = 0$ means that the constant-time hypersurfaces are orthogonal to the worldlines of particles whose rest frames coincide these hypersurfaces. $\mathbb{D} = 0$ means that the geometry on the constant-time hypersurfaces is isotropic.

[1] This is the definition cosmologists adopt. Particle physicists' GR does not require the field equations be Einstein's.

- **Comoving gauge:** $\mathbb{V} = \mathbb{D} = 0$, where we define $\mathbb{V}$ by the 4-velocity (of a specified matter species I) $u_\mu^{(I)} = a(1 - \mathbb{A}, \boldsymbol{\nabla_i}\mathbb{V}^{(\boldsymbol{I})})$. This gauge is well-defined as long as fluid vorticity is negligible.
- **Synchronous gauge:** $\mathbb{A} = \mathbb{B} = 0$. note that this does not eliminate all gauge freedom, so one has to beware of gauge artefacts. Here we have set of comoving observers who have fixed spatial coordinates on their constant-time hypersurfaces as they follow their geodesics.

Table 1: Abbreviations used in this thesis.

Abbr	Definition
CDM	Cold Dark Matter
CMB	Cosmic Microwave Background
cN	Conformal Newtonian
DE	Dark Energy
DM	Dark Matter
EdS	Einstein-de Sitter: flat, matter-only FLRW
e.o.m.	Equation(s) of motion
EP	Equivalence Principle
EEP	Einstein's Equivalence Principle
FLRW	Friedman-Lemaître-Robertson-Walker
GR	General Relativity
MG	Modified Gravity
MWh	Milky Way halo
NL	Non-linear/ Non-linearities
NR	Non-relativistic
PN	Post-Newtonian
PPN	Parametrized Post-Newtonian formalism
(n)QS	(non-) Quasi-static
QSA	Quasi-static approximation
SC	Synchronized-Comoving
SEP	Strong Equivalence Principle
SR	Special Relativity
SS	Solar System
ST	Scalar-Tensor
WEP	Weak Equivalence Principle

Table 2: General quantities in Part I.

Symbol	Definition

$g_{\mu\nu}$	Einstein frame (geometric) metric
$\tilde{g}_{\mu\nu}$	Jordan frame (physical) metric
$\Gamma^{\alpha}_{\mu\nu}$	Connection associated with covariant differentiation. In GR, it is defined to be the Levi-Civita connection defined entirely by the metric, $\Gamma^{\alpha}_{\mu\nu} = (g^{\mu\nu}/2)(g_{\alpha\nu,\beta} + g_{\beta\nu,\alpha} - g_{\alpha\beta,\nu})$.
$R_{\mu\nu}$	Ricci tensor
R	Ricci scalar curvature, $g^{\mu\nu}R_{\mu\nu}$.
$G_{\mu\nu}$	Einstein tensor, $R_{\mu\nu} - (1/2)g_{\mu\nu}R$
$\tilde{\mathcal{Q}}$	Object $\mathcal{Q}$ defined w.r.t. the Jordan frame metric, $\tilde{g}_{\mu\nu}$
$C(\phi, X)$	Conformal factor
$\mathcal{D}(\phi, X)$	Disformal factor
R	Ricci scalar
$M_{\rm pl}$	Reduced Planck mass, $1/\sqrt{8\pi G}$
G	Gravitational constant, not necessarily equal to the locally-measured Newton's constant, $G_{\rm N}$, $(8\pi M_{\rm pl}^2)^{-1}$
$G_{\rm N}$	Newton's gravitational constant, measured locally
X	Kinetic term of the scalar field, $-\frac{1}{2}g^{\mu\nu}\partial_\mu\phi\partial_\nu\phi$
$\Phi_{\rm N}$	Newtonian potential, solves the Poisson equation. Identified with GR metric potential Φ in the Newtonian limit, when time derivatives of Φ are negligible
$\Phi_{\rm cN}(\mathbf{k}, t)$	Metric potential in g_{00} in the cN gauge, not equivalent to $\Phi_{\rm N}$
$\Psi_{\rm cN}(\mathbf{k}, t)$	Metric potential in g_{ij} in the cN gauge
ψ_i	Matter fields, species labelled by i
ϕ	Scalar field, normalized to be dimensionless
β_ϕ	Coupling strength of ϕ to matter, $M_{\rm pl}\left[\ln C(\phi)\right]_{,\phi}$
$T^{\rm m}_{\mu\nu}$	Energy-momentum tensor of the matter fields in the Einstein frame, $(2/\sqrt{-g})\delta(\sqrt{-\tilde{g}}\tilde{\mathcal{L}}_{\rm m})/\delta g_{\mu\nu}$
$T^{\phi}_{\mu\nu}$	Energy-momentum tensor of the scalar field in the Einstein frame, $M_{\rm pl}^2\left[\nabla_\mu\phi\nabla_\nu\phi - g_{\mu\nu}\left(\frac{1}{2}\nabla_\mu\phi\nabla^\mu\phi + V(\phi)\right)\right]$
$T_{\rm m}$	Trace of the matter energy-momentum tensor in the Einstein frame, $g_{\mu\nu}T^{\mu\nu}_{\rm m}$
$\tilde{\rho}_{\rm m}$	NR matter density in Jordan frame, $-\tilde{T}_{\rm m}\big\vert_{\rm NR}$, conserved in the Jordan frame, $C^4\rho_{\rm m}$
$\rho_{\rm m}$	NR matter density in Einstein frame, $-g_{\mu\nu}T^{\mu\nu}_{\rm m}$ in the NR limit, not conserved, $-T_{\rm m}\big\vert_{\rm NR}$
$\rho^{\rm cons}_{\rm m}$	NR matter density conserved in the Einstein frame, $C^{-1}(\phi)\rho_{\rm m}$
$\rho_{\rm crit}$	Critical density of the Universe, $3H^2M_{\rm pl}^2$
$V(\phi)$	Scalar-field potential, to be distinguished from the effective potential $V_{\rm eff}(\phi)$.

Part I

Screening in Scalar-Tensor Theories

Chapter 1

Introduction

Einstein's theory of General Relativity (GR) has been phenomenal at reproducing and predicting phenomena in the Solar System (SS), such as the bending of light by the Sun. (Chapter 3) However, the observable universe is much larger than the SS, so the structure of gravity could be very different on large cosmological scales. In fact, observational data from supernovae suggest that the expansion of the universe is accelerating [111].

On such large scales, gravity is the only relevant force in cosmology, yet if gravity is just GR without the cosmological constant (CC) even on cosmological scales, working in a universe made of cold dark matter and radiation, both of which are gravitationally attractive, the expansion should really be decelerating. As alluded to earlier, GR allows for a CC, which could drive large scale acceleration and is consistent with all current observations. (Section 1.1.) However, it is plagued by the infamous cosmological constant problem. So despite the brilliant results of GR in the SS, we must not have the complete picture of gravity.

One way to go is to stick to GR without a CC on all scales and throw in some gravitationally-repulsive dark energy, in addition to the attractive matter (including radiation). Then when it comes to dominate cosmological evolution, it would drive the observed acceleration. (Section 2.4.)

However, there is another way. This route is adopted in this thesis.

Consider that GR is not the complete picture of gravity but simply a limit of it. This would be analogous to how Newtonian gravity is the limit of GR when all objects involved move slowly and their gravitational potentials are weak. What we would like is to build a theory of gravity that reduces to GR in the SS but works differently on cosmological scales, such that it naturally drives the acceleration. A way to do this is to introduce a new degree of freedom, a scalar field. This field interacts with matter (again, includes radiation), giving rise to a fifth force that makes them deviate from their geodesics. (Section 2.) Furthermore, the field interacts with different massive bodies differently, depending on their composition, thus allowing for environment-dependent behaviour. This differs from GR with a CC, where all macroscopic massive bodies regardless of composition follow the same geodesics, i.e. inertial and gravitational mass are equivalent. (Section 2.5.2.)

One problem we face when building such a theory is that, on face value, in order to

comply with the highly precise SS measurements, we have to fine-tune our model parameters. This tends to lead us back to square one, with GR on all scales. It would therefore be sensible to make use of the environmental-dependency of the fifth force and design our model to allow for large deviations from GR on large scales, while hiding modifications that would land us in trouble in the SS. These are called screening mechanisms. Since the SS is much denser than the mean density of the visible universe, why not let this environment-dependency be of matter density? Two examples of such mechanisms are the symmetron and the chameleon mechanisms. (Section 2.6.) We will also look into an alleged new screening mechanism called disformal screening, which we shall show to be misguided, and without it, the more complex disformal gravity model does no better than standard GR with a CC (ΛCDM). (Section 4.)

Until recently, these screening mechanisms have been studied under the quasi-static approximation (QSA). This is where one takes the equation of motion for interacting relativistic particles (Klein Gordon equation in a potential); assert that since we are working with scales much smaller than the observable universe (subhorizon limit) and that the relevant potentials and fields are sourced by matter that evolve on the Hubble time scale (vary very slowly) thus do the same themselves, we can drop their time derivatives. We are then left with the familiar Poisson-type equation, like in Newtonian gravity, which doesn't allow for wave propagation. (Chapter 5.)

Recently, however, symmetron waves have been found in cosmological simulations when one relaxes the QSA [81]. Scalar waves appear because in low-density regions, the symmetronâĂŹs effective potential offers two possible vacuum states, resulting in different regions (cells) of space where the field has chosen different vacua. The smooth transition region between these cells is called a domain wall, which can spontaneously collapse when one cell flips its vacuum state to join its neighbour, ending up in a more energetically favourable configuration.

Another source of scalar waves is violent astrophysical events, such as supernovae explosions, where less dense massive stars (unscreened, carries a scalar charge that allows it to experience the fifth force) collapse into highly dense neutron stars or black holes (screened, no scalar charge, blind to the fifth force). Think of an electrically charged isolated body becoming electrically neutral, the object has to somehow get rid of its charge. It's the same here, scalar charge is therefore radiated away, creating these scalar waves. Note that only sources in unscreened regions are relevant, since if it's screened by its background, it starts off uncharged anyway. In the case of the Milky Way halo (MWh) then, the sources to be considered have to be outside of its inner screened region.

It has been suggested that scalar waves of cosmological and astrophysical sources can observably disrupt the MWh's screening of the SS, such that a light-ray could experience an observably different amount of bending as it passes by the Sun. [51] numerically studied the effects of an incoming spherical symmetron wave centred on the MWh has on its screening of the SS. In this study, only the screening ability of the background halo is considered. It was concluded that screening can be significantly disrupted by scalar radiation, such that there could be an observable difference in the bending of light, potentially violating the current observational bounds, hence ruling out previously viable models. Such effects are

said to be relevant for any modified gravity theories with extra degrees of freedom with wave-type equations of motion. However, we find that these disruptions are observationally negligible for physically-relevant scenarios.

1.1 General Relativity (ΛCDM)

The requirements for an observationally-viable relativistic theory of gravity include:

- Foundational requirements imposed by construction: Universality of free fall and the isotropy of space.
- Compatibility with various observations and tests pertaining to its null- and time-like geodesics, which have been found to concur with GR to very high precision. Of course upcoming tests of even higher precision have yet to cast their verdicts.

In order to highlight the modifications we make to GR, here is a lightning-speed recap of it. For a more comprehensive review, see [121]. GR is a theory of gravity where spacetime is treated as a 4-dimensional manifold with two additional structures imposed upon it, namely a connection $\Gamma^{\alpha}_{\mu\nu}$(to do with covariant differentiation ∇_μ) and a metric $g_{\mu\nu}$ that defines distances on said manifold. The two additional structures are in general independent of each other, but in GR we make two further assumptions that would link them together. We assume that the torsion of $\Gamma^{\alpha}_{\mu\nu}$ vanishes, such that only the symmetric part remains, describing the curvature of the manifold. We further assume metric-compatibility of the connection, $\nabla_\alpha g_{\mu\nu} \equiv 0$, such that now we can define the Levi-Civita connection with all its components (Christoffel symbols) uniquely defined by $g_{\mu\nu}$. Therefore, in GR, $g_{\mu\nu}$ determines all quantities to do with distances and parallel transport in spacetime.

What we end up with is then a (pseudo-[1]) Riemannian manifold, which has various important implications for the theory. For example, that we can locally recover Minkowski spacetime and hence SR in the tangent space to any point in spacetime up to tidal forces, a.k.a. normal coordinates. This is essential for Einstein's Equivalence Principle which we shall later study. Another crucial one is the contracted Bianchi identities, giving us $\nabla_\mu G^{\mu\nu} \equiv 0$, where $G^{\mu\nu}$ is the Einstein tensor.

The familiar Einstein-Hilbert action for GR is

$$S = \int \mathrm{d}^4x\sqrt{-g}\frac{M_{\rm pl}^2}{2}(R - 2\Lambda_{\rm CC}) + S_{\rm m}[g_{\mu\nu};\psi_i], \tag{1.1}$$

which we vary this action with respect to the metric to get the familiar Einstein field equations

$$G_{\mu\nu} = 8\pi G T_{\mu\nu} - g_{\mu\nu}\Lambda_{\rm CC}, \quad \text{then } \nabla_\mu T^{\mu\nu} = 0. \tag{1.2}$$

The covariant conservation of $G_{\mu\nu}$, as mentioned previously, implies the covariant conservation of the energy-momentum tensor and that test particles follow the geodesics of the metric.

[1] The "pseudo-" is just to reflect that the metric is not positive-definite.

The $\sqrt{-g}$ factor in the action Eq. 1.1 ensures that the Lagrangian densities (hence the actions) are invariant under general coordinate transformation. It follows that and that the Einstein field equations in Eq. 1.2 remain covariantly-conserved.

In the NR limit of GR and the conformal Newtonian gauge for the metric, which is perturbed around the Minkowski metric,

$$ds^2 = -(1 + 2\Phi_{\rm cN}(\mathbf{x}))\mathrm{d}t^2 + (1 - 2\Psi_{\rm cN}(\mathbf{x}))\mathrm{d}\mathbf{x}^2. \tag{1.3}$$

Since we are in the NR limit, $v \ll 1$ for the test particle and $P \ll \rho$ for the density source. We may also identify the time-independent metric potentials $\Phi_{\rm cN}$ with the Newtonian potential, $\Phi_{\rm N}$. Then the $00-$th Einstein equation gives us NewtonâĂŹs law of gravitation, the Poisson equation $\nabla^2\Phi_{\rm N} = 4\pi G_{\rm N}\rho$.

There are two particular significant implications of GR:

- Lovelock's theorem: The 4-dimensional (pseudo-)Riemannian manifold (i.e. metric theory) underpinning GR requires that any action for the gravitational field must be constructed from $g_{\mu\nu}$. Then the only field equations that are second order or less from any such actions (not necessarily the Einstein-Hilbert action in Eq. 1.1, which is the simplest of them) must be EinsteinâĂŹs equations and/or a cosmological constant, as in Eq. 1.2.

  This means some of the properties we can change to build a metric theory of gravity different from GR, include: consider a higher dimensional spacetime (e.g. Brane Cosmology); add extra fields [2](e.g. ST theories); allow field equations to have higher than second-order derivatives of the metric (e.g. Galileon) [3]; etc.

- BirkhoffâĂŹs theorem: All spherically-symmetric vacuum solutions of EinsteinâĂŹs equations (i.e. RHS of Eq. $1.2 = 0$) must be locally isometric to a region in Schwarzschild spacetime[101]. A generalized version of the theorem includes the cosmological constant and states that the unique spherically-symmetric vacuum solution to EinsteinâĂŹs equation is locally isometric to a region in Schwarzschild-de Sitter spacetime.

  While this setup is never strictly realized, the theorem says that the gravitational field of an isolated mass far away from it is negligible, like in Newtonian gravity. It justifies our studying the weak-field limit of GR as a perturbation about $\eta_{\mu\nu}$. Note however that in MG, we don't have EinsteinâĂŹs equations as solutions, so the common way of studying these theories the same way is mainly motivated by intuition.

For a non-vanishing $\Lambda_{\rm CC}$ in Eq. 1.2, we have practically just added a new contributor species to the energy-momentum tensor, which is often identified with vacuum energy.

[2]but to preserve the metric nature of the theory, we need that the scalar field to couple to matter only via the metric.

[3]Otherwise we risk encountering Ostrogradski's ghosts, which are pathological physical excitations (fields) that admit of negative energy states or negative norm when quantised. Propagating ghosts in a theory means that the vacuum is unstable and we run into quantization problems.

Species that make up $T_{\mu\nu}$ in the standard cosmological model behave as perfect fluids and don't interact with each other. In other words, they don't exchange energy such that $\nabla_\mu T_i^{\mu\nu} = 0$ for each individual species i. This modifies the Newtonian Poisson equation to

$$\nabla^2\Phi = 4\pi G\rho_{\rm m} + \frac{\Lambda_{\rm CC}}{2}. \tag{1.4}$$

This means we now have a contribution to the metric potentials that grow as $\propto r^2$, kicking in on cosmological scales. Thankfully, $\Lambda_{\rm CC}r^2$ has been constrained by observations [3] to be negligible on small scales, such that Newtonian gravity is safe there.

To study/incorporate cosmological dynamics, in particular, the evolution of the physically observable Hubble parameter H, we should adopt an FLRW background metric instead of the Minkowskian one. The choice of background/asymptotic metric can be important. We shall see that in the disformal model, cosmological dynamics, which are non-existent in the Minkowski case, contribute to the scalar charge of a field thus influencing the strength of any fifth force. This is so despite us working in the NR limit and on time-scales much less than Hubble, such that $a(t) \simeq 1$. The FLRW metric is the most general form that satisfies the cosmological principle, which says that the universe is spatially homogeneous (in particular, the curvature of space is the same everywhere) and isotropic on sufficiently large scales. For Euclidean/flat space, [5] the FLRW line element is

$$\mathrm{d}s^2 = -\,\mathrm{d}t^2 + a^2(t)\left[\mathrm{d}r^2 + r^2\left(\mathrm{d}\theta^2 + \sin^2\theta\,\mathrm{d}\phi^2\right)\right] = -\,\mathrm{d}t^2 + a^2(t)\,\mathrm{d}x^2. \tag{1.5}$$

The first Friedmann equation, i.e. the 00−th component of Einstein's field equations 1.2, and noting that $\dot{a} > 0$ always, tells us when each species dominates and how $a(t)$ evolves in the corresponding epochs. We are currently in between matter and cosmological constant domination. The comparability of the current energy density of the $\Lambda_{\rm CC}$ and (dark) matter is the coincidence problem.

The second Friedmann equation, which follows from the first Friedmann equation together with the trace of 1.2, gives

$$\frac{\ddot{a}}{a} = -\frac{4\pi G}{3}\left(\rho_{\rm m} + 3P\right) + \frac{\Lambda_{\rm CC}}{3}, \tag{1.6}$$

which makes clear that during the cosmological constant's domination, with its $w_{\Lambda_{\rm CC}} = -1$, $\ddot{a} > 0$. In fact, it makes explicit that any dominating fluid with $w < -\frac{1}{3}$ will get us $\ddot{a} > 0$.

ΛCDM, where the background is taken to be FLRW while the matter fields are dominated by $\Lambda_{\rm CC}$ and CDM, is in good agreement with many physical observations and is called the concordance model.

However, ΛCDM is not quite perfect. The most infamous problem plaguing $\Lambda_{\rm CC}$ is the (old) cosmological constant problem. It is a naturalness problem, where the observed value of $\Lambda_{\rm CC}$, identified with the vacuum energy density, is around 120 orders of magnitude smaller than expected by quantum field theory. The identification follows from considering the most general Lorentz- invariant form for the vacuum energy-momentum tensor, which is $T^{\rm vac}_{\mu\nu} = -\rho_{\rm vac}g_{\mu\nu}$, for some constant $\rho_{\rm vac}$. In other words, the vacuum can treated as a

perfect fluid with equation of state equalling -1. Adding such a perfect fluid to the existing energy-momentum tensor has the same effect as the $\Lambda_{\rm CC} g_{\mu\nu}$ term in Eq. 1.2. The vacuum energy density and cosmological constant are therefore identified, s.t. $\rho_{\rm vac} \equiv \Lambda_{\rm CC}/8\pi G$.

By dimensional analysis, we know that energy density $\rho_{\rm vac} \sim [L]^4$, where L denotes a unit of length. Note that $\Lambda_{\rm CC} \sim [L]^{-2}$. However, there is no preferred length scale offered by classical GR.

For quantum vacuum (zero-point) fluctuations however, a natural length scale would be the cutoff of quantum field theory, which is the Planck scale $M_{\rm pl} \sim 10^{18}$ GeV, s.t. $\rho_{\rm vac} \sim (10^{18}\ {\rm GeV})^4$. On the other hand, cosmological observations constraining $\Lambda_{\rm CC}$ [5] imply that $\rho_{\rm vac} \lesssim (10^{-12}\ {\rm GeV})^4$. This results in the infamous 120 orders of magnitude discrepancy mentioned above.

$\Lambda_{\rm CC}$ also suffers from a coincidence problem, to do with the surprisingly similar order of magnitude of $\rho_{\Lambda_{\rm CC}}$ and the average $\rho_{\rm m}$ today. This is odd because $\rho_{\Lambda_{\rm CC}}$ and $\rho_{\rm m}$ scale very differently with the size of the Universe.

Meanwhile, we should explore alternatives.

Chapter 2

Scalar-Tensor Theories

GR is the unique Lorentz-invariant, low-energy theory of a massless spin-2 particle, the graviton[66]. Hence to modify gravity, we have to introduce new degrees of freedom, ϕ, with mass of order Hubble today $m_\phi \sim H_0$ – remember we want the theory to give self-accelerating cosmological solutions and that DE only recently began to dominate DM (the coincidence problem). In this thesis we shall focus on scalar-tensor theories, where an additional scalar field, ϕ, couples (conformally and/or disformally) to matter via the metric.

Bekenstein showed that the most general relation with an extra scalar field thrown in that preserves causality is, in the Einstein frame,

$$S = \int \mathrm{d}^4x\sqrt{-g}\, M_{\rm pl}^2 \left[\frac{R}{2} - \frac{1}{2}\nabla_\mu\phi\nabla^\mu\phi - V(\phi)\right] + S_{\rm matter}[\tilde{g}_{\mu\nu}; \psi_i], \tag{2.1}$$

where the modifications of GR are introduced through the coupling of the scalar to matter via the Jordan frame metric

$$\tilde{g}_{\mu\nu} = C^2(\phi, X)\, g_{\mu\nu} + \mathcal{D}^2(\phi, X)\, \partial_\mu\phi\partial_\nu\phi, \quad X \equiv -\frac{1}{2}g^{\mu\nu}\partial_\mu\phi\partial_\nu\phi. \tag{2.2}$$

$C(\phi, X)$ is dimensionless and describes the conformal coupling. $\mathcal{D}(\phi, X)$, also dimensionless, controls the strength of the derivative interaction, known as the disformal coupling. This thesis will only focus on the case where $C(\phi, X) = C(\phi)$ and $\mathcal{D}(\phi, X) = \mathcal{D}(\phi)$. However, our leading constraints can be generalized to models dependent on X also[1].

The system of equations to be solved are:

- The field equations from varying the Lagrangian w.r.t. the metric;
- The e.o.m. of the scalar field ϕ from varying the Lagrangian w.r.t. ϕ;
- The covariant conservation of the total energy-momentum tensor (including the contribution from the scalar field) in the Einstein frame, or equivalently, the conservation

[1]Unless if the model is fine-tuned such that $D \to 0$ as $X \to 0$. However, in that case, the model is cosmologically uninteresting like for the the minimal disformal model, Section 4.1.

of the matter component of the energy-momentum tensor in the Jordan frame. This follows from the first point by taking the covariant-derivative of the field equations.

We are looking for models where deviations from GR are dominant on cosmological scales, while simultaneously satisfy the strong laboratory and SS bounds (on small scales).

This is facilitated by the introduction of screening mechanisms, c.f. Section 2.6 that can hide the fifth-force locally.

2.1 Einstein vs Jordan frames for Scalar-Tenor Theories

There are two physically-equivalent frameworks in which ST theories are studied, called the Einstein and Jordan frames. In this thesis we are only concerned with single-field ST theories that admit both frames, as opposed to say doubly-coupled bimetric theories that have no well-defined Jordan frame metric. Care must be taken when transforming quantities between the frames.

For concreteness, we shall illustrate the frames using conformal ST theories of a canonically normalizable scalar field. While we also consider disformal theories in this thesis, their Jordan forms are unwieldy and don't provide much more insight for our purposes. For a derivation of the Jordan frame action for disformal ST theories, see Appendix A in [99].

For a conformal ST theory then, let's define

$$\tilde{g}_{\mu\nu} = C^2(\phi) g_{\mu\nu}. \tag{2.3}$$

In the Einstein frame,

$$S = \int \mathrm{d}^4x\sqrt{-g}\left[\frac{M_{\rm pl}^2}{2}R - \frac{1}{2}\phi_{;\mu}\phi^{;\mu} - V(\phi)\right] + S_{\rm m}[\tilde{g}_{\mu\nu};\psi_i]. \tag{2.4}$$

Here ϕ couples minimally to gravity (GR) but couples directly to matter via $\tilde{g}_{\mu\nu}$ (non-minimal coupling). The nonminimal coupling, which translates to the interaction between the scalar field and matter, causes test particles in the Newtonian limit to feel a fifth force $\propto \nabla \ln C(\phi)$, such that $\nabla_\mu T^{\mu\nu}_{\rm m} \neq 0$. Instead, it is $T^{\mu\nu}_{\rm total} = T^{\mu\nu}_{\rm m} + T^{\mu\nu}_{\phi}$ that is covariantly conserved. This means that test particles do not follow the geodesics of $g_{\mu\nu}$.

In the Jordan frame, this takes the form

$$S = \frac{M_{\rm pl}^2}{2}\int \mathrm{d}^4x\sqrt{-\tilde{g}}\left[\Psi_{\rm BD}\tilde{R} - \frac{w_{\rm BD}(\Psi_{\rm BD})}{\Psi_{\rm BD}}(\Psi_{\rm BD})_{;\tilde{\mu}}(\Psi_{\rm BD})^{;\tilde{\mu}} - \frac{2}{M_{\rm pl}^2}\Psi_{\rm BD}^2 V(\Psi_{\rm BD})\right] \tag{2.5}$$

$$+ S_{\rm m}[\tilde{g}_{\mu\nu};\psi_i], \tag{2.6}$$

where $\Psi_{\rm BD} \equiv C^{-2}(\phi)$. Here, ϕ couples non-minimally to gravity (not GR) but matter only couples directly to this frame's metric, $\tilde{g}_{\mu\nu}$ (minimal coupling). In other words, test particles follow the geodesics of the metric in this frame and $\tilde{\nabla}_\mu \tilde{T}^{\mu\nu}_{\rm m} = 0$.

One well-studied case is the (massless) Brans-Dicke theory, where

$$w_{\rm BD}(\Psi_{\rm BD}) \equiv w_{\rm BD}, \quad V(\phi) = 0. \tag{2.7}$$

We'll see later that this is not very cosmologically-interesting since setting $V(\phi) = 0$ disables screening mechanisms. (Section 2.6.) Also, SS tests constrains $w_{\rm BD} \gtrsim 4 \times 10^4$, requiring that the field's coupling to matter be so weak that we essentially have a DE model. (Section 2.5.2.)

2.2 Brans-Dicke Theory

In this section only we shall drop the tildes that mark Jordan frame quantities for notational simplicity.

A special case of conformal ST theories is the Brans-Dicke theory which is usually formulated in the Jordan frame (compare with Eq. 2.5),

$$\mathcal{L}_{\rm BD} = \frac{1}{16\pi G}\sqrt{-g}\left[\Psi_{\rm BD}R - \frac{w_{\rm BD}}{\Psi_{\rm BD}}\Psi_{{\rm BD};\mu}\Psi_{\rm BD}{}^{;\mu} - 2U(\Psi_{\rm BD})\right] + \mathcal{L}_{\rm m}, \tag{2.8}$$

where $w_{\rm BD}$ is the Brans-Dicke parameter and is a constant. $U(\Psi_{\rm BD})$ is the potential term, s.t. $U_{,\Psi_{\rm BD}\Psi_{\rm BD}}$ gives $\Psi_{\rm BD}$ a mass $m_{\rm BD}$, to be distinguished from its effective mass. We can freeze out the dynamics of $\Psi_{\rm BD}$ by making both or either the kinetic and/or potential terms very big as makes attaining them very energetically costly.

We are interested in constraining ST theories using SS tests. One such test is the amount of light bending by Sun (or equivalently, the Shapiro time-delay effect) measured by the Cassini probe. The length (equivalently, 1/mass) scale of interest is therefore the size of the SS, the Astronomical Unit (AU). Whereas the length scale associated with a massive $\Psi_{\rm BD}$ is $1/m_{\rm BD}$ (for the bare potential).

[91] found that the amount of light bending predicted by a theory depends on the relative sizes of $1/m_{\rm BD}$ and the AU. We shall examine this further in Section 3.1.1.

2.3 Cosmological Implications

Since the motivation of MG is cosmological, we must look at the cosmological phenomenology of MG. This generally come in 3 classes:

- Background evolution, which has to do with the expansion history and is mainly geometrical. We want this to be different from GR, addressing the accelerated expansion observed.
- Linear scales, which has to do with structure formation. Here we consider small perturbations around the background and solve the system to linear order in said perturbation.
- Nonlinear scales, which has to do with small-scale dense structures, like the SS and requires N-body simulations.

2.3.1 Background Evolution

The background scalar field is spatially homogeneous, such that $\phi_{\rm bkgd} \equiv \phi_{\rm bkgd}(t)$, and evolves in a FLRW universe, $\mathrm{d}s^2 = -\mathrm{d}t^2 + a^2(t)\mathrm{d}x^2$. The matter components (i.e. all species except DE and ϕ) are taken to be a set of non-interacting perfect fluids, each with a constant equation of state $w_i^{\rm eos}$. The expansion history is described by the two Friedmann equations[2], closed with the continuity equations. Explicitly, for a spatially flat universe in the recent epoch of CDM and DE/ϕ domination, dropping the subscript$_{\rm bkgd}$ in this subsection for notational simplicity,

$$H^2 = \frac{\rho_{\rm tot}}{3M_{\rm pl}^2} = \frac{1}{3M_{\rm pl}^2}\left[\frac{\dot\phi^2}{2} + V_{\rm eff}(\phi)\right], \tag{2.9}$$

$$\frac{\ddot a}{a} = -\frac{\rho_{\rm m}^{\rm cons} + (1+3w_\phi^{\rm eos})\rho_\phi}{6M_{\rm pl}^2} \tag{2.10}$$

$$\dot\rho_{\rm tot} + 3H(\rho_{\rm tot} + P_{\rm tot}) = 0, \quad \ddot\phi + 3H\dot\phi + V_{{\rm eff},\phi} = 0 \tag{2.11}$$

where we have defined ρ_ϕ, P_ϕ and $w_\phi^{\rm eos}$ via

$$\rho_{\rm tot} \equiv \rho_{\rm m}^{\rm cons} + \rho_\phi, \quad \text{such that } \rho_\phi = \frac{\dot\phi^2}{2} + V_{\rm eff}(\phi) \tag{2.12}$$

$$P_{\rm tot} \equiv P_\phi = \frac{\dot\phi}{2} - V(\phi) \tag{2.13}$$

$$w_\phi^{\rm eos} \equiv \frac{P_\phi}{\rho_\phi} = \frac{\dot\phi^2 - 2V(\phi)}{\dot\phi^2 + 2V_{\rm eff}(\phi)}. \tag{2.14}$$

Note that the total energy-momentum, $\rho_{\rm tot}$, is conserved in the Einstein frame.

If we let $C(\phi) \equiv 1$ and $V_{\rm eff}(\phi) \equiv V(\phi)$, we get the quintessence/DE system. If we further let $\dot\phi \equiv 0$, then we get the standard ΛCDM system.

2.3.2 Growth of Structure on Linear Scales

On large enough scales, structure formation can be described by the evolution of linear perturbations on top of the homogeneous and isotropic background. The epoch of interest is matter dominated, so we take the stress-energy perturbations to be fully captured by the CDM linear density contrast, $\delta_{\rm m}$, in cN gauge (perturbed flat FLRW metric, described fully by the 2 potentials $(\Phi_{\rm cN}(\mathbf{k},t),\ \Psi_{\rm cN}(\mathbf{k},t))$. In momentum-space the individual modes evolve independently at linear order, so it makes sense to work in Fourier space ($\mathbf{x} \to \mathbf{k}$). We are mainly interested in large but subhorizon scales and shall assume adiabatic initial

[2]Sometimes the first Friedmann equation is referred to as the Friedmann equation and the second one the acceleration equation.

conditions,

$$\text{Linear regime: } \delta_{\rm m} \ll 1 \tag{2.15}$$

$$\text{CDM density contrast: } \delta_{\rm m} \equiv \delta\rho_{\rm m}/\rho^{\rm m}_{\rm bkgd} \tag{2.16}$$

$$\text{cN gauge: } {\rm d}s^2 = -[1+2\Phi_{\rm cN}]{\rm d}t^2 + a^2[1+2\Psi_{\rm cN}]{\rm d}x^2 \tag{2.17}$$

$$\text{Sub-horizon: } k \gg aH \tag{2.18}$$

$$\text{Linear growth Eq: } \ddot{\delta}_{\rm m} + 2H\dot{\delta}_{\rm m} - \frac{3}{2}\Omega_{\rm m}H^2\left[1+2\beta_\phi^2\left(1+m_{\rm eff}^2a^2/k^2\right)^{-1}\right]\delta_{\rm m} = 0, \tag{2.19}$$

where $\Omega_{\rm m} = \rho_{\rm m}/\rho_{\rm crit}$.

We can use the Friedmann equation to arrange Eq. 2.19 into the exact form of the e.o.m. for $\delta_{\rm m}$ in a ΛCDM universe, .by defining an effective Newton's "constant" $G_{\rm N}$,[22]

$$G_{\rm N} \equiv \left(1+2\beta_\phi^2\left(1+m_{\rm eff}^2a^2/k^2\right)^{-1}\right)G. \tag{2.20}$$

This makes explicit the scale-dependence of the gravitational "constant". Notice that this enhancement is only relevant on scales smaller than the Compton wavelength of ϕ, such that $k \gg m_{\rm eff}$.

2.3.3 Non-linear Structure Formation

On small scales, $\delta_{\rm m} \gtrsim 1$, linear perturbation theory is no longer valid. Here $k-$modes couple to each other and we generally can't get an analytical solution. On the upside, here is where NL screening mechanisms kick in. (Section 2.6.)

2.4 Dark Energy

One way to go is to promote $\Lambda_{\rm CC}$ to a dynamical field, ϕ, that, via some mechanism, arrives at $w_\phi \simeq w_{\Lambda_{\rm CC}} = -1$ today. This is dark energy.

A simple example of such a field is quintessence,

$$S = \int {\rm d}^4x\sqrt{-g}\left[\frac{M_{\rm pl}^2}{2}R - \frac{1}{2}\nabla_\mu\phi\nabla^\mu\phi - V(\phi)\right] + S_{\rm m}[g_{\mu\nu};\psi_i], \tag{2.21}$$

where ϕ does not directly couple to R or ψ_i, i.e. it only minimally couples to gravity. It's time-dependent equation of state is

$$w_\phi = \frac{\dot{\phi}^2 - 2V(\phi)}{\dot{\phi}^2 + 2V(\phi)}. \tag{2.22}$$

The observed $w_\phi \simeq 1$ is achieved if the field's evolution today is potential dominated. In other words, ϕ is slow-rolling. In some quintessence models, the energy density in the DE field can be made to closely track that in (dark) matter but stay sub-dominant until the near past, where some mechanism kicks it into gear and it dominates, addressing the coincidence problem. There are more elaborate DE models, called k-essence. However, since DE is not the focus of this thesis, interested readers are referred to [7].

2.5 Distinguishing Modified Gravity and Dark Energy theories

2.5.1 Equivalence Principles

Before we start, let us first discuss the 3 equivalence principles. A main feature of GR is that there isn't a preferred frame for the laws of physics. In the flat spacetime limit (no gravity) this necessarily implies special relativity. However, when we include gravity, things get more complicated. There are 3 levels of the EP, which from weak to strong are:

- Weak equivalence principle (WEP): any uncharged free-falling test body [3] of given initial position and velocity would follow the same spacetime trajectory, independently of their composition. Mathematically, all matter species couple to the Jordan-frame metric, such that inertial and gravitational mass are equivalent. This is supported by Eötvös type torsion-balance, where we essentially measure the relative acceleration of test bodies of two different materials, hence different compositions, towards distant astrophysical bodies, such as the Sun, using a torsion balance. The "test body" nature of the test masses involved here is crucial. This distinguishes the Eötvös type laboratory experiments (verifying WEP) from Nordtvedt effect experiments where the test masses have non-negligible gravitational fields (verifying SEP)[116].

- Einstein equivalence principle (EEP): WEP + any free-falling observer (following the same trajectory as the WEP test body) recover the same laws of special relativistic physics locally, up to tidal gravitational forces, independent of its position or velocity. This is a statement about the laws of physics obeyed by the freely falling bodies whose trajectories are described by WEP. This is also the condition for a metric theory of gravity, where we have a unique metric and connection. There are no background vector or tensor fields that singles out a preferred frame. This is supported by Hughes-Drever experiments, which test for local spatial anisotropies by looking at atomic spectral lines, to see if any other gravitational fields other than the single rank-2 tensor[4] are allowed to couple directly to matter fields. If more directly-coupled fields were permissible, matter fields would no longer be following the geodesics of any one metric. This means we won't have (pseudo-)Riemannian geometry that allowed us to locally recover Minkowski spacetime in the tangent space at every point in spacetime (up to tidal forces), which in turn translated to SR at every point in spacetime. Theories that obey the EEP are called metric theories of gravity. Section 1.1

  Note that this does not disallow other fields/degrees of freedom in the theory. It only requires that these field interact with matter purely through the rank-2 tensor[5].

[3] an object that is sufficiently small that its self-gravity and backreaction on the gravitational field can be neglected

[4] Unless the fields are rank-2 tensor fields that couple to matter in a linear combination, since we can just define the effective metric of the theory as the linear combination of these various fields.

[5] Though the current observational constraints may allow wiggle-room for some additional weak interactions.

- Strong equivalence principle (SEP): WEP applies also to massive gravitating objects. EEP again applies to all free-falling frames. In other words, for SEP the laws of physics are blind to the objects' composition or gravitational binding energy, such that they follow the geodesics of Jordan frame metric, $\tilde{g}_{\mu\nu}$, without fail. The Earth and a black hole of the same mass would follow the same geodesics, e.g. the same orbit around the Sun! This is tested by examining the Nordtvedt effect, such that if the result is non-null, would imply a violation of SEP, killing GR. The test consists of tracking the separation of the Earth and Moon to high precision by LLR, where lasers on Earth are reflected off reflectors on the Moon and the time for it to return translates to the separation. The separation therefore tells us whether test masses with different gravitational binding energies fall towards the Sun at different rates, polarizing the lunar orbit.

2.5.2 MG, DE and Equivalence Principles

Models of DE satisfy the SEP, such that we are effectively just adding another species to the matter content of a fundamentally GR universe.

Whereas the models of MG only satisfy the EEP. This means that different objects, say with different gravitational binding energies (diffuse stars versus compact black holes, for example [67]) can experience the additional force due to ϕ, aka. the fifth force, differently, resulting in different motions.

In this thesis, we only concern ourselves with scalar-tensor theories that satisfy the EEP at the level of the action. Mathematically, say we have an action in the Einstein frame

$$S = \int \mathrm{d}^4x\sqrt{-g}\, M_{\rm pl}^2 \left[\frac{R}{2} - \frac{1}{2}\nabla_\mu\phi\nabla^\mu\phi - V(\phi)\right] + S_{\rm m}[(\tilde{g}_i)_{\mu\nu}; \psi_i]. \tag{2.23}$$

Since both DE and MG must obey EEP at the level of the action [6], we need $(\tilde{g}_i)_{\mu\nu} \equiv \tilde{g}_{\mu\nu}$. Then the split of DE and MG models manifests via $\tilde{g}_{\mu\nu} = g_{\mu\nu}$ for DE and $\tilde{g}_{\mu\nu} \neq g_{\mu\nu}$ for MG.

This thesis focuses on scalar-tensor theories of the MG type.

2.6 Screening mechanisms in Scalar-Tensor theories

We shall first look at screening in conformal ST theories. The action here is

$$S = \int \mathrm{d}^4x\sqrt{-g}\, M_{\rm pl}^2 \left[\frac{R}{2} - \frac{1}{2}\nabla_\mu\phi\nabla^\mu\phi - V(\phi)\right] + S_{\rm m}[C^2(\phi)g_{\mu\nu}; \psi_i]. \tag{2.24}$$

The geodesic equation (Euler-Lagrange equation) then has an extra source term additional to the usual $\boldsymbol{\nabla}\Phi_{\rm N}$, which we call the fifth-force (per unit test mass, i.e. acceleration) in

[6] Microscopic level. Macroscopic objects can apparently violate the EEP via, say, screening mechanisms [54].

the Einstein frame,

$$F_\phi = \boldsymbol{\nabla} \ln C(\phi) = \frac{\beta_\phi}{M_{\rm pl}} \boldsymbol{\nabla}\phi. \tag{2.25}$$

The goal is then to have $F_\phi \ll F_N$.

If we vary the action 2.24 w.r.t. ϕ, we find the field's equation of motion,

$$\Box\phi = V_{{\rm eff},\phi}, \quad \text{where } V_{\rm eff} = V(\phi) + C(\phi)\,\rho_{\rm m}^{\rm cons}. \tag{2.26}$$

ϕ's dependence on $V_{\rm eff}$ which in turn depends on the environmentally-dependent $\rho_{\rm m}^{\rm cons}$, means that by engineering a suitable $V_{\rm eff}$ by choosing the model quantities, V and C, we can tailor ϕ's behaviour to the environment.

The screening mechanisms can be classified according to how the regions in which they are active depend on $\Phi_{\rm N}$ in the Newtonian limit [67]. This corresponds terms in the Lagrangian at $\mathcal{O}(\delta\phi^2)$, where $\phi = \phi_{\rm bkgd} + \delta\phi$. Explicitly, the Lagrangian to $\mathcal{O}(\delta\phi^2)$ is

$$\frac{\mathcal{L}}{\sqrt{-g}} \sim -\frac{1}{2} Z^2(\phi_{\rm bkgd})\, \nabla^\mu\delta\phi\, \nabla_\mu\delta\phi - m_{\rm eff}^2(\phi_{\rm bkgd})\, \delta\phi^2 - \frac{\beta_\phi(\phi_{\rm bkgd})}{M_{\rm pl}}\, \delta\phi\, \rho_{\rm m} \tag{2.27}$$

Table 2.1: Classification of screening mechanisms in conformal ST theories according to their dependence on the Einstein-frame Newtonian potential $\Phi_{\rm N}$ in relation to some threshold mass scale, $\Lambda_{\rm thres}$. [67]

Active site	Fifth-force suppression in active region
$\Phi_{\rm N} > \Lambda_{\rm thres}$	$Q/M_{\rm source}$ suppressed in dense objects, s.t. one of the following happens: ϕ's force range $\sim m_{\rm eff}^{-1} \lesssim 10^{-6}$m (chameleon); ϕ-matter coupling becomes negligible, $\beta_\phi \ll 1$ (symmetron, dilaton)
$\nabla\Phi_{\rm N} > {\Lambda_{\rm thres}}^2$	$\nabla\Phi_{\rm N} \sim \ddot{\vec{x}}$. Large kinetic self-interactions: $\partial\phi/{\Lambda_{\rm thres}}^2 \gg 1$. ($k$-mouflage [8]). We shan't dwell on these here.
$\nabla^2\Phi_{\rm N} > {\Lambda_{\rm thres}}^3$	$\nabla^2\Phi_{\rm N} \sim \rho$, i.e. curvature. Scalar-gradients sourced by dense objects are suppressed. Large NL in the second derivatives: $\Box\phi/{\Lambda_{\rm thres}}^3 \gg 1$. $\beta_\phi \ll Z$ (Vainshtein)

Table 2.2: Screening-related quantities.

Symbol	Definition
M	Constant parameter of the ST model with the dimension of mass, appearing in $V(\phi)$
$\phi_{\rm min}$	The field value that minimizes $V_{\rm eff}$.
F_N	Newtonian force from Newton's second law

F_ϕ	Fifth-force (exists in the Einstein frame) mediated by the added light universally-coupled degree of freedom, ϕ.
$m_{\text{eff}}(\phi)$	Effective mass of ϕ, given by $V_{\text{eff},\phi\phi}(\phi)$. $m_{\text{eff}}^{-1}(\phi_{\text{min}})$, where $V_{\text{eff},\phi}(\phi_{\text{min}}) = 0$, is the characteristic range of the force mediated by the scalar field in the given medium.
μ_{sym}, λ_{sym}	Free parameters in the symmetron model
$\mathcal{X}(t, \mathbf{x})$	Metric and/or field perturbations, generally inhomogeneous and time-dependent.

We shall examine two well-studied subsets of ST theories belonging to the first class of screening listed in Table 2.1, $\Phi_{\text{N}} > \Lambda_{\text{thres}}$. This screening by a deep potential well is a result of invoking the thin-shell effect, which for spherically symmetric sources requires that a (thin-shell) suppression factor of the fifth-force relative to the gravitational force $\propto 1/\Phi_{\text{N}}$, the surface Newtonian potential of the source, to be $\ll 1$.

2.6.1 Conformal Screening: Chameleon

$V(\phi)$ and $C(\phi)$ are chosen such that m_{eff} increases in high-density regions, such as the SS.

A common choice is

$$V(\phi) = \frac{M^{4+n}}{\phi^n}, \quad C(\phi) = \mathrm{e}^{\beta_\phi \phi/M_{\text{pl}}}, \quad n \in \mathbb{R}_{>0}, \tag{2.28}$$

which has

$$m_{\text{eff}}^2(\rho) = n(n+1)\frac{M^{4+n}}{\phi_{\text{min}}^{2+n}}, \quad \text{where } \phi_{\text{min}}(\rho) = \left(\frac{nM^2M_{\text{pl}}^3}{\beta_\phi \rho}\right)^{\frac{1}{n+1}}. \tag{2.29}$$

We see that m_{eff} increases with ρ, such that we can choose to make it several orders of magnitude bigger in the high-density SS than it is in the low-density background. Since massive scalars obey the Yukawa force law, where $F_\phi \propto \mathrm{e}^{-m_{\text{eff}}r}/r^2$, we can make m_{eff} big enough via the choice of M, such that the force range is so small it is irrelevant to observable tests. Think of the familiar fundamental forces âĂŞ the strong force and the electromagnetic force, for example. While the strong force is, well, strong, macro- dynamics is blind to it because its force carriers are very massive, such that it is only relevant on very tiny scales. On the other hand, we have the electromagnetic force, which is mediated by massless photons, giving it infinite range and we can experience it in everyday scenarios.

In short, for sufficiently massive sources, the chameleon minimizes the effective potential deep inside them, resulting in the fluctuations of the chameleon field acquiring a large mass (hence Yukawa suppression) there. The exterior profile is then dominated only by the contribution from a thin shell right beneath the source's surface, which thickness is given by the thin-shell factor $\Delta R/R \propto 1/\Phi_{\text{N}}\big|_{\text{surface}} \ll 1$ for screened sources. The resulting chameleon-mediated force on an exterior test particle is consequently suppressed by the factor of $\Delta R/R$ relative to the gravitational force.

2.6.2 Conformal Screening: Symmetron

$V(\phi)$ and $C(\phi)$ are chosen such that the coupling of ϕ to matter in high-density regions is highly suppressed. It relies on ϕ having a vacuum-exectation energy that depends on the ambient matter density. The VEV is small in regions of high density, and large in regions of low density. In addition, the coupling of the scalar to matter is proportional to this VEV, hence the scalar couples with gravitational strength in regions of low density, but couples much more weakly in regions of high density.

A common choice is

$$V(\phi) = -\frac{1}{2}\mu_{\text{sym}}^2\phi^2 + \frac{1}{4}\lambda_{\text{sym}}\phi^4, \quad C(\phi) = 1 + \frac{\phi^2}{2M^2}, \tag{2.30}$$

which has

$$V_{\text{eff}}(\phi) = \frac{1}{2}\mu_{\text{sym}}^2\phi^2\left(\frac{\rho}{\rho_{\text{sym}}} - 1\right) + \frac{1}{4}\lambda_{\text{sym}}\phi^4, \tag{2.31}$$

where ρ_{sym} is a constant determined by the model parameters, such that in high-density regions $\rho > \rho_{\text{sym}}$, the model enjoys a $\mathbb{Z}_2$ symmetry, with $\phi_{\text{min}} = 0$, which means that the coupling function $C(\phi_{\text{min}}) = 0$, so no fifth-force exists. In low-density regions $\rho < \rho_{\text{sym}}$, however, the $\mathbb{Z}_2$ symmetry is spontaneously broken and $\phi_{\text{min}} \neq 0$, a fifth-force is thus introduced.

It is worth noting that the symmetron mechanism works very differently from the chameleon. Here m_{eff} remains small in high-density regions, so the force range is still very large. What is changed is instead the coupling strength of ϕ to matter. Explicitly, in order that the fifth-force is screened at sub-cosmological densities, we need $\mu_{\text{sym}}^2 \lesssim H_0^2$, corresponding to $m_{\text{eff}} \lesssim H_0$.

The thin-shell story here is very similar to that of the chameleon. For an object in vacuum, say, we know that the symmetron has to asymptote to its symmetry-breaking VEV. If the source is sufficiently massive, then symmetry is restored deep inside it, s.t. $\phi \approx 0$ there and the symmetron only weakly couples to matter. In order for the field to asymptote to its symmetry-breaking VEV far away frm the source, there needs to exist a thin-shell near its surface where the field deviates from $\phi \approx 0$. The symmetron field then effectively only couples to this thin shell and the resulting symmetron-mediated force on an exterior test particle is suppressed by a thin-shell factor $1/\alpha \propto 1/\Phi_{\text{N}}\big|_{\text{surface}}$ relative to the gravitational force.

Chapter 3

Newtonian and Post-Newtonian Gravity

Newtonian limit is defined to be the NR ($v^2/c^2 \ll 1$) [1] , weak field limit of gravity ($\Phi_{\rm N} \sim v^2/c^2$, from integrating Newtonian's second law) in a stationary, spherically symmetrical, asympotically-flat spacetime (essentially $g_{\mu\nu} \to \eta_{\mu\nu}$ as $|x^\mu| \to \infty$ [2]). In this limit, we should get the Poisson equation and Newton's second law. The relevance of the speed of light c lies in it being the speed of gravitational waves, propagated by massless gravitons. [3]

Post-Newtonian limit has the same requirements on $v^2, \Phi_{\rm N}$ and the geometry of spacetime but retain the next-to-leading-order terms in v/c. While these corrections are subdominant to the Newtonian terms, the effects are compounded over time, rendering them observable. Objects that are of order $\mathcal{O}(1/c^{2n})$ will be denoted as $\mathcal{O}_{\rm PN}(n)$. Solutions that truncate at $(v/c)^{2n} = \mathcal{O}_{\rm PN}(n)$, is referred to as nPN.

There are very precise tests of gravity in the SS, which constraints must be satisfied by any new theory of gravity. This would mean that given an action for a new proposed theory, we would have to vary it w.r.t. to the metric, obtain the field equations, solve for the metric in the non-relativistic, weak field limit, then plugging it into the geodesic equations to get the equations of motion for relevant objects. This is tedious. Thankfully, Will and Nordtvedt developed a framework called the parametrized post-Newtonian formalism (PPN)[122] that allows us to compare a large number of metric theories of gravity with the SS tests directly at the metric level. In particular, it is a general framework that provides a model-independent formulation of observational constraints for testing alternate theories of gravity in the SS. Deviations from GR are encoded in 10 parameters (one Newtonian and nine post-Newtonian) that appear multiplying various terms in the metric. SS experiments constrain these parameters either directly or in combinations (see [120] for a review) and so one can constrain a wide class of theories using the same experimental data. Note

[1] We mainly work in units where $c = 1$ in this thesis but c is explicitly included here for clarity.

[2] We didn't really have to specify a gauge choice, by writing limit as $\eta_{\mu\nu}$, but it is a good illustration. Technically, one wants $R^\alpha{}_{\beta\mu\nu} \to 0$ as $|x^\mu| \to \infty$. Note that the FLRW spacetime is not technically asymptotically flat, due to the time-dependent scale factor.

[3] The speed of gravitational waves in Newtonian gravity is taken to be infinite, i.e. instantaneous action. This is in conflict with observation, such as the precession of Mercury's perihelion.

however that while the PPN formalism attempts to encompass as wide a range of theories as possible, there is no guarantee that all metrics from alternate theories of gravity can be brought into PPN form.

Table 3.1: PPN-related quantities in Chapter 3.

Symbol	Definition
$\eta_{\mu\nu}$	Minkowski metric; vacuum solution of GR
$h^{(n)}_{\mu\nu}$	Metric perturbation around Minkowski of $\sim \mathcal{O}_{\rm PN}(n)$ induced by adding a NR test mass into the $\eta_{\mu\nu}$ spacetime. We are mainly concerned with $h^{(1)}_{\mu\nu}$ and shall write $h^{(1)}_{\mu\nu}$ as $h_{\mu\nu}$.
τ	Proper time for an observer moving along their worldline , s.t. $\mathrm{d}\tau \equiv g_{\mu\nu}\mathrm{d}x^\mu \mathrm{d}x^\nu$
$\Gamma^\alpha_{\mu\nu}$	Christoffel symbol for metric $g_{\mu\nu}$: $\frac{1}{2}g^{\alpha\beta}(g_{\mu\beta,\nu} + g_{\nu\beta,\mu} - g_{\mu\nu,\beta})$
$\sigma_{\rm aff}$	Affine parameter, such that $x^\mu(\sigma_{\rm aff})$ satisfies the geodesic equation: $(x^\alpha)'' + \Gamma^\alpha{}_{\mu\nu}(x^\mu)'(x^\nu)' = 0$.
t	Coordinate time (gauge/coordinate-dependent)
x^i	Coordinate spatial coordinate (gauge/coordinate-dependent)
v^i	Coordinate velocity (gauge/coordinate-dependent). For PPN purposes, it is the velocity measured by an observer in the Jordan frame, with the time-coordinate rescaled such that the lapse is unity. So unless the lapse is unity, $v^i \not\equiv \mathrm{d}x^i/\mathrm{d}t$. $\mathcal{O}_{\rm PN}(0.5)$.
$\gamma_{\rm Lorentz}$	Lorentz factor, $\mathrm{d}t/\mathrm{d}\tau = 1/\sqrt{1-(\mathrm{d}x^i/\mathrm{d}t)^2}$
u^μ	4-velocity (gauge/coordinate-independent), $\mathrm{d}x^\mu/\mathrm{d}\tau = \gamma_{\rm Lorentz}(1, \mathrm{d}x^i/\mathrm{d}t)$
$w^{\rm eos}_{(I)}$	Equation of state of species (I), $P_{(I)}/\rho_{(I)}$.
$T^{\mu\nu}_{(I)}$	Energy-momentum tensor of species (I), $\rho_{(I)}(1+w^{\rm eos}_{(I)}+\Pi_{(I)})u^\mu u^\nu + P_{(I)}g^{\mu\nu}$
$\Pi_{(I)}$	Specific internal energy (all forms of non-rest-mass) per unit $\rho_{(I)}$, such as thermal energy. $\mathcal{O}_{\rm PN}(1)$.
$\rho_{(I)}$	Rest-frame mass density of the fluid of species (I), important when transforming to PPN coordinates. $\mathcal{O}_{\rm PN}(1)$.
$P_{(I)}$	Rest-frame pressure of the fluid of species (I). $\mathcal{O}_{\rm PN}(2)$.
G	Gravitational constant, as appearing in the action, Einstein's equations, $M^2_{\rm pl} \equiv 1/8\pi G$.
$G_{\rm N}$	Locally-measured (effective) Newton's constant, not necessarily equal to G. Used to define PPN potentials, such that $g_{00} = -1+2U$ at $\mathcal{O}_{\rm PN}(1)$.
w^i	Coordinate velocity of the PPN coordinate system relative to the mean rest frame of the universe (CMB), relevant when a theory of gravity that involves a fixed external field, preferred frame effects. $\mathcal{O}_{\rm PN}(0.5)$. Varies over time scales much longer than SS time scales, such that we can ignore its time derivatives.

3.1 Parametrised post-Newtonian formalism (PPN)

The PPN framework is formulated in the weak gravitational field, non-relativistic limit around a Minkowski (asymptotically flat) background, such that $g_{\mu\nu}^{\mathrm{PPN}} = \eta_{\mu\nu} + h_{\mu\nu}$ with $h_{\mu\nu} \sim \mathcal{O}_{\mathrm{PN}}(1)$. The asymptotic $\eta_{\mu\nu}$ spacetime means that PPN is applicable for a time period over which cosmological evolution of the metric is negligible. The metric perturbations $h_{\mu\nu}$ are generated by an isolated, infinitesimal test mass embedded in the flat background. In the context of SS constraints, the test mass is the Sun, which perturbs the halo's smooth scalar field.

Explicitly, the system's negligible evolution in time means that $0 \approx \mathrm{d}/\,\mathrm{d}t = \partial_t + v^i\nabla_i$. Since we have defined $v \sim \mathcal{O}_{\mathrm{PN}}(0.5)$, it follows that $\partial_t \sim \mathcal{O}_{\mathrm{PN}}(0.5)$ and $\nabla_i \sim \mathcal{O}_{\mathrm{PN}}(0)$. Consequently, $\Phi_{\mathrm{N}} \sim \mathcal{O}_{\mathrm{PN}}(1)$ from Newton's second law and $\rho \sim \mathcal{O}_{\mathrm{PN}}(1)$ from the Poisson equation.

The fields involved are $g_{\mu\nu}, \phi, T_{\mu\nu}$. So we expand our dynamical fields in orders of smallness in perturbation, $\mathcal{O}_{\mathrm{PN}}(n)$, and solve the field equations and the equations of motion for the scalar field order by order.

Our tests measure the behaviour of the null- and time-like geodesics. To compare the predictions against measurement, we would therefore have to effectively solve for the e.o.m. of the test bodies to the necessary orders $\mathcal{O}_{\mathrm{PN}}$ for the matching. For example, for a metric ST theory,

- For time-like test bodies: To recover the Newtonian limit, we only need g_{00} to 1PN, while knowing the other metric components only at background level. To 1PN, we need g_{00} to 2PN, g_{0i} to 1.5 PN and g_{ij} to 1PN.
- For null-like test bodies: To recover the Newtonian limit, we only need all metric components only at background level since massless particles follows straight lines, to Newtonian accuracy. To 1PN, we need both g_{00} and g_{ij} to only 1PN.

We shall therefore aim for the requirements of the time-like test-bodies. We shall refer to a tensor of this scaling as being expanded to 2PN, since any scalar constructed out of it alone will be at least $\mathcal{O}_{\mathrm{PN}}(2)$.

We find that when solving for quantities needed for the 1PN e.o.m., we need to specify a gauge. After which we can always make further gauge transformations of the form $x^\mu \to x^\mu + \xi^\mu$, where $|\xi^\mu| \leq \mathcal{O}_{\mathrm{PN}}(1)$. This extra gauge freedom is valuable, as we shall see that at the end of solving the field equations to the necessary order and choosing a gauge, the resulting metric is not necessarily in the standard PN gauge, where at 1PN, g_{ij}^{PPN} is diagonal and isotropic while $g_{0i}^{\mathrm{PPN}} = 0$; the metric also contains no time-derivative terms. We shall need this remaining gauge freedom to put the metric in the PPN form, allowing for the matching to the PPN test metric.

Here is the PPN test metric to the necessary order required by time-like matter fields for their 1PN e.o.m.s, where the Jordan-frame metric components are decomposed in terms of scalar, vector and tensor potentials, and parametrized by (linear combinations of) 10 constant PN parameters (the particular combinations of which before the potentials are chosen to correspond to observable gravitational phenomena) and $G_{\rm N}$:

$$\begin{aligned}
\tilde{g}_{00} &= -1+2U-2\beta_{\rm PPN}U^2-2\xi_{\rm PPN}\Phi_W+(2\gamma_{\rm PPN}+2+\alpha_3+\zeta_1-2\xi_{\rm PPN})\Phi_1 \\
&\quad +2(3\gamma_{\rm PPN}-2\beta_{\rm PPN}+1+\zeta_2+\xi_{\rm PPN})\Phi_2+2(1+\zeta_3)\Phi_3+2(3\gamma_{\rm PPN}+3\zeta_4-2\xi_{\rm PPN})\Phi_4 \\
&\quad -(\zeta_1-2\xi_{\rm PPN})\mathcal{A}-(\alpha_1-\alpha_2-\alpha_3)w^2U-\alpha_2 w^i w^j U_{ij}+(2\alpha_3-\alpha_1)w^i V_i, \qquad (3.1)\\
\tilde{g}_{0i} &= -\frac{1}{2}(4\gamma_{\rm PPN}+3+\alpha_1-\alpha_2+\zeta_1-2\xi_{\rm PPN})V_i-\frac{1}{2}(1+\alpha_2-\zeta_1+2\xi_{\rm PPN})W_i-\frac{1}{2}(\alpha_1-2\alpha_2)w^iU \\
&\quad -\alpha_2 w^j U_{ij}, \qquad (3.2)\\
\tilde{g}_{ij} &= (1+2\gamma_{\rm PPN}U)\delta_{ij}, \qquad (3.3)
\end{aligned}$$

where

The 1PN gravitational potentials are

$$U\equiv G_{\rm N}\int \mathrm{d}^3\mathbf{x}'\frac{\rho_{\rm tot}(\mathbf{x}')}{|\mathbf{x}-\mathbf{x}'|},\quad \text{and}\quad U_{ij}\equiv G_{\rm N}\int \mathrm{d}^3\mathbf{x}'\frac{\rho_{\rm tot}(\mathbf{x}')(\mathbf{x}-\mathbf{x}')_i(\mathbf{x}-\mathbf{x}')_j}{|\mathbf{x}-\mathbf{x}'|^3}. \qquad (3.4)$$

U is familiar Newtonian gravitational potential solving the Newtonian Poisson equation.

The 2PN post-Newtonian gravitational potentials are

$$\begin{aligned}
&\Phi_1\equiv G_{\rm N}\int \mathrm{d}^3\mathbf{x}'\frac{\rho_{\rm tot}(\mathbf{x}')v^2(\mathbf{x}')}{|\mathbf{x}-\mathbf{x}'|},\quad \Phi_2\equiv G_{\rm N}\int \mathrm{d}^3\mathbf{x}'\frac{\rho_{\rm tot}(\mathbf{x}')U(\mathbf{x}')}{|\mathbf{x}-\mathbf{x}'|},\\
&\Phi_3\equiv G_{\rm N}\int \mathrm{d}^3\mathbf{x}'\frac{\rho_{\rm tot}(\mathbf{x}')\Pi(\mathbf{x}')}{|\mathbf{x}-\mathbf{x}'|},\quad \Phi_4\equiv G_{\rm N}\int \mathrm{d}^3\mathbf{x}'\frac{P_{\rm tot}(\mathbf{x}')}{|\mathbf{x}-\mathbf{x}'|},\\
&V_i\equiv G_{\rm N}\int \mathrm{d}^3\mathbf{x}'\frac{\boldsymbol{v}_i(\mathbf{x}')\rho_{\rm tot}(\mathbf{x}')}{|\mathbf{x}-\mathbf{x}'|},\quad W_i\equiv G_{\rm N}\int \mathrm{d}^3\mathbf{x}'\frac{\rho_{\rm tot}(\mathbf{x}')\boldsymbol{v}\cdot(\mathbf{x}-\mathbf{x}')(\mathbf{x}-\mathbf{x}')_i}{|\mathbf{x}-\mathbf{x}'|^3},\\
&\Phi_W\equiv G_{\rm N}^2\int \mathrm{d}^3\mathbf{x}'\,\mathrm{d}^3\mathbf{x}''\frac{\rho_{\rm tot}(\mathbf{x}')\rho_{\rm tot}(\mathbf{x}'')(\mathbf{x}-\mathbf{x}')}{|\mathbf{x}-\mathbf{x}'|^3}\cdot\left(\frac{\mathbf{x}'-\mathbf{x}''}{|\mathbf{x}-\mathbf{x}''|}-\frac{\mathbf{x}-\mathbf{x}''}{|\mathbf{x}'-\mathbf{x}''|}\right)\quad\text{and}\\
&\mathcal{A}\equiv G_{\rm N}\int \mathrm{d}^3 vecx'\frac{\rho_{\rm tot}(\mathbf{x}')\left[\boldsymbol{v}(\mathbf{x}')\cdot(\mathbf{x}-\mathbf{x}')\right]^2}{|\mathbf{x}-\mathbf{x}'|^3}. \qquad (3.5)
\end{aligned}$$

Notice that the PPN formalism assumes that the SS metric is stationary, such that all the metric potentials are time-independent. Since it admits a non-zero $0i$-component, however, it is not static (there is rotation in the spacetime geometry – the time direction is not exactly orthogonal to the spatial hypersurfaces).

The 10 parameters $\gamma_{\rm PPN}$, $\beta_{\rm PPN}$, $\xi_{\rm PPN}$, ζ_i and α_i are arbitrary constants whose value depends on the specific theory in question. GR has $\gamma_{\rm PPN}=\beta_{\rm PPN}=1$ and $\xi_{\rm PPN}=\zeta_i=\alpha_i=0$. Canonical conformally-coupled ST theories on the other hand, typically lead to different values of $\gamma_{\rm PPN}$ and $\beta_{\rm PPN}$ while the other PPN parameters remain at their vanishing GR

values. The PPN parameters have been measured using a variety of different probes [120] and are all consistent with GR. One can then calculate them in alternate theories and use the bounds to constrain the model parameters. We shall elaborate on two specific PPN parameters, $\gamma_{\rm PPN}$ and α_2 as they are most relevant to this thesis. The other PPN parameters are described in Table 3.2.

We see that all the precisely-measured physical phenomena are in good agreement with GR's predictions. This means when in order for any MG theory to be observationally viable, it must look a lot like GR in the weak field limit.

Table 3.2: PPN parameters. These parameters are chosen to pertain to specific physical observations.[120]

Symbol	Definition	Constraint (0 in GR)
$\gamma_{\rm PPN}-1$	Eddington light bending parameter. Measures the amount of spatial curvature produced per unit rest mass, thus changing the motion of light relative to NR bodies, resulting in light deflection and time delay. Constrained by light bending by the Sun or more stringently by the Shapiro time-delay effect, both measured by the Cassini probe.	2.3×10^{-5}
$\beta_{\rm PPN}-1$	Measures the degree of NL in the superposition law for gravity. Constrained by the anomalous perihelion precession of the orbit of Mercury. If we assume that only $\{\gamma_{\rm PPN},\beta_{\rm PPN}\}$ are non-vanishing and $\gamma_{\rm PPN}$ is given by observations of the Shapiro time delay effect, then we can obtain a tighter constraint from the Nordtvedt effect measured by LLR as discussed in Section 2.5.1.	3×10^{-3}; 2×10^{-4}
$\xi_{\rm PPN}$	Whitehead parameter. Measures anisotropies in $G_{\rm N}$in three-body systems, resulting in large tides on Earth as the SS moves through the MW. Constrained by gravimeter data on Earth tides.	10^{-3}
α_1,α_2	Measures preferred-frame effects, the presence of a fixed cosmological background field, violating Lorentz invariance. When non-zero indicates a semi-conservative theory (conserves only P^μ not $J^{\mu\nu}$). Constrained by Lunar Laser Ranging data on orbital polarisation and the spin precession of the alignment of the Sun's axis with its ecliptic, respectively.	10^{-4}, 4×10^{-7}
α_3	Measures preferred-frame effects and is a conservation law parameter, such that it being non-zero indicates a non-conservative theory (conserves neither P^μ or $J^{\mu\nu}$). Constrained by pulsar spin-down statistics.	4×10^{-20}

ζ_i, $i = 1,2,3,4$	Conservation law parameters, such that one or more of them being non-zero indicates a non-conservative theory (conserves neither P^μ or $J^{\mu\nu}$). Constrained by combined PPN bounds, binary pulsar acceleration, Newton's third law measured by lunar acceleration and the Kreuzer experiment, respectively.	2×10^{-2}, 4×10^{-5}, 10^{-8}, 4×10^{-1}

3.1.1 Eddington light-bending parameter, $\gamma_{\rm PPN}$

A PPN parameter of particular interest to this thesis is the Eddington light-bending parameter, $\gamma_{\rm PPN}$. Comparing Eq.s 3.1 and 3.3, we see that $\gamma_{\rm PPN}$ is given by the ratio of the space-like to time-like metric perturbations of the Jordan frame metric in the SS *in PPN form* at $\mathcal{O}_{\rm PN}(1)$, i.e.

$$\gamma_{\rm PPN} = \frac{\tilde{g}^{[1]}_{ij}|_{i=j}}{\tilde{g}^{[1]}_{00}}, \tag{3.6}$$

where again we emphasize that this definition applies to the Jordan frame metric in the PPN form, as will be demonstrated in Section 4.1.5.

$|\gamma_{\rm PPN} - 1|$ has been constrained by Cassini data – by combining photon propagation, in particular, light bending by the Sun (Shapiro time delay: where a radio signal's round-trip across the SS, passing by the Sun, yields an a observable time delay) with the EarthâĂŹs orbital dynamics – to be $\lesssim 2 \times 10^{-5}$ in the SS. This tight constraint illustrates the need to have modifications in gravity be scale- and/or environment-dependent, in order to have a theory that is viable and cosmologically interesting.

There has been some confusion regarding the proper definition of $\gamma_{\rm PPN}$. In Ref. [51], the authors defined $\gamma_{\rm PPN}$ as the ratio of the space-like to time-like perturbations of the Jordan-frame metric of the smoothed halo in which the SS is a perturbing test mass, this gives[4]

$$\gamma_{\rm PPN} - 1\Big|_{\rm halo} = -\frac{\phi^2}{M^2}\frac{2}{\frac{\phi^2}{M^2} + 2\Psi\left(1 + \frac{\phi^2}{M^2}\right)}. \tag{3.7}$$

We reiterate: this is the PPN parameter valid for the smooth spherically symmetric density profile of the halo. Contrast this with the arguably more relevant definition of $\gamma_{\rm PPN}$, which is the ratio of space-like to time-like perturbations generated in the metric by a test mass (the Sun) embedded in the smooth halo. This second definition is also more consistent with the PPN framework, which is formulated around an asymptotically flat spacetime, corresponding to an isolated central mass. In this case, one obtains [53] [Eq. (32) with Eq. (18) there]

$$\gamma_{\rm PPN} - 1\Big|_{\rm SS} = -\frac{4\beta^2_{\rm sym}(\phi/\phi_{\rm vac})^2}{1 + 8\beta^2_{\rm sym}(\phi/\phi_{\rm vac})^2} \approx -4\beta^2_{\rm sym}\left(\frac{\phi}{\phi_{\rm vac}}\right)^2, \tag{3.8}$$

[4]Here we have corrected a sign error in [51].

where $\beta_{\rm sym}$ is the dimensionless symmetron coupling constant. It measures the strength of scalar force in vacuum relative to gravity, such that $F_\phi = 2\beta_{\rm sym}^2 F_{\rm N}$ and is taken to be of order unity. [51]

In Section 2.2, we saw that Brans-Dicke theory the mass scale associated with a massive $\Psi_{\rm BD}$ given by its bare potential (as opposed to its effective potential) is $m_{\rm BD}$. For SS tests, the relevant mass (equivalently, 1/length) scale corresponds to the size of the SS, i.e. (Astronomical Unit)$^{-1}$, which we shall denote by $m_{\rm AU}$.

[91] found that the expression for $\gamma_{\rm PPN}$ is dependent on the relative sizes of $m_{\rm BD}$ and $m_{\rm AU}$. The two extreme cases are as follows:

- $m_{\rm BD} \ll m_{\rm AU}$: We get the familiar $\gamma_{\rm PPN} = (1+w_{\rm BD})/(2+w_{\rm BD})$. Note that in strict BD theory, $w_{\rm BD}$ is a constant and therefore cannot be environmentally-dependent, to be distinguished from the environmentally-dependent models, such as the symmetron (Section 2.6.2), for example, which we shall call Brans-Dicke-like models, where $w_{\rm BD}$ is generalized to the field-dependent Brans-Dicke parameter, $w_{\rm BD}(\Psi_{\rm BD})$.This means we can design it to become big in regions of high-density, so that the scalar field effectively decouples from matter.

- $m_{\rm BD} \gg m_{\rm AU}$: Note that this corresponds to $\Psi_{\rm BD}$ having a very small range, s.t. it is effectively not excited on SS scales regardless of $w_{\rm BD}$.

For the inbetween region, we need an "effective $\gamma_{\rm PPN}$". The physical setup considered in [91] is as follows: For the background quantities, we have the Minkowski metric and $\Psi_{\rm BD}^{\rm bkgd}$ is spatially uniform and time-independent. Note that the time-independence is valid since $\Psi_{\rm BD}$'s evolution is expected to be on cosmological time-scales, which are much greater than that of the SS, hence the time dependency can be ignored. On top of the background solution are perturbations in the metric and in $\Psi_{\rm BD}$, with we shall denote as $h_{\mu\nu}$ and $\Psi_{\rm BD}^{\rm pert}$. Here [91] adopted the quasi-static limit to the SS's system of equations, where time-derivatives are ignored relative to spatial ones. This is valid even where there are time-dependent perturbations in the embedding halo, as the SS itself is static and the PPN metric describes the effect of the (effectively infinitesimal in size) test mass – the SS. The halo provides a smooth background field which the SS, a test mass, disturbs. At linear order in the wave amplitude, waves in the halo would only enter the SS's solution by modifying its effective mass and coupling constant, the solution itself remains static.Matter fields are taken to be dominated by CDM with vanishing pressure.

The resulting expression of $\gamma_{\rm PPN}$ is then found to be

$$\gamma_{\rm PPN}(w_{\rm BD}, m_{\rm BD}, m_{\rm AU}) \equiv \frac{h_{ij}|_{i=j}}{h_{00}} = \frac{1 - {\rm e}^{(-m_{\rm eff}^{\rm BD} m_{\rm AU})}/(2w_{\rm BD}+3)}{1 + {\rm e}^{(-m_{\rm eff}^{\rm BD} m_{\rm AU})}/(2w_{\rm BD}+3)}, \tag{3.9}$$

where $m_{\rm eff} = m_{\rm eff}^{\rm BD}(w_{\rm BD}) \equiv m_{\rm BD}\sqrt{2\Psi_{\rm BD}^{\rm bkgd}/(2w_{\rm BD}+3)}$ is the effective mass of $\Psi_{\rm BD}$ and restricts its force's range to $1/m_{\rm eff}^{\rm BD}$. If $m_{\rm BD} \sim 0$, i.e. vanishing potential term, then, we recover the expression for $m_{\rm BD} \ll m_{\rm AU}$.

3.1.2 Preferred frame effect parameter α_2

Preferred frame effect parameters $\alpha_i,\ i = 1, 2, 3$ contribute in (and only in) the coefficients of the PPN potentials whose definitions involve $\mathbf{v}$. α_2, in particular, is constrained by the near perfect alignment of the Sun's spin axis with the orbital angular momenta of the planets. The term in the PPN metric proportional to α_2 leads to a torque on the Sun which induces a precession of the Sun's spin axis, contributing to the misalignment of the axes of spin and planetary orbital angular momenta. Ref. [89] obtained a constraint on α_2 by integrating the motion of the SS relative to the cosmological reference frame over the past 5 Gyr. Caveats to this treatment given the uncertainties of galactic evolution have been pointed out in [59]. As shown there, the orbit of Mercury provides an independent constraint $|\alpha_2| \lesssim 4\times10^{-5}$, with further improvements possible. While a detailed discussion of the α_2 constraints goes beyond the scope of this thesis, it is worth noting that an integration time of 5 Gyr is still relatively short compared to the Hubble time, over which the background scalar field evolves.

As we shall see in Section 4.1.2, that we don't lose the preferred-frame effects by calculating the PPN metric in the CMB rest frame.This is possible because preferred frame effects are present implicitly within the matter velocities $v_i^{\rm CMB}$ in the CMB-frame metric. To see this, note that at lowest order of $v_i^{\rm CMB}$ can be decomposed into $v_i^{\rm CMB}(\mathbf{x}) = v_i^{\rm SS}(\mathbf{x}) + w_i$, where $v_i^{\rm SS}$ is the matter velocity with respect to the centre of mass of the SS frame.

Chapter 4

Disformal ST theories

Table 4.1: Disformal gravity-related quantities in Chapter 4

Symbol	Definition
ϕ	Scalar field that we have normalized to be dimensionless *in this chapter*.
$\phi_{\rm CMB}(t)$	Cosmological background field in the CMB frame. Homogeneous, time-dependent. $\mathcal{O}_{\rm PN}(0)$.
$\mathcal{D}(\phi, X)$	Disformal factor, $C(\phi, X)D(\phi, X)/\Lambda_{\rm disf}$
$\Lambda_{\rm disf}$	Disformal coupling mass scale, controls the amplitude of disformal effects, with smaller values of $\Lambda_{\rm disf}$ leading to larger effects.
$\hat{\beta}_\phi$	Rescaled conformal coupling strength, $\beta_\phi/M_{\rm pl} = [\ln C(\phi)]_{,\phi}$.
$\hat{\Delta}_\phi$	Rescaled disformal coupling strength, $[\ln D(\phi)]_{,\phi}$
H_0	Hubble parameter today
$a(t)$	Einstein frame scale factor
$\tilde{a}(t)$	Jordan frame scale factor, $C(\phi_{\rm CMB})\, a(t)$
N	Lapse function, relates coordinate time t and proper time τ along curves normal to "spatial" hypersurfaces of constant t.
$v^i_{\rm SS}$	Matter velocity (in unitary lapse coordinates) w.r.t. the centre of mass of the SS frame.
$v^i_{\rm CMB}$	Matter velocity (in unitary lapse coordinates) w.r.t. the CMB.
w^i	Coordinate velocity of the PPN coordinate system (SS) w.r.t. CMB frame (in unitary lapse coordinates), $\mathcal{O}_{\rm PN}(0.5)$.
$(\phi_{\rm CMB,\mu})_{\rm SS}$	Four-gradient of $\phi_{\rm CMB}$ in the SS frame, as opposed to $\partial_\mu\phi_{\rm CMB}$ which defined in the CMB frame.
ϕ_n	$\mathcal{O}_{\rm PN}(n)$ term in ϕ, s.t. $\phi = \phi_{\rm CMB} + \sum_{n=1}^{\infty}\phi_n$
Υ	$\dot{\phi}^2_{\rm CMB}/{\Lambda_{\rm disf}}^2$
Σ	$\ddot{\phi}_{\rm CMB}/{\Lambda_{\rm disf}}^2$
$\dot{\mathcal{Q}}$	Time derivative (w.r.t. coordinate time) of the quantity $\mathcal{Q}$, $\mathrm{d}\mathcal{Q}/\mathrm{d}t$

t	Coordinate time
τ	Proper time, $\sqrt{-g_{\mu\nu}x^\mu x^\nu}$
$T^{\mu\nu}_{\rm m}$	Einstein frame energy-momentum tensor for matter, $(2/\sqrt{-g})\delta(\sqrt{-\tilde{g}}\tilde{\mathcal{L}}_{\rm m})/\delta g_{\mu\nu}$
$T^{\mu\nu}_{\phi}$	Einstein frame energy-momentum tensor for ϕ, $(2/\sqrt{-g})\delta(\sqrt{-g}\mathcal{L}_\phi)/\delta g_{\mu\nu} = M_{\rm pl}^2\left(\phi^{,\mu}\phi^{,\nu} - g^{\mu\nu}\phi^{,\alpha}\phi_{,\alpha}/2 - g^{\mu\nu}V(\phi)\right)$
$T^{\rm tot}_{\mu\nu}$	Total energy-momentum tensor, $T^{\rm m}_{\mu\nu} + T^{\phi}_{\mu\nu}$, such that $\nabla_\mu T^{\mu\nu}_{\rm tot} = 0$.
Q	Local scalar charge, $\left[\hat{\beta}_\phi + (D/\Lambda_{\rm disf})^2\left(\ddot{\phi}_{\rm CMB} + \dot{\phi}^2_{\rm CMB}(\hat{\Delta}_\phi - \hat{\beta}_\phi)\right)\right]/(1 - D^2\dot{\phi}^2_{\rm CMB}/{\Lambda_{\rm disf}}^2)$, such that the fifth-force $\mathbf{F}_5 = -Q\boldsymbol{\nabla}\phi$ and $\nabla_\mu T^{\mu\nu}_{\phi} = -\nabla_\mu T^{\mu\nu}_{\rm m} \equiv Q\nabla^\nu\phi$.
λ	Model parameter of the concrete model defined by $V(\phi) = m_0^2 e^{-\lambda\phi}$, Eq. 4.64.

So far we have only discussed conformal ST theories and their screening mechanisms. However, the most general relation that preserves causality is Bekenstein's Eq. 2.1. The addition of the disformal coupling term, $D(\phi, X)\partial_\mu\phi\partial_\nu\phi$, to any theory does not introduce a ghost by itself, assuming that the signs of C and D are chosen appropriately.

When C and D depend on ϕ only the theory is a subset of the Horndeski class[1] [55, 20], and when D depends on ϕ and X the theory fits into the "beyond Horndeski" class [47]. The latter case contains hidden constraints that render the equations of motion second-order [126]. Disformal coupling, in contrast to conformal coupling, has only recently begun to be studied in detail [68, 71, 124, 88, 30, 125, 29, 25, 23, 24, 96, 97, 28, 70, 50, 43]. Until recently, most studies have focused on the cosmology of disformal ST theories and, unlike the conformal coupling [41, 64, 27, 94, 112, 98, 95, 73], little attention has been given to astrophysical and SS effects.

As a reminder, canonical disformal gravity theories are described by the ST action:

$$S = \int \mathrm{d}^4x\sqrt{-g}\, M_{\rm pl}^2\left[\frac{R}{2} - \frac{1}{2}\nabla_\mu\phi\nabla^\mu\phi - V(\phi)\right] + S_{\rm matter}[\tilde{g}_{\mu\nu}; \psi_i], \tag{4.1}$$

which describes a massless spin-2 graviton and an additional scalar degree of freedom in the Einstein frame. The modifications of general relativity arise due to a coupling of the scalar to matter via the Jordan frame metric

$$\tilde{g}_{\mu\nu} = C^2(\phi, X)\left[g_{\mu\nu} + \frac{D^2(\phi, X)}{{\Lambda_{\rm disf}}^2}\partial_\mu\phi\partial_\nu\phi\right], \quad X \equiv -\frac{1}{2}g^{\mu\nu}\partial_\mu\phi\partial_\nu\phi. \tag{4.2}$$

Note that we have normalized ϕ to be dimensionless. Here we will only study the case where the coupling functions depend solely on the scalar field, ϕ. Our leading constraints will also apply to models that generalize this to $D = D(\phi, X)$.

[1] Unless non-Horndeski terms are present in the action $S[g_{\mu\nu}, \phi]$.

The equations of motion in the Einstein frame are [96]

$$G_{\mu\nu} = 8\pi G\left(T^{\rm m}_{\mu\nu} + T^{\phi}_{\mu\nu}\right) \tag{4.3}$$

$$\left(1 - \frac{2XD^2}{{\Lambda_{\rm disf}}^2}\right)\Box\phi = \frac{8\pi GD^2}{{\Lambda_{\rm disf}}^2}T^{\mu\nu}_{\rm m}\nabla_\mu\nabla_\nu\phi - 8\pi G\hat{\beta}_\phi T_{\rm m} - \frac{8\pi GD^2}{{\Lambda_{\rm disf}}^2}(\hat{\beta}_\phi - \hat{\Delta}_\phi)T^{\mu\nu}_{\rm m}\partial_\mu\phi\partial_\nu\phi + \left(1 - \frac{2XD^2}{{\Lambda_{\rm disf}}^2}\right)V_{,\phi}, \tag{4.4}$$

The energy-momentum tensors in the Einstein frame, $T^{\rm m}_{\mu\nu}$ and $T^{\phi}_{\mu\nu}$, are not separately covariantly conserved quantities due to the coupling of the scalar to matter, only their sum is. Equation (4.3) is simply Einstein's equation, which is a consequence of working in the Einstein frame. Equation (4.4) is the equation of motion for the scalar and this is where the modifications of gravity become apparent. Note that the physical metric is the Jordan frame metric (4.2); it is this metric that governs the motion of test particles. The energy-momentum tensor of matter appears in equation (4.4) and so the field is sourced by any non-zero matter distribution characterised by $T^{\rm m}_{\mu\nu}$. In NR systems, the gravitational field is sourced mainly by matter and not the scalar, in which case the solution of (4.3) is identical to the GR solution. The physical metric, and correspondingly the motion of test particles, then deviates from the GR prediction.

In order to calculate this theory's SS observables, we want to find its physical (Jordan frame) metric to post-Newtonian (PN) order. The PN predictions of purely conformal ST theories have been well-studied (see [119, 120] and reference therein) but, to date, the PN behaviour of disformal theories has yet to be derived. We therefore focus on the disformal part of (4.2), setting $C \equiv 1$ thus $\hat{\beta}_\phi = 0$. Furthermore, we set $D(\phi)$ to be constant ($\hat{\Delta}_\phi = 0$), and absorb its value into $\Lambda_{\rm disf}$ to set $D \equiv 1$.

Let's look at a minimal model first. In fact, in Section A we show that the general model yields no new constraints compared with the minimal model. This is because the conformal and disformal couplings are independently constrained by different PPN parameters, so that any interaction of the two effects is highly suppressed, although this is far from obvious a priori. Ref. [96] has examined the Newtonian behaviour of these theories and has shown that the disformal terms are only active when one accounts for the fact that the space-time is asymptotically FRW and not Minkowski and that the disformal terms are sourced by the time-derivative of $\phi_{\rm CMB}$. The constraints for the non-minimal model are then essentially the same when setting $D \to D(\phi_{\rm CMB}(t_0))$.

4.1 The Minimal Disformal Model

The minimal model is described by the Jordan frame metric

$$\tilde{g}_{\mu\nu} = g_{\mu\nu} + \frac{\partial_\mu\phi\partial_\nu\phi}{{\Lambda_{\rm disf}}^2}\,. \tag{4.5}$$

The inverse Jordan frame metric is given by

$$\tilde{g}^{\mu\nu} = g^{\mu\nu} - \frac{1}{{\Lambda_{\rm disf}}^2}\left(1 - \frac{2X}{{\Lambda_{\rm disf}}^2}\right)^{-\frac{1}{2}} g^{\mu\alpha}g^{\nu\beta}\partial_\alpha\phi\partial_\beta\phi\,. \tag{4.6}$$

We will treat the scalar as a light, cosmological scalar driving the acceleration of the cosmic expansion. $V(\phi)$ and its derivatives are then all of order H_0, and we can neglect the mass of the scalar on the scales of interest. Screening mechanisms such as the chameleon and symmetron can render the field locally massive and thus hide it from local observations. In that case however, there is nothing to add to the standard conformally coupled screened theories in the PPN context, and we will not consider this case here.

4.1.1 Choice of Coordinates

We begin by setting up a coordinate system in which to solve the equations. The equations of motion are simplest in the Einstein frame, so this is where we will start. The Einstein frame solution at $\mathcal{O}_{\rm PN}(0)$ in the CMB rest-frame is simply Minkowski space, $\eta_{\mu\nu}$. We can ignore FRW corrections of the $\mathcal{O}_{\rm PN}(0)$ solution since these are negligible on SS scales.

Explicitly, the vacuum solution of the field equations:

$$\mathrm{d}s^2 = -\,\mathrm{d}t^2 + \delta_{ij}\,\mathrm{d}x^i\,\mathrm{d}x^j. \tag{4.7}$$

The corresponding Jordan frame metric is

$$\mathrm{d}\tilde{s}^2 = -N^2\,\mathrm{d}t^2 + \delta_{ij}\,\mathrm{d}x^i\,\mathrm{d}x^j\,, \tag{4.8}$$

where the lapse is

$$N^2 = 1 - \frac{\dot{\phi}^2_{\rm CMB}}{{\Lambda_{\rm disf}}^2}\,. \tag{4.9}$$

This differs from unity due to the presence of a time-dependent cosmological field $\phi_{\rm CMB}$. In this sense, the proper time for a physical observer is not coincident with the coordinate time and so it is clear that even at $\mathcal{O}_{\rm PN}(0)$, $\tilde{g}_{\mu\nu}$ is not in the PPN gauge with this choice of coordinates. The Jordan frame and Einstein frame energy-momentum tensors are related by [125, 96]:

$$T^{\mu\nu}_{(I)} = \sqrt{1 - \frac{2X}{{\Lambda_{\rm disf}}^2}}\,\tilde{T}^{\mu\nu}_{(I)}. \tag{4.10}$$

We will consider the metric sourced by a static object of finite extent and will hence treat its internal structure using a fluid description. Since the Jordan-frame $\tilde{T}^{\mu\nu}_{\rm m}$ (rather than $T^{\mu\nu}_{\rm m}$) is the covariantly conserved energy-momentum tensor, all fluid variables such as the density and pressure must be defined in this frame. We will hence consider the Einstein frame as a calculation tool; we will not assign any physical meaning to $T^{\mu\nu}_{\rm m}$, it is simply a source in the field equations. We will transform quantities to the Jordan-frame PPN gauge once the solutions at 1PN and 2PN have been found.

4.1.2 Preferred Frame Effects

Our goal is to derive the PPN metric in the rest frame of the SS, since that is the frame in which observations are being made. There are two possible ways to proceed. First, one could directly derive the solution for the field in the SS frame. In this frame, the background field gradient, which is simply $\partial_\mu \phi_{\rm CMB} = \dot{\phi}_{\rm CMB}(1,0,0,0)$ in the CMB frame, is Lorentz-boosted to

$$
\begin{aligned}
(\partial_0 \phi_{\rm CMB})_{\rm SS} &= \dot{\phi}_{\rm CMB}\left(1+\frac{w^2}{2}+\frac{3w^4}{8}\right) \\
(\partial_i \phi_{\rm CMB})_{\rm SS} &= -\dot{\phi}_{\rm CMB}\left(1+\frac{w^2}{2}\right) w_i \,,
\end{aligned}
\tag{4.11}
$$

where we have expanded to 2PN. Once the solution is obtained, one performs a gauge transformation including terms involving w to obtain the metric in PPN form, Eqs. (3.1)–(3.3). One can immediately see why this theory predicts preferred frame effects: $\dot{\phi}_{\rm CMB}(t)$ is only isotropic in the CMB rest frame. In any other frame it has a spatial gradient proportional to w_i. In any scalar-tensor theory, an evolving background field leads to preferred-frame effects. In purely conformal theories, these are suppressed by powers of the ratio of the SS time-scale (years) to the Hubble time since $\dot{\phi}_{\rm CMB} \sim H_0$. These effects are usually neglected and we do the same here. The disformal coupling, on the other hand, adds additional explicit preferred-frame effects in factors of $\dot{\phi}_{\rm CMB}/\Lambda_{\rm disf}$. Hence, for novel effects in cosmology, we require that $\Lambda_{\rm disf} \sim H_0$.[28]

The second approach solves the field equations in the rest frame of the CMB, where the bulk motion of the SS is included in the energy momentum tensor; to lowest order, $v_i^{\rm CMB}(\mathbf{x}) = v_i^{\rm SS}(\mathbf{x}) + w_i$. This means that preferred-frame effects are present implicitly within the matter velocities v^i in the CMB-frame metric. One then performs a gauge transformation to the PPN gauge in the absence of bulk motion, i.e. Eqs. (3.1)–(3.3) with w_i set to zero. Finally, the PPN metric is boosted to the SS frame by a Lorentz boost ("post-Galilean transformation"), as described in Sec. 4.3 of [119], which reintroduces the terms involving w^i in Eqs. (3.1)–(3.3).

Both approaches are equivalent since the underlying theory is Lorentz invariant, and since the physical relative velocity between CMB and SS frames is included in either case (it is merely absorbed in $\tilde{T}_{\mu\nu}$ in the second approach). While the first approach in principle keeps the physics more clear, the gauge transformation from the Einstein-frame, in which the field solution is obtained, to PPN gauge is somewhat cumbersome in this approach, as many terms involving powers of w^i and various contractions with PPN potentials need to be kept. The second approach on the other hands avoids these complications and so we follow it here. Thus, we begin by deriving the Einstein frame field solution in the CMB rest-frame, and then transform the resulting CMB Jordan-frame metric to the PPN form with $w = 0$.

Ansatz for the Solution

The field to 2PN is

$$\phi = \phi_{\rm CMB} + \phi_1 + \phi_2. \tag{4.12}$$

We expect that $\dot{\phi}_{\rm CMB} \sim H_0$ and $\ddot{\phi}_{\rm CMB} \sim H_0^2$ in the CMB frame since the evolution of $\phi_{\rm CMB}$ is driven by the cosmological background (recall that ϕ is normalized to be dimensionless for our discussions on disformal ST theories). Looking at equation (4.4) with $\hat{\beta}_\phi = \hat{\Delta}_\phi = 0$ one can see that, at lowest order, there are two parameters multiplying the source terms for the field:

$$\Upsilon \equiv \frac{\dot{\phi}_{\rm CMB}^2}{{\Lambda_{\rm disf}}^2} \quad \text{and} \quad \Sigma \equiv \frac{\ddot{\phi}_{\rm CMB}}{{\Lambda_{\rm disf}}^2}. \tag{4.13}$$

We will take both of these to be small numbers and will work only to leading-order in both. We will see that this approximation is self-consistent once the constraints from the PPN parameters have been imposed. We expand the Einstein frame metric as $g_{\mu\nu} = \bar{g}_{\mu\nu} + h_{\mu\nu}$, and impose the gauge choice

$$\partial_\mu h^\mu_0 - \frac{1}{2}\partial_0 h^\mu_\mu = -\frac{1}{2}\partial_0 h_{00} \quad \text{and} \tag{4.14}$$

$$\partial_\mu h^\mu_i - \frac{1}{2}\partial_i h^\mu_\mu = 0, \tag{4.15}$$

with $h^\mu_\nu \equiv \eta^{\mu\alpha} h_{\alpha\nu}$. With this gauge choice, one can write the Einstein frame metric as[2]

$$\begin{array}{ll} g_{00} = -1 + 2\chi_1 + 2\chi_2, & g^{00} = -1 - 2\chi_1 - 2\chi_2 - 4\chi_1^2 \\ g_{0i} = B_i, & g^{0i} = -B^i \\ g_{ij} = (1 + 2\Psi_1)\delta_{ij}, & g^{ij} = (1 - 2\Psi_1 + 4\Psi_1^2)\,\delta^{ij}, \end{array} \tag{4.16}$$

where our gauge choice implies

$$\partial_k B^k = 3\partial_0 \Psi_1 \tag{4.17}$$

$$\partial_0 B_k = \partial_k \chi_2, . \tag{4.18}$$

The PPN order of the metric perturbations is $\chi_1 \sim \Psi_1 \sim \mathcal{O}_{\rm PN}(1)$, $B_i \sim \mathcal{O}_{\rm PN}(1.5)$ and $\chi_2 \sim \mathcal{O}_{\rm PN}(2)$. The resulting expression for the Jordan frame metric to $\mathcal{O}_{\rm PN}(2)$ is given below in Eq. (4.45).

The Energy-Momentum Tensor

As remarked above, the energy-momentum tensor for matter must be defined in the Jordan frame and so one has

$$\tilde{T}^{\mu\nu}_{\rm m} = \rho_{\rm m}\left[1 + \frac{P_{\rm m}}{\rho_{\rm m}} + \Pi\right] u^\mu u^\nu + P_{\rm m}\tilde{g}^{\mu\nu}, \tag{4.19}$$

[2]Note that the symbol χ is often used to denote a quantity referred to as the *superpotential* in the literature [119]. We will not use the superpotential in this work and use χ to refer to perturbations of the 00-component of the metric.

We will ultimately want to change coordinates so that the lapse is unity, which we can do by setting $\mathrm{d}T = N\,\mathrm{d}t$, and so the velocity measured by an observer in the Jordan frame is

$$v^i = \frac{\mathrm{d}x^i}{\mathrm{d}T} = \frac{1}{N}\frac{\mathrm{d}x^i}{\mathrm{d}t}. \tag{4.20}$$

In this case we have

$$u^\mu = \frac{\mathrm{d}x^\mu}{\mathrm{d}\tau} = \gamma_{\text{Lorentz}}\left(1, Nv^i\right). \tag{4.21}$$

In this case, one can calculate γ_{Lorentz} using the normalisation condition $\tilde{g}_{\mu\nu}u^\mu u^\nu = -1$ to find

$$\gamma_{\text{Lorentz}} = \frac{1}{N}\left(1 + \frac{\chi_1}{N^2} + \frac{v^2}{2}\right) + \mathcal{O}_{\text{PN}}(2), \tag{4.22}$$

Using this, we can find the Jordan-frame energy-momentum tensor to 2PN:

$$\tilde{T}^{00}_{\text{m}} = \frac{\rho_{\text{m}}}{N^2}\left[1 + \Pi + v^2 + \frac{2\chi_1}{N^2}\right], \tag{4.23}$$

$$\tilde{T}^{0i}_{\text{m}} = \frac{\rho_{\text{m}}v^i}{N}, \tag{4.24}$$

$$\tilde{T}^{ij}_{\text{m}} = \rho_{\text{m}}v^iv^j + P_{\text{m}}\delta^{ij}. \tag{4.25}$$

We can then find the Einstein-frame energy-momentum tensor using equation (4.10). Note that $\sqrt{1 - 2X/\Lambda_{\text{disf}}{}^2} = 1 - \Upsilon/2 + \mathcal{O}_{\text{PN}}(1) = N + \mathcal{O}_{\text{PN}}(1)$. Then to 2PN, we simply have $T^{0i}_{\text{m}} = N\tilde{T}^{0i}_{\text{m}}$ and $T^{ij}_{\text{m}} = N\tilde{T}^{ij}_{\text{m}}$. $\tilde{T}^{00}_{\text{m}}$ contains both $\mathcal{O}_{\text{PN}}(1)$ and $\mathcal{O}_{\text{PN}}(2)$ terms. To 1PN we have $X = (1 - 2\chi_1)\dot{\phi}^2_{\text{CMB}}/2$ and hence

$$T^{00}_{\text{m}} = \frac{\rho_{\text{m}}}{N}\left[1 + \Pi + v^2 + \frac{2\chi_1}{N}\right]. \tag{4.26}$$

We will also need the lowered form of the energy-momentum tensor and the trace to 2PN,

$$T^{\text{m}}_{00} = \frac{\rho_{\text{m}}}{N}\left[1 + \Pi + v^2 - 2\chi_1 N\right], \tag{4.27}$$

$$T^{\text{m}}_{0i} = -T^{0i} = -\rho_{\text{m}}v^i \tag{4.28}$$

$$T^{\text{m}}_{ij} = T^{ij}_{\text{m}} = N[\rho_{\text{m}}v^iv^j + P_{\text{m}}\delta^{ij}] \tag{4.29}$$

$$T_{\text{m}} = -\frac{\rho_{\text{m}}}{N}\left[1 + \Pi + v^2 + \chi_1\Upsilon\right] + \rho_{\text{m}}v^2N \tag{4.30}$$

These are all the quantities that we need to compute the solution at 2PN. We will do this by solving the trace-reversed form of Einstein's equation,

$$R_{\mu\nu} = 8\pi G\left(T^{\text{tot}}_{\mu\nu} - \frac{1}{2}g_{\mu\nu}T^{\text{tot}}\right), \tag{4.31}$$

and the equation of motion (4.4) for ϕ to the appropriate order. Note that the contribution of the scalar field to the energy-momentum tensor contains terms proportional to $\dot{\phi}_{\text{CMB}}$ that

are unpaired with factors of ${\Lambda_{\rm disf}}^{-1}$, which we neglect. Compared to the matter variables and terms proportional to Υ and Σ, they are suppressed by the ratio of the dynamical time of the system (of order a year in the SS) to the Hubble time H^{-1} which is of order 10^{10} years.

4.1.3 Solution at 1PN

At 1PN the only quantities we need to calculate are χ_1, Ψ_1 and ϕ_1. We are working in the Einstein frame, where due to the absence of anisotropic stress we have $\chi_1 = \Psi_1$. The 00-component of (4.31) in the NR limit is

$$\nabla^2\chi_1 = \nabla^2\Psi_1 = -\frac{4\pi G\rho_{\rm tot}}{N}, \tag{4.32}$$

the solution of which is

$$\chi_1 = \Psi_1 = \frac{U}{N}. \tag{4.33}$$

Next, we need the field equation for ϕ_1, which is

$$\nabla^2\phi_1 = 8\pi G\,\Sigma\,\rho_{\rm m}, \tag{4.34}$$

which is solved by

$$\phi_1 = -2\Sigma U \tag{4.35}$$

to leading-order in Σ. These are all of the solutions at 1PN.

4.1.4 Solution at 2PN

At 2PN we need to find the metric potentials $\chi_2 \sim \mathcal{O}_{\rm PN}(2)$ and $B_i \sim \mathcal{O}_{\rm PN}(1.5)$ as well as the field ϕ_2. The following identities will be useful:

$$U_{,0i} = -\frac{N}{2}\nabla^2(V_i - W_i) \tag{4.36}$$

$$U_{,i}U^{,i} = \nabla^2\left(\frac{1}{2}U^2 - \Phi_2\right). \tag{4.37}$$

Note that these differ from their usual form in the literature [119] because we are working in a coordinate system with a non-trivial lapse. Specifically, for our Jordan-frame metric Eq. (4.8), the continuity equation becomes at lowest order

$$N^{-1}\dot{\rho}_{\rm m} + \partial_i(\rho_{\rm m}v^i) = 0\,. \tag{4.38}$$

The components R_{00} and R_{0i} of the Ricci tensor are given in many standard references (see [119] for example) but the calculation implicitly uses the 1PN solutions (4.33) and the identities (4.36) and (4.37) in the standard forms without the factors of N. The reader

attempting to reproduce the calculations in this subsection should bear this in mind and, in particular, calculate these components explicitly.

We begin with the vector B_i. The $0i$-component of (4.31) is

$$\frac{1}{2}\nabla^2 B_i + \frac{1}{2}\Psi_{1,0i} = 8\pi G \rho_{\rm tot} v_i. \tag{4.39}$$

Using the solution (4.33) and the identity (4.36), one finds

$$B_i = -\frac{7}{2}V_i - \frac{1}{2}W_i. \tag{4.40}$$

Next, we find χ_2 using the 00-component of (4.31), which gives

$$\chi_2 = -\frac{U^2}{N^2} + 2\Phi_1 + \frac{2}{N^3}\Phi_2 + \frac{1}{N}\Phi_3 + 3N\Phi_4. \tag{4.41}$$

Finally, we need the scalar to second order. Using the scalar's equation of motion (4.4), we find

$$\nabla^2\phi_2 = \ddot{\phi}_1 - \Sigma\left(8\nabla^2\Phi_2 + 2\nabla^2\Phi_3 + 2\nabla^2\Phi_1\right) \tag{4.42}$$

at $\mathcal{O}_{\rm PN}(2)$. The term proportional to $\ddot{\phi}_1$ can be dealt with by combining the gauge conditions (4.17) and (4.18) to find

$$\frac{3}{N}\ddot{U} = \nabla^2\chi_2. \tag{4.43}$$

Using this, one finds

$$\phi_2 = \Sigma\left(\frac{2}{3}U^2 - \frac{10}{3}\Phi_1 - \frac{28}{3}\Phi_2 - \frac{8}{3}\Phi_3 - 2\Phi_4\right). \tag{4.44}$$

These are all of the 2PN quantities.

4.1.5 The Jordan Frame Metric

Now that we have all of the metric potentials and field solutions, we can calculate the Jordan frame metric using (4.8). We continue to work to leading-order in Υ and Σ in what follows and we obtain

$$\tilde{g}_{00} = -N^2\left(1 - \frac{2\chi_1}{N^2} - \frac{2\chi_2}{N^2} - \frac{2\dot{\phi}_{\rm CMB}\dot{\phi}_1}{{\Lambda_{\rm disf}}^2}\right) + \mathcal{O}_{\rm PN}(3) \tag{4.45}$$

$$\tilde{g}_{0i} = B_i + \frac{\dot{\phi}_{\rm CMB}\phi_{1,i}}{{\Lambda_{\rm disf}}^2} + \frac{\dot{\phi}_{\rm CMB}\phi_{2,i}}{{\Lambda_{\rm disf}}^2} + \mathcal{O}_{\rm PN}(2.5) \tag{4.46}$$

$$\tilde{g}_{ij} = (1 + 2\Psi_1)\,\delta_{ij} + \mathcal{O}_{\rm PN}(2). \tag{4.47}$$

This result is clearly not in PPN form: the lapse is not unity, and the last term in $\tilde{g}_{00}$ is $\mathcal{O}_{\rm PN}(1.5)$. Also, there are $\mathcal{O}_{\rm PN}(1)$ and $\mathcal{O}_{\rm PN}(2)$ terms in the $0i$-component. We need to perform a gauge transformation to get this into the standard PPN gauge.

We begin by changing coordinates such that $\mathrm{d}T = N\,\mathrm{d}t$. This leaves the ij-components unchanged but the other components are

$$\tilde{g}_{TT} = -1 + \frac{2\chi_1}{N^2} + \frac{2\chi_2}{N^2} + \frac{2\dot{\phi}_{\rm CMB}\dot{\phi}_1}{{\Lambda_{\rm disf}}^2} \quad \text{and} \tag{4.48}$$

$$\tilde{g}_{Ti} = \frac{B_i}{N} + \frac{\dot{\phi}_{\rm CMB}\phi_{1,i}}{{\Lambda_{\rm disf}}^2} + \frac{\dot{\phi}_{\rm CMB}\phi_{2,i}}{{\Lambda_{\rm disf}}^2}\,, \tag{4.49}$$

thus eliminating the lapse.

Next, we need to perform a post-Newtonian gauge transformation $x^\mu \to \tilde{x}^\mu$ to bring this into the PPN gauge. This is a second-order transformation and so we write $\tilde{x}^\mu = x^\mu - \xi_1^\mu - \xi_2^\mu$, where ξ_n is $\mathcal{O}_{\rm PN}(n)$ in the PPN counting scheme. One must then expand the formula

$$\hat{g}_{\mu\nu}(\tilde{x}^\alpha) = \frac{\partial x^\sigma}{\partial \tilde{x}^\mu}\frac{\partial x^\lambda}{\partial \tilde{x}^\nu}\tilde{g}_{\sigma\lambda}(x^\alpha(\tilde{x}^\rho)), \tag{4.50}$$

where a hat denotes the new metric in the new coordinate system, to second order. The perturbations in the new gauge can be computed explicitly using the relations given in [31, 82, 113]. Note that since the new metric is written in terms of the new coordinates we do not need to expand the metric potentials separately.

The $\mathcal{O}_{\rm PN}(1.5)$ term in $\tilde{g}_{00}$ as well as the $\mathcal{O}_{\rm PN}(1)$ term in $\tilde{g}_{0i}$ can be removed by choosing

$$\xi_1^\mu = \frac{\dot{\phi}_{\rm CMB}\phi_1}{{\Lambda_{\rm disf}}^2}\left(1\,,\ \vec{0}\right)\,. \tag{4.51}$$

Note that in the transformation of the metric, ξ_1^μ always induces terms of order Υ. Since we work to linear order in that parameter, any terms $\mathcal{O}_{\rm PN}(\xi_1^2)$ can be neglected.

Finally, we can remove the $\mathcal{O}_{\rm PN}(2)$ term in $\tilde{g}_{0i}$ by performing a time shift at $\mathcal{O}_{\rm PN}(2)$,

$$\xi_2^T = \frac{\dot{\phi}_{\rm CMB}}{{\Lambda_{\rm disf}}^2}\left(2\phi_2 - 4\Sigma U^2\right)\,, \quad \xi_{2\,i} = 0\,. \tag{4.52}$$

Inserting the field solution, the metric then becomes

$$\tilde{g}_{00} = -1 + \frac{2U}{N^3} - \frac{2U^2}{N^4} + \frac{4\Phi_1}{N^2} + \frac{4\Phi_2}{N^5} + \frac{2\Phi_3}{N^3} + \frac{6\Phi_4}{N} + \mathcal{O}_{\rm PN}(3) \tag{4.53}$$

$$\tilde{g}_{0i} = -\frac{1}{N}\left[\frac{7}{2}V_i + \frac{1}{2}W_i\right] + \mathcal{O}_{\rm PN}(2.5) \tag{4.54}$$

$$\tilde{g}_{ij} = \left(1 + \frac{2U}{N}\right)\delta_{ij} + \mathcal{O}_{\rm PN}(2). \tag{4.55}$$

Comparing (4.53) with (3.1), we can see that the metric is still not in PPN form, since the coefficient of U in $\tilde{g}_{00}$ is not unity. The reason for this is that $G \equiv 1/8\pi M_{\rm pl}^2$ is not equal to the locally measured value of Newton's constant $G_{\rm N}$. We need to normalise the metric to PPN form and so we define

$$G_{\rm N} \equiv \frac{G}{N^3} = G\left[1 + \frac{3}{2}\Upsilon\right]. \tag{4.56}$$

This is the gravitational constant measured in the SS. Next, we rescale every metric potential so that $G_{\rm N}$ and not G appears in their definition. That is, U is now defined such that $\nabla^2 U = -4\pi G_{\rm N}\rho_{\rm tot}$. Doing this, we find

$$\tilde{g}_{00} = -1 + 2U + -2N^2U^2 + 4N\Phi_1 + 4N\Phi_2 + 2\Phi_3 + 6N^2\Phi_4 + \mathcal{O}_{\rm PN}(3) \tag{4.57}$$

$$\tilde{g}_{0i} = -\frac{7N^2}{2}V_i - \frac{N^2}{2}W_i + \mathcal{O}_{\rm PN}(2.5) \tag{4.58}$$

$$\tilde{g}_{ij} = \left(1 + 2N^2U\right)\delta_{ij} + \mathcal{O}_{\rm PN}(2). \tag{4.59}$$

This metric is in the proper PPN form in the CMB frame, where $w^i = 0$. Next, we proceed to transform it to the SS frame.

4.1.6 Lorentz Boost to SS Rest Frame

The Lorentz transformation described in Section 4.1.2 preserves the PN character of our metric since $w = \sqrt{w_i w^i}$ is the speed with respect to the CMB dipole and hence $w_i \sim 370$ km/s $\sim \mathcal{O}_{\rm PN}(0.5)$. An explicit treatment of the transformation has been well-documented (Sec. 4.3 in [119]) and our metric takes the form

$$\tilde{g}_{00} = -1 + 2U - 2N^2U^2 + 4N\Phi_1 + 4N\Phi_2 + 2\Phi_3 + 6N^2\Phi_4 + 3\Upsilon w^2 U + \Upsilon w^i w^j U_{ij} + 4\Upsilon w^i V_i, \tag{4.60}$$

$$\tilde{g}_{0i} = -\frac{7N^2}{2}V_i - \frac{N^2}{2}W_i + \Upsilon w_i U + \Upsilon w^j U_{ij}, \tag{4.61}$$

$$\tilde{g}_{ij} = \left(1 + 2N^2U\right)\delta_{ij}. \tag{4.62}$$

4.1.7 The PPN Parameters

We are finally in a position to extract the PPN parameters, which can be done by comparing the metric Eq. (4.60) with equations (3.1)–(3.3). We obtain the following non-vanishing PPN parameters:

$$\gamma_{\rm PPN} = \beta_{\rm PPN} = 1 - \Upsilon, \quad \alpha_1 = -4\Upsilon, \quad \text{and} \quad \alpha_2 = -\Upsilon. \tag{4.63}$$

The parameters $\gamma_{\rm PPN}$ and $\beta_{\rm PPN}$ are the PPN parameters that are commonly modified in scalar-tensor theories. α_1 and α_2 parametrize preferred-frame effects due to the motion of the SS relative to the cosmological background gradient $\dot{\phi}_{\rm CMB}$. Due to the relative motion of the SS with respect to the cosmological rest frame, it induces (apparent) preferred spatial directions locally. We will discuss some observable consequences of this below.

The preferred-frame parameter α_3 as well as the integral conservation-law parameters ζ_i on the other hand all vanish, as does the Whitehead parameter ξ. One may worry that this is true to leading-order in Υ and Σ only and that one should go to next-to-leading-order to derive their values. This is not the case. According to a theorem of Lee, Lightman and Ni [77], any diffeomorphism-invariant theory of gravity that can be derived from a Lagrangian

is at least semi-conservative, which implies that the above mentioned parameters are zero to all orders. Our theory falls into this class and so there is no need to go beyond leading-order. The Whitehead parameter is also zero to all orders since the Whitehead potential Φ_W does not appear in the solutions for the metric potentials or the field. Equation (4.63) constitutes the main result of this section.

In Appendix A we show that the disformal contributions are unchanged when considering the general conformal/disformal theory $C(\phi)$, $D(\phi)$. Specifically, $\gamma_{\rm PPN}$ independently constrains $\hat{\beta}_\phi \lesssim 10^{-3}$. [46] This reduces any interactions of conformal and disformal effects to negligible levels. The parameter values given in equation (4.63) then remain valid apart from a trivial rescaling $\Upsilon \to D^2(\phi_{\rm CMB})\Upsilon$. The parameters $\hat{\Delta}_\phi$ and $\hat{\Delta}'_\phi$ are only constrained very weakly ($\hat{\Delta}_\phi \lesssim 10^5$, $\hat{\Delta}'_\phi \lesssim 10^9$) through their contributions to the PPN parameter $\beta_{\rm PPN}$ (see Appendix A).

4.2 Constraints

4.2.1 A concrete model

We have seen above that only Υ and not Σ is constrained by SSs experiments. The strongest constraint comes from α_2, which is constrained to satisfy $|\alpha_2| < 4 \times 10^{-7}$ [89, 120] from limits on the Sun's spin precession, implying $|\Upsilon| < 4 \times 10^{-7}$ (we will discuss this constraint in Section 6.1). In order to investigate the implications for disformal gravity, we study a concrete representative of the disformal models considered in the cosmological context:

$$C(\phi) = e^{\hat{\beta}_\phi \phi}, \quad D(\phi) = e^{\hat{\Delta}_\phi(\phi - \phi_{\rm CMB})} \quad \text{and} \quad V(\phi) = m_0^2 e^{-\lambda\phi}. \tag{4.64}$$

Following the discussion above, we set the conformal coupling $\hat{\beta}_\phi = 0$ from here on. This is the model studied by [97] who found a dark energy dominated fixed point with

$$\dot{\phi}_{\rm CMB} = \lambda H_0 \quad \text{and} \quad \ddot{\phi}_{\rm CMB} = -\frac{\lambda^3 H_0^2}{2} \tag{4.65}$$

when $\lambda < \sqrt{6}$. Note that this implies $\Upsilon = -2\Sigma/\lambda$, which is consistent with our assumption that $\Upsilon \sim \Sigma$. Assuming that we are close to this fixed point today, the constraint becomes

$$\lambda^2 \left(\frac{H_0^2}{{\Lambda_{\rm disf}}^2} \right)^2 < 4 \times 10^{-7}. \tag{4.66}$$

The region in the $\Lambda_{\rm disf}/H_0$–λ plane where this is satisfied is shown below in figure 4.1. One can see that $\Lambda_{\rm disf}/H_0 \gtrsim 3 \times 10^3$ is required, which gives $\Lambda_{\rm disf} \gtrsim 10^{-30}$ eV. The disformal coupling is often stated in the form [23]

$$\frac{\mathcal{L}}{\sqrt{-g}} \supset \frac{T^{\mu\nu}_{\rm m} \partial_\mu\phi\partial_\nu\phi}{\mathcal{M}^4} \tag{4.67}$$

in the decoupling limit. In this case, one has the relation $\mathcal{M}^4 = M_{\rm pl}^2 {\Lambda_{\rm disf}}^2$ [96] and so our constraint translates into the bound $\mathcal{M} \gtrsim 10^2$ eV. Note that this is two orders-of-magnitude stronger than the previous bound using SS tests $\mathcal{M} \gtrsim \mathcal{O}(\text{eV})$ [96], which was found using an estimate of the Eddington light bending parameter $\gamma_{\rm PPN}$.

An independent constraint can be obtained from the time-variation of Newton's constant in the SS. Taking the time derivative of equation (4.56), we find

$$\frac{\dot{G}_{\rm N}}{G_{\rm N}} = \frac{3\dot{\Upsilon}}{2(1+\frac{3\Upsilon}{2})} \approx \frac{3\dot{\Upsilon}}{2}. \tag{4.68}$$

Lunar Laser Ranging (LLR) constrains this quantity to be less than 1.5×10^{-13} yr^{-1} [110], which gives

$$\frac{3}{2}\lambda\Upsilon\left(2\hat{\Delta}_\phi - \lambda\right) < 0.002, \tag{4.69}$$

where we have used equation (4.65). This allows us to constrain $\hat{\Delta}_\phi$ as a function of λ by simultaneously imposing the constraint (4.66). In figure 4.2 we plot the excluded region in the $\hat{\Delta}_\phi$–λ plane when Υ just satisfies the constraint (4.66) i.e. $\Upsilon = 4 \times 10^{-7}$. One can see that $\hat{\Delta}_\phi$ is relatively unconstrained and values as large as 10^3 are not excluded.

4.2.2 Cosmological Implications

In this section we will show that the constraint $\frac{\Lambda_{\rm disf}}{H_0} \gtrsim 3 \times 10^3$ implies that disformal effects are negligible in the context of the cosmological evolution. We begin by studying the expansion history described in the disformal model by the modified Friedmann equation in the Einstein frame [28]

$$H^2 = \frac{\rho_{\rm tot}}{3M_{\rm pl}^2}, \tag{4.70}$$

where[3]

$$\dot{\rho}_m = -3H\rho_m - \frac{QM_{\rm pl}\dot{\phi}}{\sqrt{2}}, \quad \rho_\phi = \frac{M_{\rm pl}^2}{2}\left(\frac{1}{2}\dot{\phi}^2 + m_0^2 e^{-\lambda\phi}\right) \quad \text{and} \tag{4.71}$$

$$\ddot{\phi} + 2H\dot{\phi} - \lambda m_0^2 e^{-\lambda\phi} = \frac{\sqrt{2}}{M_{\rm pl}}Q\,. \tag{4.72}$$

Note that we have coupled the field to all species of matter, unlike [28] who only couple ϕ to the CDM component. The disformal effects enter through the coupling Q given by

$$M_{\rm pl}Q = \frac{\rho_{\rm m}}{{\Lambda_{\rm disf}}^2}\frac{\frac{3}{\sqrt{2}}H\dot{\phi} - \frac{\lambda m_0^2}{\sqrt{2}}e^{-\lambda\phi} - \hat{\Delta}_\phi\dot{\phi}^2}{1 + \left(\rho_m - \frac{M_{\rm pl}^2}{2}\dot{\phi}^2\right)/({\Lambda_{\rm disf}}^2 M_{\rm pl}^2)} \lesssim 10^{-7}\,\rho_m \quad (z=0), \tag{4.73}$$

[3] Comparing the definitions of the actions, $\phi = \frac{\sqrt{2}}{M_{\rm pl}}\phi_{\rm ref}$ and $V = \frac{2}{M_{\rm pl}^2}V_{\rm ref}$, where $\phi_{\rm ref}, V_{\rm ref}$ are the corresponding quantities defined in [28]. Also, $D(\phi) = D^2/ldisf^2 M_{\rm pl}^2$ in our notation.

where we have defined $\phi_{\rm CMB}$ such that $D = 1$ and for the order-of-magnitude estimate at the epoch today, we have used $\rho_m \sim M_{\rm pl}^2 H_0^2$, $\dot{\phi} \sim H_0 \phi$, and $\Lambda_{\rm disf}/H_0 \gtrsim 3 \times 10^3$. Note that the 10^{-7} bound was found assuming that $\hat{\Delta}_\phi \sim \mathcal{O}_{\rm PN}(1)$, which is the theoretically natural value. This parameter is only weakly constrained by PPN measurements and we have found that it can be as large as $\mathcal{O}_{\rm PN}(10^3)$, in which case the bound above is weakened to $M_{\rm pl} Q \lesssim 10^{-4} \rho_m$. In fact, values of $\hat{\Delta}_\phi \gtrsim \mathcal{O}_{\rm PN}(1)$ lead to phantom universes and are hence strongly disfavoured [99]. It is then clear that the fractional modification to the background expansion Eq. (4.70) due to the disformal coupling is of order 10^{-7}–10^{-4} or less for models that satisfy SS constraints. This is much smaller than current and near future observational uncertainties [6].

We now turn to the growth of linear density perturbations, $\delta_m = \delta\rho_m/\rho_m$. The growth equation for δ_m has been derived in [28][4]:

$$\ddot{\delta}_m + \left(H - \frac{Q M_{\rm pl} \dot{\phi}}{\sqrt{2}\rho_m} \right) \dot{\delta}_m = \left(4\pi G + \frac{Q^2}{\rho_m^2} \right) \rho_m \delta_m \,. \tag{4.74}$$

This again reduces to the GR result if Q is set to zero. We then see that the fractional correction to the growth factor is constrained to be less than 10^{-7}–10^{-4} due to our by SS constraints. In fact, the effect will be smaller numerically, as the disformal coupling only becomes relevant at late times, when $\rho_{\rm de} \sim \rho_m$, so that the growth is modified by order Q only over the last Hubble time.

We see that for models satisfying the constraints from the SS derived in the previous section, in particular from α_2, the impact on all cosmological observables is highly suppressed. Finally, we point out that there are two ways to evade these constraints: first, one could add one of the well-known screening mechanisms to the scalar field action, i.e. the Chameleon or Vainshtein screening. Second, one could drop the weak equivalence principle and let the scalar field couple only to dark matter and not to baryons. In the latter case, the SS constraints do not apply as they were derived from baryonic objects.

4.3 Disformal screening (or lack thereof...)

it is worth examining the screening situation via a different route, by considering the fifth force $\mathbf{F}_5$. In particular, following the lines of [96], we examine the significance of the asymptotic spacetime (Minkowski v.s. FLRW) and the validity of assumptions made in [72], which claimed the existence of a novel disformal screening mechanism.

To do so, we shall examine the NR limit.

In the PPN formalism, the metric is asymptotically $\eta_{\mu\nu}$ by definition. We have shown that for a Minkowski background metric, the SS is not screened from disformal effects up to 2PN. This agrees with the finding in [96], where the e.o.m. of ϕ in the NR limit is

$$\nabla^2 \phi = 8\pi G \hat{\beta}_\phi \rho_{\rm m} + V(\phi)_{,\phi}. \tag{4.75}$$

[4]Note that [28] work in conformal time. We have translated their results into coordinate time.

We want ϕ to drive cosmic acceleration on large scales, hence $V_{,\phi} \ll G\rho_{\rm m}$. We also have the fifth-force (including PN terms)

$$\mathbf{F}_5 = -\left(1 - \frac{2D^2X}{{\Lambda_{\rm disf}}^2}\right)^{-1}\left[\hat{\beta}_\phi + \frac{D^2}{{\Lambda_{\rm disf}}^2}\left(\ddot{\phi} + (\hat{\Delta}_\phi - \hat{\beta}_\phi)\dot{\phi}^2\right)\right]\ \boldsymbol{\nabla}\phi, \tag{4.76}$$

which in the Newtonian limit reduces to $\mathbf{F}_5 \sim \hat{\beta}_\phi \boldsymbol{\nabla}\phi \sim \hat{\beta}_\phi^2 \boldsymbol{\nabla}\Phi_{\rm N} \sim \hat{\beta}_\phi^2 \mathbf{F}_{\rm N}$.This is identical to that of any ST theory with a scalar potential and conformal coupling only. In other words, only conformal screening mechanisms are relevant here and no novel disformal screening mechanism is possible.

While [72], also took the metric to be asymptotically $\eta_{\mu\nu}$, when applying the condition

$$\frac{C^2D^2\rho_{\rm m}}{{\Lambda_{\rm disf}}^2} \gg M_{\rm pl}^2 \tag{4.77}$$

to Eq. 4.4, inadvertently imposed instead the condition

$$\frac{C^2D^2\rho_{\rm m}}{{\Lambda_{\rm disf}}^2}\ \ddot{\phi} \gg M_{\rm pl}^2\,\nabla^2\phi, \tag{4.78}$$

which is not justified[96]. This removed the radial profile of ϕ when we should really get Eq. 4.75 in the NR limit.

In short, there is no disformal screening if spacetime is asymptotically Minkowskian.

Suppose that spacetime is instead asymptotically FLRW. In this case, there exists terms $\propto \dot{\phi}_{\rm CMB}$, $\ddot{\phi}_{\rm CMB}$, such that $\hat{\beta}_\phi \to Q$ in Eq. 4.75 and $\mathbf{F}_5 = -Q\boldsymbol{\nabla}\phi \sim Q^2\mathbf{F}_{\rm N}$. Notice that now, disformal contributions enter via Q in the form of Υ, Γ, i.e. cosmological dynamics source spatial gradients on small scales for an FLRW background. For a detailed derivation, please refer to [96].

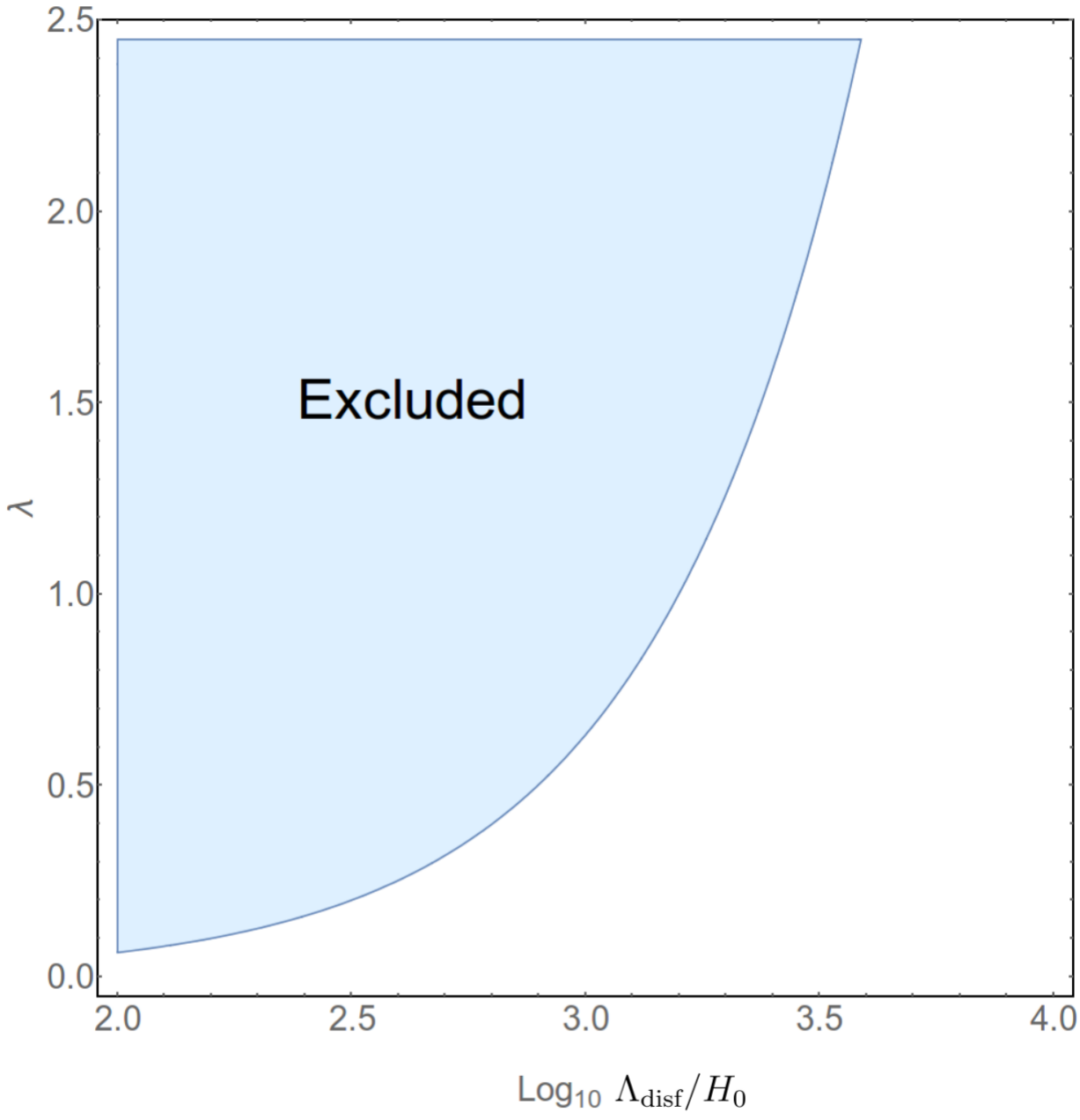

Figure 4.1: The region in the λ-$\log_{10}\Lambda_{\rm disf}/H_0$ plane where the constraint from measurements of α_2 is satisfied.[60]

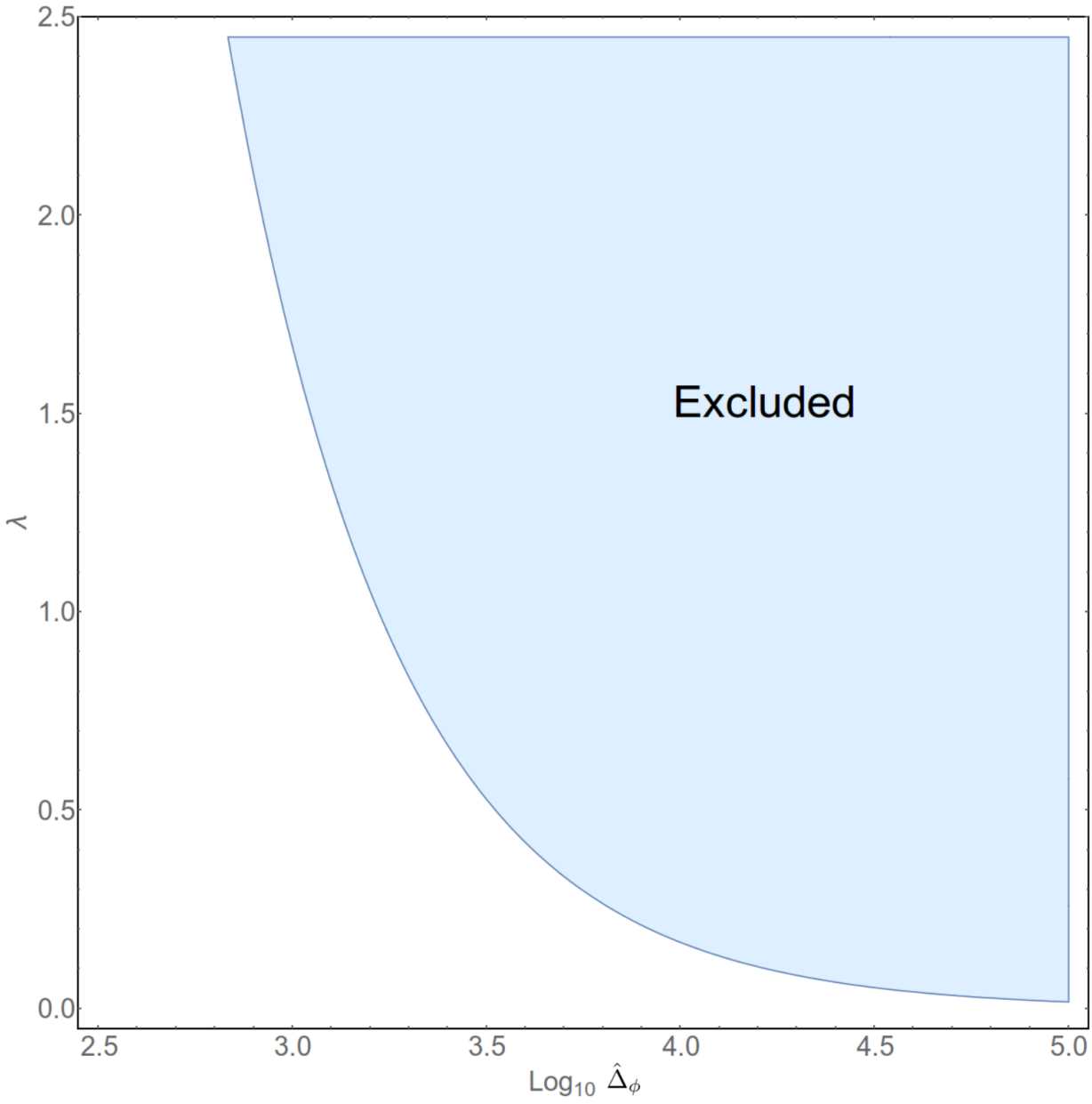

Figure 4.2: The region in the λ-$\log_{10}\hat{\Delta}_\phi$ plane where the constraint from LLR measurements of the time-variation of G are satisfied.[60]

Chapter 5

Quasistatic Approximation (QSA)

We have discussed ST theories, where we have introduced a relativistic scalar field, and the need for screening mechanisms, focusing on the chameleon and symmetron types as examples.

While we can effectively take into account relativistic effects for linear cosmological (early times/large-scales) perturbations of homogeneous spacetimes, using linear, relativistic Boltzmann codes, such as CAMB and CLASS, the linear approximation is no longer valid as we enter late times/small scales of gravitational evolution. As we enter the epoch of matter domination, matter perturbations grow with time and the gravitational collapse of matter must be described non-linearly (NL). Eventually of course, the whole perturbation approach breaks down, but we shall not concern ourselves with that here.

N-body simulations are often used to study NL LSS evolution but it is governed by Newtonian gravity, i.e. it is intrinsically NR. This therefore only applies when relativistic effects and species are negligible. On the other hand, implementing the full evolution equations in numerical simulations is horribly computationally expensive [26]. Appropriate compromises/approximations are therefore necessary.

Notice that when we studied screening mechanisms previously, we did so under the quasistatic (QS) approximation. This is really two separate assumptions combined as

$$|\dot{\mathcal{X}}| \sim \mathcal{H}|\mathcal{X}| \ll |\nabla_i \mathcal{X}|. \tag{5.1}$$

. We shall look at each condition separately : [105]

1. Time derivatives of metric and field perturbations are suppressed relative to their spatial derivatives. Explicitly, the perturbations evolve on Hubble time-scales, such that for a given gravitational field (metric or ϕ), $\mathcal{X}$,

$$|\dot{\mathcal{X}}| \lesssim \mathcal{H}|\mathcal{X}|. \tag{5.2}$$

   This (in natural units) corresponds to spatial gradients much smaller that those pertaining to the system concerned.
   Why should this apply to the scalar field? Technically, it could well evolve with

non-negligible time-derivatives, such as oscillating rapidly. However, there are model-specific constraints on such behavior for observationally-viable modified gravity models.
For the chameleon models, in order for the screening to work such that SS constraints are satisfied, we need $\dot{\phi}$ to effectively slow-roll, which translates to the suppression of time derivatives [106].
For symmetron models, however, due to the $\mathbb{Z}_2$ symmetry breaking in low-density regions, $V_{\rm eff}$ offers two possible vacuum states $\phi^{\pm}_{\rm min}$, resulting in different regions (cells) of space where ϕ has chosen different vacua, $\phi^{\pm}_{\rm min}$. The smooth transition region between these cells is called a domain wall, which can spontaneously âĂİcollapseâĂİ when one cell flips its vacuum state to conform to its neighbour to obtain an overall more energetically-favourable configuration. The release of energy takes the form of scalar waves that could oscillate quickly. In fact, symmetron waves have been found in cosmological simulations when one relaxes the QSA [81].

2. The sub-horizon approximation, $k^2 \gg \mathcal{H}^2$, such that

$$\mathcal{H}^2\mathcal{X} \ll |\nabla^2\mathcal{X}|. \tag{5.3}$$

This allows us to justify ignoring the slow evolution of the inhomogeneous part of ϕ, in addition to any high-frequency oscillations in the metric perturbations. Without specifying the model, this is only justifiable on sub-horizon scales, where the background (large-scale) field is essentially homogeneous.

While for ΛCDM models, the $X_{,(I)}$ evolves on Hubble/expansion time-scales. This means that $k \ll \mathcal{H}$ automatically implies $|\dot{\mathcal{X}}| \lesssim \mathcal{H}|\mathcal{X}| \ll |\nabla_i\mathcal{X}|$, this implication does not hold for a general MG theory.

A particular conseqence of the QSA is that it prohibits wave propagation. More precisely, the dynamical Klein-Gordon equation with a source, which describes the evolution of a relativistic scalar field, ϕ, in some background potential, V, reduces to an elliptic Poisson-type equation.

$$\Box\phi = -V_{\rm eff,\phi}, \quad \text{where } \Box \equiv g^{\mu\nu}\nabla_\mu\nabla_\nu. \tag{5.4}$$

becomes

$$\boldsymbol{\nabla}^2\phi = V_{\rm eff,\phi}, \quad \text{for } a(t) \approx 1. \tag{5.5}$$

Until recently, screening mechanisms have been studied under the QSA. We have mentioned above that the QSA is not a hard and fast rule for all ST theories. It therefore behoves us to investigate what happens when we drop the QSA.

5.1 QSA and screening in ST theories

Llinaries and Mota [81] went beyond the QSA and found scalar waves in non-QS cosmological simulations for the symmetron model. These appear because, at a certain cosmological

epoch, the field enters a symmetry-breaking phase. This leads to large domains where the field is in different vacua, which can then rapidly transition as they come into contact. Together with Hagala [51], they further numerically studied how a *spherical incoming wave* of the symmetron field centred on the MW halo affects the screening of the SS, which is dominated by the halo's potential well. Astrophysical and cosmological sources for such waves were suggested. They concluded that the amplitude of the fifth force and $|\gamma_{\rm PPN} - 1|$ can consequently increase by several orders of magnitude, potentially reaching $> 10^{-5}$. In other words, they concluded that screening can be significantly disrupted by scalar radiation, causing previously viable models to violate current bounds. Such effects could in principle be relevant for any modified gravity theories with extra degrees of freedom with wave-type equations of motion. Potential sources of this scalar radiation include the Mpc-scale waves generated in the process of structure formation in the case of the symmetron model, as found by [81]. Specifically, they found a peak amplitude of waves (at $a \approx 0.4$, where a is the cosmological scale factor) corresponding to a fractional field perturbation of $\delta\phi/\phi \sim 0.03$, although typical wave amplitudes are significantly smaller. Further, in both symmetron and chameleon models, any unscreened astrophysical object that collapses to form a screened object has to radiate away its scalar charge. This in particular includes the collapse of massive stars to neutron stars or black holes (which we will hereafter refer to as Supernovae). In this case, assuming that the scalar field couples with approximately gravitational strength, the wave amplitude can be estimated to be of order $\phi \sim \Phi_\star R_\star / r$, where $\Phi_\star$ is the surface gravitational potential of the star and $R_\star$ is the stellar radius (both before collapse), and r is the distance to the source. Note that only sources in unscreened regions are relevant, since otherwise the star does not carry scalar charge even before collapse. This means that the sources considered here are outside of the screened part of the MW halo, so that $r \gtrsim 100$ kpc.

In this chapter, we shall obtain analytical solutions for the influence of spherical as well as planar incoming waves, in order to obtain better physical insight into this scenario. We linearise the system and consider a tophat halo in order to obtain closed-form solutions. While linear theory breaks down for incoming waves of very large amplitudes, we can nonetheless gain physical insight. In particular, purely geometrical effects are expected to qualitatively hold for larger wave amplitudes as well. We expect planar waves to be generally the most physically relevant wave configuration. Clearly, given the large distance compared to the source size, the planar-wave assumption should be very accurate for astrophysical events. For symmetron waves of cosmological origin, this is less clear, as they are produced throughout the Universe and we are not necessarily in the far-field limit. Nevertheless, it seems reasonable to expect that the cosmological symmetron radiation field can be represented as a superposition of plane waves with random wavevectors and phases. We will mostly consider the spherical case in order to make the connection to the setup considered in [51]. This case corresponds to a spherical shell of emitters centred on the MW halo with a *single coherent phase*.

Table 5.1: Physical quantities in Chapter 5.

Symbol	Definition	Value
	Global quantities:	
$g_{\nu\mu}$	Einstein frame (geometric) metric	
$\tilde{g}_{\nu\mu}$	Jordan frame (physical) metric, $\tilde{g}_{\nu\mu} = C^2(\phi) g_{\nu\mu}$	
R	Ricci scalar	
$\mathcal{L}_m$	Lagrangian for matter fields ψ	
h	Dimensionless Hubble parameter (today), $\frac{H_0}{100 \text{ km s}^{-1}}$	0.67 [4]
M_{pl}	Reduced Planck mass, $\sqrt{1/8\pi G}$	2×10^{18} GeV/c^2
$\rho(x)$	Total matter density	
ρ_c	Critical density of the universe	$9.5 \times 10^{-27}\,\text{kg}\,\text{m}^{-3}$
$\rho_m := \Omega_m \rho_c$	Background matter density of the universe	$2.6 \times 10^{-27}\,\text{kg}\,\text{m}^{-3}$
a	Expansion factor of the universe	1 today
H	Hubble parameter	
γ_{PPN}	PPN parameter measuring the space-curvature produced by a unit rest mass [121], tracked by the Cassini probe.	$\lvert\gamma_{\text{PPN}} - 1\rvert < 2 \times 10^{-5}$ [16]
$\Delta_{\lvert\gamma_{\text{PPN}}-1\rvert}$	Fractional deviation of the PPN parameter from the QS case: $\lvert\lvert\gamma_{\text{PPN}} - 1\rvert_{\text{non-QS}} - \lvert\gamma_{\text{PPN}} - 1\rvert_{\text{QS}}\rvert / \lvert\gamma_{\text{PPN}} - 1\rvert_{\text{QS}}$	
P_L	Legendre polynomial of order L	
j_L	Spherical Bessel function of order L	
	Halo parameters:	
R_h	MW halo's virial radius taken to be the tophat halo radius	200 kpc
r_{SS}	Radial distance of the SS from the center of the MW halo	8 kpc
$\rho_h = 200\rho_c$	Average interior density of the MW halo, obtained from virial mass and radius	$1.9 \times 10^{-24}\,\text{kg}\,\text{m}^{-3}$
M_h	Mass of the MW halo	$8.4 \times 10^{11} M_\odot$
Φ_{in}	Gravitational potential inside the halo	$\frac{GM_h(3R_h^2 - r^2)}{2R_h^3}$

Unfortunately, we will generally find a very small impact of scalar waves on the SS, even when considering wave amplitudes at the upper limit of what is physically expected.

Table 9.1 lists the notation and quantities used throughout the paper. Table 5.2 lists the quantities, including their definitions, notations and adopted values, for the symmetron model, while Table 5.3 lists those for the chameleon model.

5.2 Non-QS symmetron

We shall consider a tophat Milky Way halo (MWh) subjected to spherical and planar incoming waves. We do so by linearising the Klein-Gordon equation, including potential, in the time-dependent perturbation $\delta\phi$. This yields a linear Klein-Gordon equation with an effective mass that depends on radius. In the case of the tophat halo, the mass is given by a step function, assuming its cosmological value outside of the halo, and a larger value inside.

The symmetron model is a special case of the general ST action for canonical scalar fields,

$$S = \int d^4x\sqrt{-g}\left[\frac{M_{\rm pl}^2}{2}R - \frac{1}{2}g^{\nu\mu}\partial_\mu\phi\partial_\nu\phi - V(\phi)\right] + \int d^4x\sqrt{-\tilde{g}}\mathcal{L}_m(\psi,\tilde{g}_{\nu\mu})\,, \tag{5.6}$$

where ψ denotes the matter fields and $\tilde{g}_{\nu\mu}$ is the Jordan-frame metric. In the symmetron case, the latter is given by

$$\tilde{g}_{\nu\mu} = C^2(\phi)g_{\nu\mu}, \quad C(\phi) = 1 + \frac{\phi^2}{2M^2} + \mathcal{O}\left(\frac{\phi^4}{M^4}\right) \tag{5.7}$$

and the quartic Symmetron potential is

$$V(\phi) = -\frac{1}{2}\mu^2\phi^2 + \frac{1}{4}\lambda\phi^4 + V_0, \tag{5.8}$$

with μ, λ, V_0 being free parameters. Our adopted values are defined in Table 5.2.

Table 5.2: Symmetron-related quantities in Sections 5.2 and 5.3.

Symbol	Definition	Value
$\lambda_{\rm vac}$	Symmetron range in vacuum	0.37 Mpc [51]
μ	Mass scale defined via $V(\phi)$, $1/(\sqrt{2}\lambda_{\rm vac})$	$1.9\,{\rm Mpc}^{-1}$
M	Mass scale defined in $C(\phi) = 1 + \frac{\phi^2}{2M^2} + \mathcal{O}\left(\frac{\phi^4}{M^4}\right)$	8.2×10^{14} GeV
$\phi_{\rm vac}$	Vacuum expectation value of ϕ with the symmetron coupling constant set to 1, given by $\mu/\sqrt{\lambda}$, which $\approx M^2/M_{\rm pl}$	2.8×10^{11} GeV
$\beta_{\rm sym}$	$:= \phi_{\rm vac}M_{pl}/M^2$, Dimensionless symmetron coupling constant. It measures the strength of scalar force in vacuum relative to gravity, such that $F_\phi = 2\beta_{\rm sym}^2 F_{\rm N}$. In order that $F_\phi \sim F_{\rm N}$, we we need $\phi_{\rm vac}/M^2 \sim 1/M_{\rm pl}$. Note that this is not β_ϕ applied to the symmetron model.	1 [51]
$a_{\rm SSB}$	Expansion factor at the time of spontaneous symmetry breaking, such that $\rho_m\vert_{a=1}\,{a_{\rm SSB}}^{-3} = M^2\mu^2$[49]	0.5[51]

$\phi_{\rm QS}(r)$	Background scalar field under QSA	
$\delta\phi(\vec{x},t)$	Time-dependent field perturbation, without QSA	
$m_{\rm eff,in}$	Effective mass of the field inside the halo	$16\ {\rm Mpc}^{-1}$
$r_{\rm BC}$	Edge of the simulation in [51]	$6.0\,{\rm Mpc}$
A	Dimensionless wave amplitude defined at $r_{\rm BC}$	0.01 [51]
$\mathcal{A}$	Wave amplitude, $A\phi_{\rm vac}$	$2.8\times10^9\,{\rm GeV}$
w	Frequency of incoming wave	$40\,{\rm Myr}^{-1}$
k	Wavenumber of incoming wave, w/v_p	$1.3\times10^2\ {\rm Mpc}^{-1}$
v_p	Phase velocity of incoming wave	$\sqrt{1+m_{\rm eff}^2/k^2}$ [80]

The Einstein-frame metric, for negligible backreaction of ϕ on the metric which applies in the weak gravity case, is

$$ds^2=-(1+2\Psi)dt^2+(1-2\Psi)a^2(t)d\vec{x}^2. \tag{5.9}$$

At this order, $\Psi=\tilde{\Psi}$, where $\tilde{\Psi}$ is the Jordan-frame gravitational potential.

We direct the reader to the discussion on the relevant definition of $\gamma_{\rm PPN}$ in Section 3.1.1. The definition adopted by [51] is really applicable to the smooth spherically symmetric density profile of the halo and is given by

$$\gamma_{\rm PPN}-1\Big|_{\rm halo}=-\frac{\phi^2}{M^2}\frac{2}{\frac{\phi^2}{M^2}+2\Psi\left(1+\frac{\phi^2}{M^2}\right)}\,. \tag{5.10}$$

However, we have argued in Section 3.1.1 that the more relevant definition of $\gamma_{\rm PPN}$ should pertain to perturbations generated in the metric by a test mass embedded in the halo, i.e. the Sun. In this case, we have

$$\gamma_{\rm PPN}-1\Big|_{\rm SS}=-\frac{4\beta_{\rm sym}^2(\phi/\phi_{\rm vac})^2}{1+8\beta_{\rm sym}^2(\phi/\phi_{\rm vac})^2}\approx-4\beta_{\rm sym}^2\left(\frac{\phi}{\phi_{\rm vac}}\right)^2\,. \tag{5.11}$$

In order to compare with the analysis of [51], we will present results for both definition of $\gamma_{\rm PPN}$ in this paper. Of course, the underlying field solution is the same. Moreover, our main conclusions hold for both choices of $\gamma_{\rm PPN}$. We will find that the fractional difference in $\Delta_{|\gamma_{\rm PPN}-1|}$ is small ($\lesssim0.1$) inside the halo, with the major deviations located towards the edge of the halo, far from $r_{\rm SS}$. The apparent discrepancy in applying the PPN framework formulated in the quasi-static limit to a setup with a propagating plane wave perturbation dissipates when one realizes that the PPN formulism really only assumes that the SS metric is stationary (not even static, as there can be a nonzero $0i$ component). The SS, dominated by the Sun, is indeed spherically-symmetric and non-relativistic. It is embedded in a large-scale scalar-field background on which the wave perturbation exists. Throughout, we take the wavelength of the propagating wave to be much longer than the time scales pertaining to the SS that are on the order of years.

The equation of motion of the symmetron field ϕ, in the absence of the QSA, is the Klein-Gordon equation,

$$\Box\phi \approx \ddot{\phi} - \nabla^2\phi = -V_{\text{eff},\phi}, \quad \text{where } V_{\text{eff}}(\phi) = V(\phi) + [C(\phi) - 1]\,\rho, \tag{5.12}$$

and $\Box$ is the D'Alembertian, a dot denotes a partial derivative with respect to cosmic time t, and ρ is the matter density; more precisely, the field is sourced by the trace of the stress-energy tensor, but we assume pressureless matter throughout. In the second equality we have again assumed the weak-gravity and subhorizon regime. Here and throughout, we assume the subhorizon regime today, so that we can neglect H relative to ∂_t and ∂_x, and can set $a = 1$ for the scale factor. We now make the following ansatz for the field:

$$\phi(\vec{x}, t) = \phi_{\text{QS}}(r) + \delta\phi(\vec{x}, t)\,, \tag{5.13}$$

where $\phi_{\text{QS}}(r)$ is the spherically symmetric static background, and $\delta\phi$ is the wave perturbation. At zeroth and linear order in $\delta\phi$, this yields, respectively,

$$\nabla^2\phi_{\text{QS}} = V_{\text{eff},\phi}(\phi_{\text{QS}}) \tag{5.14}$$

$$\partial_t^2\delta\phi - \nabla^2\delta\phi = -\,m^2_{\text{eff,in}}(\phi_{\text{QS}})\delta\phi, \quad \text{where} \tag{5.15}$$

$$m^2_{\text{eff,in}}(\phi_{\text{QS}}) = V_{\text{eff},\phi\phi}(\phi_{\text{QS}}) = \frac{1}{2\lambda^2_{\text{vac}}}\left(\frac{3\phi^2_{\text{QS}}}{\phi^2_{\text{vac}}} - 1\right) + \frac{\rho}{M^2}\,. \tag{5.16}$$

We shall take $m_{\text{eff,out}}(\phi_{\text{QS}}) \approx 0$ outside the halo, assuming that the sources are within the Compton length of the field in the background. This is conservative, since including the background mass would further dampen in the waves. Inside the halo, $\left(\frac{\phi_{\text{QS}}}{\phi_{\text{vac}}}\right)^2 \ll 1$[1], such that $m^2_{\text{eff,in}} \approx \frac{1}{2\lambda^2_{\text{vac}}}\left(\frac{a^3_{\text{SSB}}\rho_h}{\rho_m} - 1\right)$, where we have introduced the expansion factor at the time of spontaneous symmetry breaking, a_{SSB}. This yields $m_{\text{eff,in}} \approx 16\text{Mpc}^{-1}$.

The incoming waves enter as boundary conditions. A planar incoming wave can be expressed as a sum of spherical waves by the plane wave expansion:

$$\delta\phi(r_{\text{BC}}, t) = \text{Re}\left[\mathcal{A}\,\text{e}^{i(\vec{k}\cdot\vec{r}_{\text{BC}} - wt)}\right] = \text{Re}\left[\mathcal{A}\,e^{-iwt}\sum_{L=0}^{\infty}(2L+1)i^L j_L(k\,r_{\text{BC}})P_L(\cos\theta)\right]. \tag{5.17}$$

We choose the wavevector to be along the z-axis, $\vec{k} = (0, 0, k)$. A spherical incoming wave is the special case of angular independence, such that $L = 0$,

$$\delta\phi(r_{\text{BC}}, t) = \mathcal{A}\sin(wt). \tag{5.18}$$

[1] While in real life, the halo's edge is not a step function, note that we are considering models for which the SS is screened in the quasi-static case, such that the thin-shell condition is satisfied. We are considering perturbations with wavelengths much greater than the thickness of the thin-shell, hence the progation of waves is not expected to be significantly modified by the precise field profile within the thin shell. In fact, even if the wavelength of the perturbation is to be comparable to the thin-shell's thickness, there would not be extra focusing effects on the wave.

5.3 Symmetron solution for the different types of incoming waves

Under the approximations explained above, the system can now be solved straightforwardly by continuously matching the spherical-wave expansions of the Klein-Gordon solutions for $m_{\text{eff,out}} = 0$ and $m_{\text{eff,in}}$, respectively. For the incoming plane wave, we obtain

$$\delta\phi = \text{Re}\left[\mathcal{A}e^{-iwt}\sum_{L=0}^{\infty}(2L+1)i^L\frac{j_L(kR_h)}{j_L(\sqrt{k^2-m_{\text{eff,in}}^2}R_h)}\,j_L(\sqrt{k^2-m_{\text{eff,in}}^2}\,r)P_L(\cos\theta)\right]. \tag{5.19}$$

This result includes all linear optics effects such as refraction (diffraction is not relevant, as there are no barriers involved). Indeed, one expects refraction effects as the wave enters the halo due to the change in its phase velocity, $v_p = c\sqrt{1+\frac{m_{\text{eff,in}}^2}{k^2}} > c$ [80]. This means that the ratio of refractive indices $\frac{n_{\text{out}}}{n_{\text{in}}} > 1$, resulting in convex wave fronts w.r.t. the halo center, as illustrated in Fig. 5.1. That is, the plane wave fronts are deformed to deviate even further from a spherical incoming wave. Our treatment does not include gravitational lensing. However, lensing effects are extremely small for sources at a distance of a few Mpc as considered here.

Figure 5.2 shows the natural logarithm of the fractional correction to the PPN γ_{PPN} parameter, i.e.

$$\ln\Delta_{|\gamma_{\text{PPN}}-1|} = \ln\left|\frac{|\gamma_{\text{PPN}}-1|_{\text{non-QS}} - |\gamma_{\text{PPN}}-1|_{\text{QS}}}{|\gamma_{\text{PPN}}-1|_{\text{QS}}}\right|, \tag{5.20}$$

for planar incoming wave in the symmetron model. Here t is set to 0, and we take the real part of the solution, as written in Eq. (5.19). The wave fronts inside the halo are convex with respect to the halo center, echoing the form predicted in Figure 5.1. Clearly, the field perturbation is not spherically symmetric around the halo center.

Quantitatively, when inserting the values used in [51], a fractional wave incoming wave amplitude $\delta\phi/\phi_{\text{QS}} = 0.01$ and $r_{\text{BC}} = 6$ Mpc (although this value is irrelevant for the plane wave), we obtain $\frac{\delta\phi}{\phi_{\text{QS}}}\big|_{r_{\text{SS}}} \sim 4$ at the SS radius. This implies that the deviation of the PPN parameter $|\gamma-1|$ is amplified by a factor of $\left(\frac{\delta\phi}{\phi_{\text{QS}}}\right)^2 \sim 16$ times over the QS value $|\gamma-1|_{\text{QS}}(r_{\text{SS}})$. This amplification holds regardless of which definition of the PPN parameter is used [Eq. (5.10) or Eq. (5.11)]. For reference, using Eq. (5.10), we approximately have $|\gamma-1|_{\text{QS}}(r_{\text{SS}}) \sim 10^{-6}$ for the tophat halo. Note that the mass distribution within the halo affects the gravitational potential at r_{SS} via the associated gravitational potential at that point, and hence affects the PPN parameter. For an NFW profile [86], we obtain $|\gamma-1|_{\text{QS}}(r_{\text{SS}}) \sim 7\times10^{-8}$, in good agreement with [51], which is smaller than in the tophat case due to the higher density in the inner regions. Clearly, the enhancement of $|\gamma-1|$ should not be taken as a literal estimate, since our linear perturbative treatment formally breaks down when $\delta\phi/\phi_{\text{QS}}$ becomes of order unity. Moreover, a tophat density profile is

clearly not realistic. A fractional wave amplitude of 0.01 is near the upper end of the range expected from waves generated during structure formation in symmetron models. Llinares and Mota [81] found that for their particular given model parameters and at some locations within the simulation box, cosmologically generated scalar waves can be such that these amplitudes are reached at today's epoch ($a = 1$). All these caveats notwithstanding, we see that the wave amplitude adopted in [51] does not lead to a violation of the Cassini bound when the field configuration is a plane wave.

It is instructive to compare these results to the case of a spherical incoming wave, in which case the solution reads

$$\delta\phi = \mathcal{A}\, r_{\rm BC} \sin wt \frac{\sin(k\, R_h)\sin(\sqrt{k^2 - m^2_{\rm eff,in}}\, r)}{\sin(k\, r_{\rm BC})\sin(\sqrt{k^2 - m^2_{\rm eff,in}}\, R_h)} \cdot \frac{1}{r}. \tag{5.21}$$

This is the setup studied numerically in [51]. Note the dependence of the spherical solution on the combination $\mathcal{A} r_{\rm BC}$, which follows from energy conservation. A coherent spherical incoming wave leads to a strong focusing effect around the origin (in this case, the center of the halo). This is in contrast with the planar case, where the plane wave (with negligible $m_{\rm eff,\,out}$) propagates freely outside the halo.

In our linear analysis, assuming a tophat halo and at a time t that maximizes the disruption (i.e. $\sin wt = 1$), we have $\frac{\delta\phi}{\phi_{\rm QS}} \sim 5 \times 10^3$, that is, an enhancement close to three orders of magnitude larger than in the plane-wave case. Correspondingly, we formally obtain a strong violation of the Cassini bound on $|\gamma - 1|(r_{\rm SS})$. The physical reason for the discrepancy is the focusing effect on the spherical wave's amplitude induced by energy conservation as $r \to 0$. This is again explicitly illustrated in the analytical solution for the spherical wave by its dependence on $\mathcal{A} r_{\rm BC}$.

The spherical incoming wave is the setup studied fully NL in [51] using a 1D simulation. The authors found for the same parameters that, while the enhancement is not as large as formally obtained using the linearised solution, $|\gamma_{\rm PPN}(r_{\rm SS}) - 1|$ can take values $> 10^{-5}$, breaching the Cassini bound. Again, for the same incoming wave parameters, and changing only the wave configuration, we find that at $r_{\rm SS}$, the perturbation in the planar case is smaller by a factor $\sim 10^{-3}$ compared to the spherical case. This is a geometrical consequence and applies also to cases where the linear treatment breaks down. We thus expect that a fully NL solution of the planar incoming wave will not yield a large effect on the screening in the SS.

5.4 Non-QS chameleon

The chameleon model is another special case of the canonical scalar-tensor theory in Eq. (5.6), where now the functions $C(\phi)$ and $V(\phi)$ are chosen to be

$$C(\phi) = e^{\frac{\beta_\phi \phi}{M_{\rm pl}}}, \quad V(\phi) = \frac{M^{4+n}}{\phi^n}, \quad \text{where we shall focus on } n = 1. \tag{5.22}$$

Our adopted values are defined in Table 5.3. The resulting field equation is then

$$\Box\phi = V_{\text{eff},\phi} := -\frac{M^5}{\phi^2} + \frac{\beta_\phi}{M_{\text{pl}}}\rho\, e^{\frac{\beta_\phi\phi}{M_{\text{pl}}}}. \tag{5.23}$$

In chameleon models, there is no symmetry breaking, and the field adiabatically follows its equilibrium position in the regime of large-scale structure. Hence, one does not expect large-scale waves of cosmological origin. Nevertheless, astrophysical sources of scalar waves such as Supernovae exist in these models. We will thus only consider the plane-wave case here. If the halo is screened, the QS solution far inside the screening radius satisfies $V_{\text{eff},\phi}(\phi_{\text{QS}}) = 0$ [92], which we will assume here. It is worth emphasizing that all considerations in this section also apply to $f(R)$ gravity [36, 108].

Table 5.3: Chameleon-related quantities in Section 5.4.

Symbol	Definition	Value
	Model parameters and quantities:	
β_ϕ	Dimensionless coupling constant	1
M	Mass scale with units of mass, defined via $V(\phi)$	2 meV [33]
$m_{\text{eff,in}}$	Effective field mass inside tophat halo at ϕ_{QS}.	$1.5 \times 10^{-30}\,\text{GeV}/c^2 \approx 2\times10^8\,\text{Mpc}^{-1}$
m_{SS}	Effective field mass of the scalar field in the SS. This is to be distinguished from $m_{\text{eff,in}}$ defined above.	$> m_{\text{eff,in}}$
$V(\phi)$	Bare potential	$M^5\phi^{-1}$
$V_{\text{eff}}(\phi)$	Effective potential, $V(\phi) + \rho\, e^{\beta_\phi\phi/M_{\text{pl}}}$	
ϕ_{QS}	Static field value minimizing V_{eff} inside the halo: $\sqrt{M^5 M_{\text{pl}}/(\beta_\phi\rho_h)}$. Valid for $r \in (0, R_{\text{roll}})$. [92]	3.1 GeV
ϕ_c	Field at cosmic mean density: $\sqrt{M^5 M_{\text{pl}}/(\beta_\phi\rho_c)}$	44 GeV
r_{sys}	Scale of the experiment or observation constraining $\lvert\gamma-1\rvert$. For Cassini, r_{sys} is the distance from Saturn to Earth on the other side of the Sun.	$\sim$ 11AU.

The linearized system then takes the same form as Eq. (5.15) with a different m^2_{eff}, such that $m^2_{\text{eff,out}} \approx 0$ outside the halo while inside,

$$m^2_{\text{eff,in}} \equiv m^2_{\text{eff}}(\phi_{\text{QS}})\,; \quad m^2_{\text{eff}}(\phi) = V_{\text{eff},\phi\phi}(\phi)\,. \tag{5.24}$$

Far inside the screening radius, the solution is consequently the same as Eq. (5.19),

$$\delta\phi = \mathrm{Re}\left[\mathcal{A}e^{-iwt}\sum_{L=0}^{\infty}(2L+1)i^L\frac{j_L(k\,R_h)}{j_L(\sqrt{k^2-m_{\mathrm{eff,in}}^2}\,R_h)}\,j_L(\sqrt{k^2-m_{\mathrm{eff,in}}^2}\,r)P_L(\cos\theta)\right]. \tag{5.25}$$

Here we have assumed that the incoming scalar field jumps from being massless to acquiring an effective mass of $m_{\mathrm{eff,in}}$ instantaneously at R_h, as in the symmetron case, neglecting the thin shell of the halo. This is sufficient given our simplified setup. Treating the Sun as a test mass, the SS γ_{PPN} parameter analogous to Eq. (5.11) is

$$\gamma_{\mathrm{PPN}}-1\Big|_{\mathrm{SS}} = -\frac{4\beta_\phi^2}{2\beta_\phi^2+e^{m_{\mathrm{SS}}r_{\mathrm{sys}}}}, \tag{5.26}$$

where r_{sys} is the scale of the experiment or observation constraining $|\gamma-1|$, and $m_{\mathrm{SS}} = m_{\mathrm{eff}}(\phi[r_{\mathrm{SS}}])$ is the mass of the large-scale field at the Solar System location, that is, in the absence of the Sun. We have used the expressions derived by [91] for massive Brans-Dicke theories, c.f. Section 2.2. We see that, if $m_{\mathrm{SS}} \gg 1/r_{\mathrm{sys}}$, the modification to the PPN γ parameter is exponentially damped.

Recall that our aim is to study the effect of a long-wavelength perturbation on the screening in the SS, which is quantified by the suppression of $\gamma-1$. For chameleon models, the incoming scalar wave, as well as the large-scale scalar field background in which the SS is embedded, thus enter through their modification of m_{SS}. Eq. (5.26) assumes that the Sun would not be screened by itself, i.e. if it were embedded in the cosmic mean density rather than the halo. If the Sun is screened, then $\gamma-1$ is further suppressed by the thin-shell factor $\delta M/M$. However, in that case we expect a negligible effect of any incoming scalar waves on the screening, since they would have to significantly modify the thin shell of the Sun. Thus, we will proceed with the assumption that the Sun is a test mass which does not screen the field by itself, for which Eq. (5.26) holds. We reiterate that Eq. (5.26) pertains in chameleon models regardless of the shape of the incoming field perturbation, as long as its wavelength is greater than the size of the SS (and hence much greater than r_{sys} as well). In that case, chameleon screening operates by making the mass of the field large (whereas the coupling remains constant).

For Cassini, r_{sys} is the distance from Saturn to Earth on the other side of the Sun. This gives $r_{\mathrm{sys}} \sim 11\mathrm{AU} \approx 5\times10^{-11}\mathrm{Mpc}$. The mass of the field given by our QS solution within the smooth halo and for the fiducial model parameters would yield $m_{\mathrm{SS}} = m_{\mathrm{eff,in}} \approx 10^8\ \mathrm{Mpc}^{-1}$ (Table 5.3). However, the actual local density within the SS is much higher than the mean halo density assumed here, and the local value m_{SS} is correspondingly expected to be several orders of magnitude larger [92]. Nevertheless, since our analytical solution is only valid for a tophat density profile, and the focus of this paper is to study the propagation of waves of screened fields in the halo, we will continue to use m_{eff} as fiducial value in the following.

In order to study the wave propagation within the halo, we now consider separately the two cases $k^2 \lesssim m_{\mathrm{eff,in}}^2$ and $k^2 \gtrsim m_{\mathrm{eff,in}}^2$. For $k^2 \lesssim m_{\mathrm{eff,in}}^2$, one can show that the wave

amplitude is strongly suppressed inside the halo, such that the Cassini bound is not spoiled for any reasonable wave amplitudes. In this regime, Eq. (5.25) becomes

$$\delta\phi = \mathrm{Re}\left[\mathcal{A}e^{-iwt}\sum_{L=0}^{\infty}(2L+1)i^L j_L(k\,R_h)\frac{i_L(\sqrt{m^2_{\mathrm{eff,in}}-k^2}\,r)}{i_L(\sqrt{m^2_{\mathrm{eff,in}}-k^2}\,R_h)}\,P_L(\cos\theta)\right], \tag{5.27}$$

where i_L is the modified spherical Bessel function of the first kind of order L, which is related to j_L by $i_L(x) = i^{-l}j_L(ix)$. It has been shown in previous literature [76] that $|j_L(x)| < 0.64\,x^{-5/6}$, $\forall L$, $x \in \mathbb{R}_{>0}$. Note however that $|j_L(x)| \leq 1\ \forall L$. It has also been shown in [75] that $\frac{I_L(x_-)}{I_L(x_+)} < \left(\frac{x_-}{x_+}\right)^L$, for $0 < x_- < x_+$ and $L > -\frac{1}{2}$, where $i_L(x) := \sqrt{\frac{\pi}{2x}}I_{L+1/2}(x)$.

A very conservative upper bound on Eq. 5.27 is then

$$\frac{\delta\phi}{\phi_{\mathrm{vac}}} < 10^{-2}\sum_{L=0}^{\infty}\left|(2L+1)j_L(kR_h)\left(\frac{1}{25}\right)^L\right|, \tag{5.28}$$

where the value for $\mathcal{A} \equiv 10^{-2}\,\phi_{\mathrm{vac}} \sim 10^{-1}\,\phi_{\mathrm{QS}}$ is adopted from [51]. $\sum_{L=0}^{\infty}\left|(2L+1)\left(\frac{1}{25}\right)^L\right| \approx 1$. Since j_L is bounded above by 1, a very conservative bound gives $\delta\phi/\phi_{\mathrm{QS}} < 10^{-1}$. For physically-relevant scenarios, k from supernovae are expected to be $\sim 10^{12}\,\mathrm{Mpc}^{-1}$, as we shall demonstrate below for the $k^2 \gtrsim m^2_{\mathrm{eff,in}}$ case. We would therefore expect that $kR_h \gg 1$ even for the less energetic scenarios. $\delta\phi/\phi_{\mathrm{QS}}$ is therefore highly suppressed by the envelope $|j_L(kR_h)| < 0.64\,(kR_h)^{-5/6}$ for physically relevant setups. While the analytical bound is more relevant to larger, physically-relevant values of k, one can numerically check that for the very low ks, $\delta\phi/\phi_{\mathrm{QS}}$ is also negligible.

These relations bound Eq. (5.27) to be numerically strongly suppressed compared to the QS solution. This can also be confirmed numerically. Thus, long-wavelength chameleon waves cannot penetrate a screened halo, and hence do not disrupt the screening. This is analogous to electromagnetic waves which cannot enter a plasma if they are below the plasma frequency.

We now consider the opposite limit, $k^2 \gtrsim m^2_{\mathrm{eff,in}}$, which is the relevant regime for astrophysical events such as Supernovae. For example, estimating $k \sim \pi/R_\star$, where $R_\star \approx 2.3 \times 10^7$ km[109], is the stellar radius before collapse, we have $k \sim 10^{12}\ \mathrm{Mpc}^{-1} \gg m_{\mathrm{eff,in}}$. Unfortunately, since $m_{\mathrm{eff,in}}R_h \gg 1$ numerically, high-order spherical Bessel functions contribute significantly. This makes the numerical evaluation of the solution Eq. (5.25) very difficult. However, when $k^2 \gg m^2_{\mathrm{eff,in}}$, as for the supernova referenced here, we can neglect $m_{\mathrm{eff,in}}$ entirely and just consider a massless field perturbation on top of the static background. This is because k and $m_{\mathrm{eff,in}}$ are the only relevant scales in the wave propagation, and any corrections to the massless case are suppressed by $m^2_{\mathrm{eff,in}}/k^2$. In other words, a very high-frequency wave of the chameleon field is unscreened inside the (smooth) halo.

Now consider the effect of such waves within the SS. In order for them to propagate within the SS, we require $k \gtrsim m_{\mathrm{SS}}$. For a chameleon model that passes SS constraints in

the static case however, we have $m_{\rm SS} \gg 1/r_{\rm sys}$, which implies $k \gg 1/r_{\rm sys}$ in order for a wave to propagate. Such high-frequency waves have periods that are much less than the time it takes light to travel the distance $r_{\rm sys}$. This suppresses observable effects within the SS (e.g. from the Cassini probe), as these average over many wave cycles leading to a cancellation. Thus, with the possible exception of a narrow window for models in which the SS is just barely screened, propagating scalar waves in chameleon models cannot lead to observable effects on SS scales.

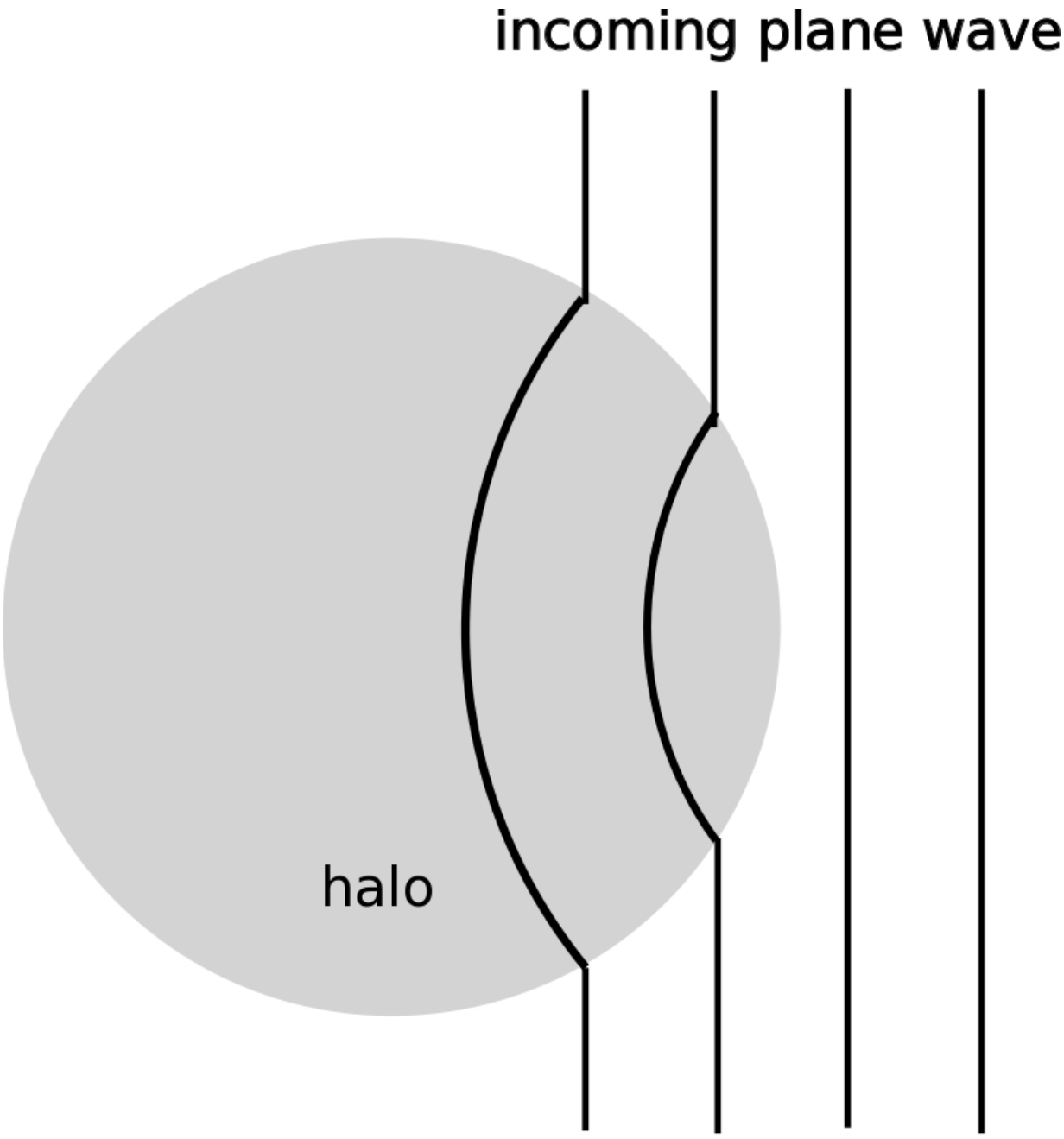

Figure 5.1: Refraction of plane waves entering the halo. Note the direction of distortion due to $v_p > c$ inside the halo.[62]

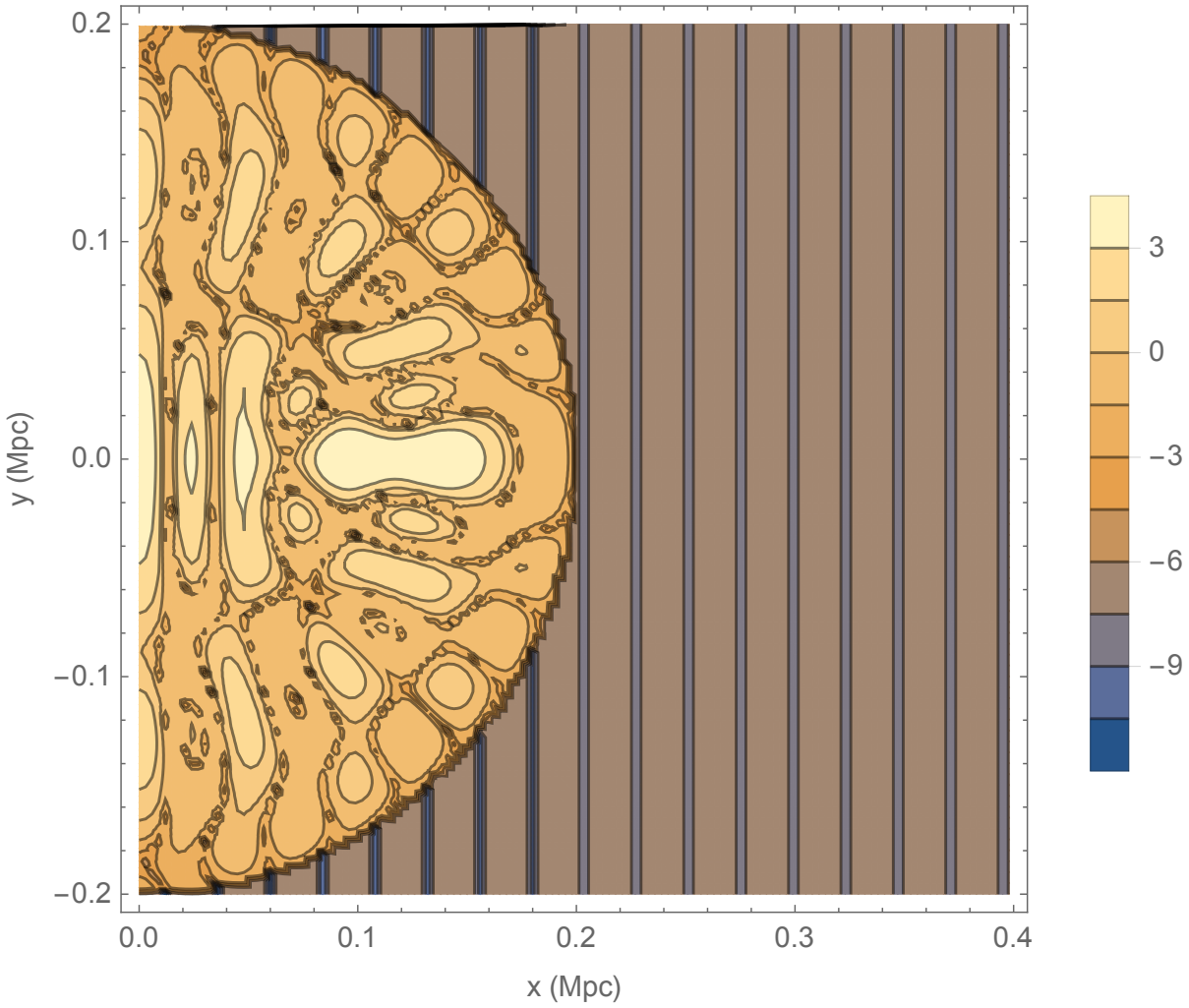

Figure 5.2: $\ln \Delta_{|\gamma_{\mathrm{PPN}}-1|}\big|_{\mathrm{SS}}$ due to an incoming plane wave in the symmetron model, for the two different definitions of the PPN parameter Eq. (5.11) (left) and Eq. (5.10) (right), respectively. The center of the halo resides at $x = y = 0$, while the SS is located at $r = \sqrt{x^2 + y^2} = r_{\mathrm{SS}} = 0.008$ Mpc. Here, t is set to 0.[62]

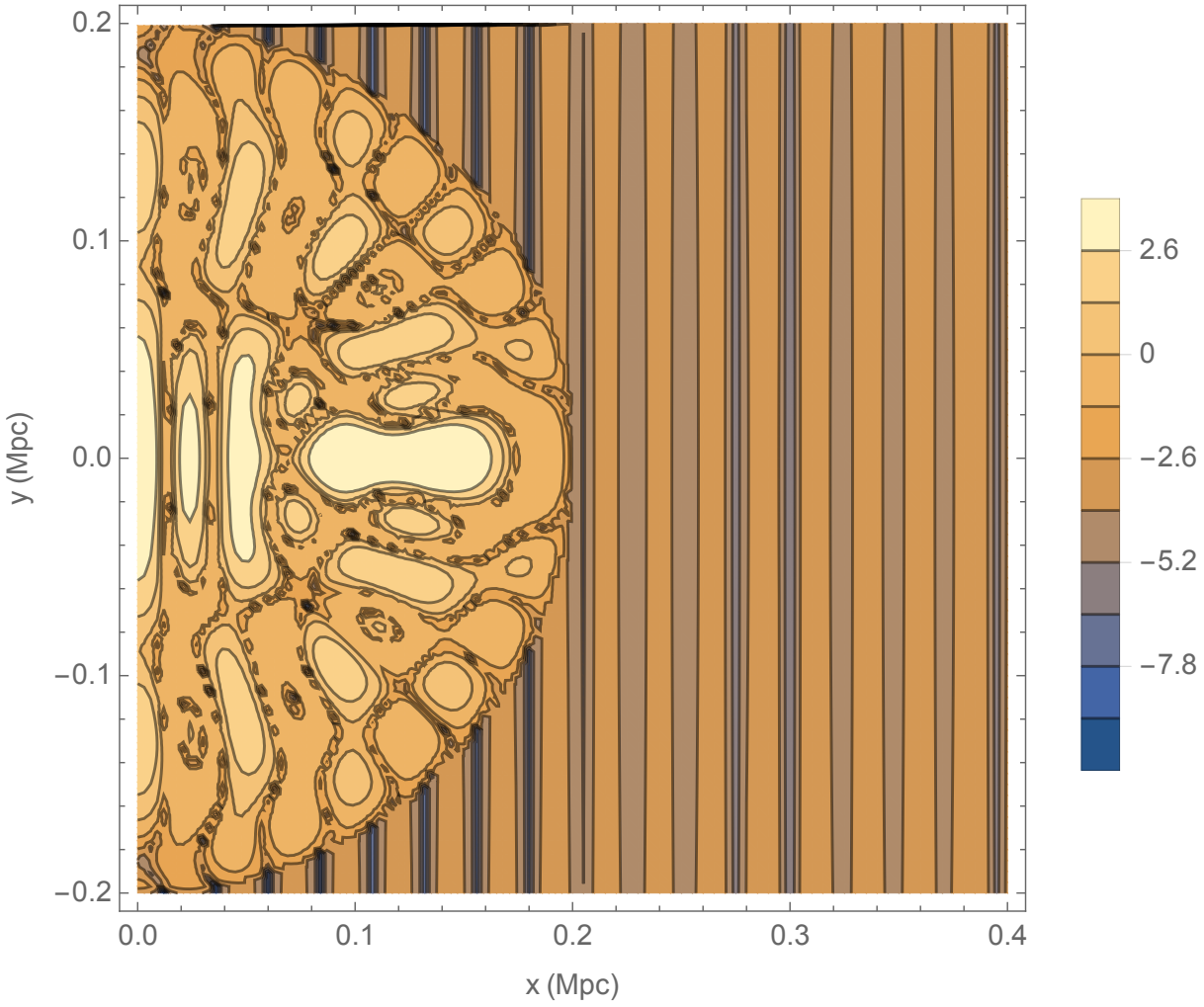

Figure 5.3: $\ln \Delta_{|\gamma_{\mathrm{PPN}}-1|}\big|_{\mathrm{halo}}$ due to an incoming plane wave in the symmetron model, for the two different definitions of the PPN parameter Eq. (5.11) (left) and Eq. (5.10) (right), respectively. The center of the halo resides at $x = y = 0$, while the SS is located at $r = \sqrt{x^2 + y^2} = r_{\mathrm{SS}} = 0.008$ Mpc. Here, t is set to 0.[62]

Chapter 6

Summary of Part I

Here is a quick summary of what we have learned in Part I of this thesis, pertaining to screening mechanisms in the scalar-tensor class of modified gravity theories.

6.1 Constrained Disformal Theories of Gravity

in Chapter 4, we saw that there is no new disformal screening mechanism up to 2PN and that at all local effects are proportional to $\dot{\phi}^2_{\rm CMB}$. As a diffeomorphism-invariant theory derived from a Lagrangian, disformally coupled scalar-tensor theories are semi-conservative, such that the parameters allowed to be non-zero are $\gamma_{\rm PPN}-1$, $\beta_{\rm PPN}-1$, ξ, α_1, α_2 . In ST theories, the evolution of the cosmological background field provides a preferred 4-vector, singling out the cosmological (CMB) frame as preferred frame. When the scalar is coupled disformally to matter, this leads to significant non-zero α_1, α_2. All of the PPN parameters are proportional to the same quantity, $\Upsilon \equiv \dot{\phi}^2_{\rm CMB}/{\Lambda_{\rm disf}}^2$. The strongest bound comes from α_2, which for generic (non-fine-tuned) models, constrains the coupling scale to $\Lambda_{\rm disf}/H_0 \gtrsim 3\times 10^3$. This is two orders-of-magnitude stronger than the previous bounds using SS constraints [96]. We were able to place a weak constraint on the first derivative of the disformal factor $\beta_\phi \lesssim 10^3$ using Lunar Laser Ranging constraints on the time-variation of $G_{\rm N}$.

In terms of the cosmology, deviations from GR are non-negligible at the background and linear level when $\mathcal{M} \lesssim \mathcal{O}(10^{-3}\text{ eV})$ [28], such that $\mathcal{M} = (M_{\rm Pl}\Lambda_{\rm disf})^{1/2} \gtrsim 10^2$ eV. In agreement with [96], we have found that there is no "disformal screening" in these theories. The natural scale for the background evolution is the Hubble scale, so that at the present time we expect $\dot{\phi}_{\rm CMB} \sim H_0\phi_{\rm CMB}$, $\ddot{\phi}_{\rm CMB} \sim H_0^2\phi_{\rm CMB}$ unless the model is fine-tuned. Since there are no non-linear screening mechanisms, the SS constraints demand that the time-derivatives of Υ, Σ be small. In this case, the effects on matter are negligible everywhere, in contrast to non-linear mechanisms that only hide the scalar field locally. These constraints then rule out disformal theories as a potential driving mechanism of the cosmic acceleration since they require a cosmology that is indistinguishable from ΛCDM. In this sense, the acceleration is due to the cosmological constant. One caveat is that the

theory we have considered here assumes that there is a Jordan frame and so the scalar couples universally to all matter species (WEP). If one were to break this assumption and couple to dark matter only our constraints would be circumvented since SS objects would not source the field.

There are other astrophysical probes that could potentially improve our constraints. Binary pulsars have provided some of the most stringent tests of general relativity and conformal scalar-tensor theories to date [40], and so one may wonder whether the same is true for disformal theories. In addition to the PPN formalism, there is a parametrised post-Keplerian (PPK) framework for binary pulsar observations. Ref. [100] have shown that three of the PPK parameters can be obtained directly from the PPN parameters $\gamma_{\rm PPN}$ and $\beta_{\rm PPN}$. These are constrained to the 10^{-6} level at most[1] and so one cannot improve the constraints found here using these measurements. The most accurately measured parameter is $P^{\rm PPK}$, the rate of orbital decay. This is constrained to the 10^{-12} level, however, the power emitted into scalar radiation typically scales as the square of the scalar charge, which scales like Υ^2, Σ^2 (see [96]) and so one expects this to yield constraints at the 10^{-6} level, which are not as strong as the bound obtained using α_2, although a more detailed calculation is required to confirm this. Future observations that constrain the PPK parameters to higher precision have the potential to improve our bounds, but, for now, they are the strongest that one can obtain using the properties of slow-moving astrophysical objects alone.

6.2 Disruption of Screening by Scalar Waves

In Chapter 5, we saw that allowing scalar waves to propagate in scalar-tensor theories by relaxing the QSA could have interesting consequences for the screening of the SS by the MW halo. This could result in a tightening of the parameter space for various modified gravity models. Here we have considered a symmetron model with parameters adopted in [51]. We have studied the impact of both planar and spherical incoming waves, where the former is the more realistic case, although the latter case could arise in certain special locations due to waves generated by rapid switching of vacua of the large-scale field. We found that planar incoming waves are significantly less disruptive than their spherical counterparts considered in [51]. This is of purely geometrical origin, due to the focusing inherent in spherical incoming waves, and does not rely on the linear analysis performed here. We have further found that the field configuration generated inside the halo by an incoming plane wave is certainly not spherically symmetric about the halo center.

The analytical approach, albeit linear, allows for a clearer understanding of the mechanisms at work. It is worth noting that for spherical waves as considered in [51], the perturbation is explicitly dependent on the combination $A r_{\rm BC}$, a constant, due to energy conservation as the spherical wave closes in. This means that the incoming wave's amplitude is greatly magnified by the time it reaches the halo. Note that $r_{\rm BC}$ corresponds to $r_{\rm max}$, which is the edge of the simulation in the study of [51] and as such corresponds to an

[1] These bounds come from the binary pulsar system PSR J0737-3039 [74].

arbitrary choice. Nevertheless, waves do propagate inside the halo in symmetron models, and could potentially have consequences for models that are just marginally screened.

We also studied waves in chameleon models, which have been claimed to also potentially suffer from disruptions of screening by incoming scalar waves. In this case, the scalar waves are necessarily of astrophysical origin and therefore planar in nature. For $k \lesssim m_{\rm eff}$, we show analytically that the effect of waves on the screening in the SS is strongly suppressed, while it is numerically difficult to compute $\delta\phi$ for $k > m_{\rm eff}$. Since the only relevant scales are k and the mass of the field $m_{\rm eff}$ inside the halo, it is clear however that if $k \gg m_{\rm eff}$, the incoming scalar wave would effectively be propagating freely within the halo. For any viable chameleon model in which the SS is screened, these waves would thus have to have periods that are much smaller than the light travel time through the SS. This means that their effects on observables such as time delay are strongly suppressed. Thus, we can effectively rule out significant observable effects of chameleon waves on SS scales. The crucial difference from the symmetron case is that the chameleon screening operates by making the field massive, thus limiting the propagation of low-frequency waves, while the symmetron screening operates by suppressing the coupling to matter.

We have not considered models of Vainshtein screening in this paper (which Ref. [51] also did not study), and leave the examination of the disruption effects on screening of this type for future work. The structure of the field equations of theores with Vainshtein screening are very different from that considered here; in particular, they are fully nonlinear rather than quasilinear. Hence, this goes beyond the scope of this paper. We refer the interested reader to studies of Galileon radiation in [93] and references therein.

In short, while disruptions of the screening of the SS by scalar waves are in principle possible in symmetron models, the effects are much less severe than previously thought when realistic wave configurations are considered. Going forward, it would be interesting to look into the influence of the halo's density distribution on the wave propagation. The dependence of the effect on the screening upon model and incoming wave parameters should also be investigated further. On the other hand, we were able to rule out any such effects for chameleon models.

Part II

A Framework Incorporating Large Scale Tidal Fields

Chapter 7

LSS in Perturbed Spacetimes

Cosmological observations strongly suggest that on large scales, our universe is well described the homogeneous, isotropic, flat FLRW spacetime that is weakly perturbed by density fluctuations that evolved from initial perturbations generated by inflation.

We wish to extract the rich information about the physical state of the very early Universe from LSS which involves NL dynamics, unlike the more straightforward linear CMB where Fourier modes evolve independently. This involves large spatial and time scales comparable to the Hubble scale, which means that we need a relativistic treatment – the NR Newtonian limit is no longer sufficient. In short, we want to probe fully NL, fully relativistic (GR) LSS formation. For this part of thesis, we shall take gravitation to be described by GR.

At the moment, we have N-body simulations to deal with NR, fully NL dynamics; and the Boltzmann code for fully relativistic, linear dynamics. Newtonian NR, linear dynamics is a special limit of these two configurations. To begin probing the unprobed (fully NL, fully relativistic) regime, we consider the widely applicable simplification where we have a distinct scale hierarchy, in which short-scale physics is modulated by a much larger scale background perturbation.

7.1 Separate Universe Picture (SUP)

The SUP is where long-wavelength isotropic adiabatic perturbations are indistinguishable from an FLRW spacetime (with different cosmological parameters) by local observations. [78, 11, 37, 84, 107, 48, 9, 104, 79, 114, 10] In other words, the short scale physics modulated by the long-wavelength perturbations are not sensitive to the latter's spatial variation, instead locally sees a homogeneous FLRW cosmology with (locally) altered parameters.

A special class of perturbations of the FLRW spacetime is that of the spherically symmetric adiabatic perturbations (spherical top-hat). Suppose we are interested in their collapse. BirkhoffâĂŹs theorem, stated in Section 1.1, tells us that the evolution of the tophat is independent of the external Universe, such that the tophat evolves without a care for the matter distribution outside, while a test particle outside would see the same metric

if the tophat was just a point source of the same mass located at the centre of the sphere. This means that the tophat is practically a different homogeneous universe, locally exactly equivalent to a different FLRW solution $a \to a_F$, where a_F obeys the Friedmann equations, as long as their wavelength is much larger than the sound horizon of all fluid components. This result holds at fully NL order [39]. That is, an observer within such a "perturbed" spacetime cannot distinguish the spacetime from exact FLRW by any local measurements, where local means on spatial scales much smaller than the wavelength of the perturbation. Note that this holds for all time, i.e. the observer could keep making spatially local measurements for several Hubble times and would continue to find agreement with FLRW. This holds for both over- and under- dense regions. In short, for a spherical perturbation, the SUP is fully NL and fully NR.

This spherical top-hat picture is of course an idealization of reality. A truer picture would include anisotropies from long-wavelength perturbations (which come from stochastical initial perturbations) that would manifest locally as a tidal shear, modulating the short-scale dynamics.

However, no neat relation to an exact solution of Einstein's equations is known for *anisotropic* adiabatic perturbations around FLRW, unlike in the perfect spherical case. While the spherically symmetric perturbations mentioned above can be equivalently seen as density or curvature perturbations, the anisotropic case is equivalent to large-scale tidal fields. It is sometimes argued that the exact solution corresponding to this case is a Bianchi I spacetime, however we show that it isn't in Section 8.

Beyond elucidating the physical interpretation of tidal fields in the relativistic context, we would also want to estimate the PN corrections appearing in NL cosmological perturbation theory. The SUP proves that all local gravitational effects of isotropic adiabatic metric perturbations (at all orders in perturbation theory) are captured by the spatial curvature in the comoving frame [39]. Our results prove that the corresponding quantity for anisotropic perturbations is the electric part of the Weyl tensor. Moreover, written in terms of locally observable quantities, the evolutionary equations only contain terms that are familiar from the subhorizon, Newtonian calculation (although, of course, they do contain post-Newtonian terms once expressed in a specific gauge such as Poisson gauge). However, in order to a obtain closed set of equations, certain terms need to be dropped. This *local tidal approximation (LTA)* [56] only recovers the correct physical evolution of the tidal field at linear order, and the density field at second order. Hence, anisotropic (tidal) adiabatic perturbations are significantly more complex than isotropic (density) perturbations.

7.2 Conformal Fermi Coordinates (CFC)

The Conformal Fermi Coordinates (CFC) is a generalization of the Fermi Normal Coordinates (FNC), so that it is applicable to cosmological studies involving large spatial and temporal scales.

FNC follows from the EEP on metric theories, see Section 2.5.1, which allows us to locally recover Minkowski spacetime in the tangent space at every point in spacetime

(up to tidal forces). In other words, for a free falling observer, the FNC is simply the standard Riemann normal coordinates parallel transported along the geodesic, inheriting the properties that in these coordinates $g_{\mu\nu}\Big|_{\text{geodesic}} \equiv \eta_{\mu\nu}$ such that the metric at any point along the geodesic looks like that of flat space âĂIJto first orderâĂİ with (tidal) corrections starting at $\mathcal{O}(x^2)$. It is then natural to do so at every point along a free-falling observer's geodesic to facilitate the interpretation of observations. However, for large spatial and temporal scales, the expansion of the universe is no longer negligible and we need to generalize the FNC to the CFC.

For the perfectly spherical perturbation case, it has been shown that the CFC observer wouldn't be able to tell, via local measurements, the difference between the local effects of a long-wavelength perturbation and an FLRW spacetime with different local parameters.[39]

CFC, $\{t_F, x^i_F\}$, is rigorously defined in [38]. Quantities defined with respect to CFC shall be denoted by a subscript F. Take an observer free-falling in some general spacetime. His worldline is then a timelike geodesic in said spacetime. For most applications of these coordinates, we take the spacetime to be perturbed Friedmann-Lemaître-Robertson-Walker (FLRW), although this is not a necessary assumption. We construct a coordinate system centered on the observer, such that he always sees an unperturbed FLRW spacetime on the geodesic, with corrections going as the spatial distance from him squared, $\mathcal{O}\left[\left(x^i_F\right)^2\right]$. Note that a power expansion in x^i_F requires that $|x^i_F|$ be less than the typical scale of variation of $h_{F\nu\mu}$, which we shall call Λ^{-1}. Since in a realistic cosmological setting, there exist metric perturbations on very small scales, we need to coarse-grain the metric (and the stress energy tensor) on a spatial scale Λ^{-1}. Then, the only contributing modes in the resulting metric perturbations have wavenumbers $k \lesssim \Lambda$. CFC is then valid over a finite region [38]. Since the absolute scale of the coarse-graining is not of relevance to the discussion here, we will not explicitly indicate the scale Λ.

We start by taking the tangent $U^\mu = \mathrm{d}x^\mu/\mathrm{d}t_F$ to his worldine, i.e. the fluid 4-velocity, to be the time direction and the hypersurface composed of all vectors orthogonal to his worldline to be the constant-time hypersurface, with the observer being at the spatial origin $x^i_F = 0$. The orthonormal tetrad thus chosen at a point on his worldline is then parallel transported along the latter, such that these properties are preserved. Then, given a scalar $a_F(x)$ that is positive in a neighborhood of the geodesics, the spatial coordinate for a given t_F is defined as follows: (t_F, x^i_F) is the point at which we arrive when starting from $P = (t_F, 0)$ (on the observer's worldline), we move along the spatial geodesic of $\tilde{g}^F_{\nu\mu}$ for a proper distance of $a_F(P)\sqrt{\delta_{ij}x^i_F x^j_F}$ in the direction defined w.r.t. the spatial components of the observer's tetrad.

For any given spacetime scalar $a_F(x)$[1], the metric can thus be made to take the form

$$g^F_{\nu\mu}(x^\mu_F) = a^2_F(\tau_F)\left[\eta_{\nu\mu} + h^F_{\nu\mu}\left(t_F, x^i_F\right)\right], \tag{7.1}$$

[1]Note that a_F has to be defined not just on the geodesic, but in a neighbourhood around it in order for us to define CFC. [38]

where

$$h^F_{00} = -\tilde{R}^F_{0l0m}(\mathbf{0})x^l_F x^m_F \tag{7.2}$$

$$h^F_{0i} = -\frac{2}{3}\tilde{R}^F_{0lim}(\mathbf{0})x^l_F x^m_F \tag{7.3}$$

$$h^F_{ij} = -\frac{1}{3}\tilde{R}^F_{iljm}(\mathbf{0})x^l_F x^m_F. \tag{7.4}$$

Here, $\tilde{R}^F_{\nu\mu\alpha\beta}(\mathbf{0})$ is the Riemann tensor of the conformally-related metric,

$$\tilde{g}^F_{\nu\mu} := a_F^{-2} g^F_{\nu\mu}\,, \tag{7.5}$$

evaluated on the central geodesic.

So far, we have not specified the local scale factor a_F. As shown in [38, 39], the natural, physically motivated choice is to define the local Hubble rate along the geodesic through

$$H_F(t_F) := a_F^{-1}\frac{\mathrm{d}a_F}{\mathrm{d}t_F} := \frac{1}{3}\nabla_\mu U^\mu\,. \tag{7.6}$$

a_F is then uniquely defined, up to an arbitrary overall multiplicative constant, by integrating the Hubble rate along the observer's geodesic. Apart from reducing to $a_F = a$ for an unperturbed FLRW spacetime, this choice ensures that H_F as well as $h^F_{\nu\mu}$ are strictly *local observables* from the point of view of the observer.[2]

Table 7.1: Quantities in Part II.

Term	Definition
$h_{\mu\nu}$	Coarse-grained metric perturbation to the FLRW spacetime in an any gauge. We assume that $\lvert h_{\mu\nu}\rvert \ll 1$ so that we can do perturbative expansion in $\lvert h_{\mu\nu}\rvert$ to simplify calculations. This is to be distinguished from a power expansion in $\boldsymbol{x}_F$.
$\boldsymbol{x}_F$	Spatial CFC coordinates (a.k.a. synchronous-comoving or fliuid spatial coordinates). Terms $\mathcal{O}(\lvert\boldsymbol{x}_F\rvert)$ do not appear in the CFC metric. CFC is valid for $\lvert\boldsymbol{x}_F\rvert \ll$the characteristic scale of variation of $h_{\mu\nu}$.
U^μ	A free-falling observer's 4-velocity, $\mathrm{d}x^\mu_{\mathrm{fl}}/\mathrm{d}t_F$, where $x^\mu_{\mathrm{fl}}(t_F)$ is the fluid trajectory and t_F is the proper time .
ρ	Proper energy density in the fluid rest frame.
Θ	4-velocity divergence/divergence of geodesic congruence, a.k.a. expansion scalar, describes the change in the volume of a sphere of test particles centred on the geodesic, $P^{\nu\mu}\nabla_\mu U_\nu$, and when on the geodesic $3H_F$.

[2] In fact, there is a residual gauge freedom to change h^F_{ij} via a purely spatial gauge transformation, as discussed in [90, 38]. However, in this paper we will not deal with h^F_{ij}.

$\sigma_{\nu\mu}$	Velocity shear tensor, the traceless symmetric part of the velocity gradient tensor, describes the rate of distortion of a sphere of test particles into an ellipsoid. Defined by Eq. 7.7.
σ_{Fij}	${a_F}^{-1}\,(P_F)^{\mu}{}_{i}\,(P_F)^{\nu}{}_{j}\sigma_{\nu\mu} = \partial^F_{(i}v^F_{j)}$
$P_{\nu\mu}(U)$	Projection tensor, projects on the subspace orthogonal to the fluid 4-velocity, $g_{\nu\mu} + U_\mu U_\nu$, becomes trivial in CFC. It also serves as the effective spatial metric for the observer in covariant form, s.t. 4-indices are raised and lowered with it.
$\omega_{\mu\nu}$	Vorticity, the antisymmetric part of the (flow-orthogonal) velocity gradient. Since we are mainly concerned with a single barotropic fluid, vorticity is not generated, and any initial vorticity decays. This is why we will generally neglect it here.
$[\nabla_\mu, \nabla_\nu]$	Commutator of the covariant derivatives, ∇_μ.
${R^\alpha}_{\beta\nu\mu}$	Riemann tensor of the metric $g_{\nu\mu}$
$E_{\nu\mu}(U)$	(Covariant) Electric part of the Weyl tensor, $C_{\mu\alpha\nu\beta}U^\alpha U^\beta$
$C_{\alpha\nu\mu\beta}$	Weyl tensor [17], the traceless part of the Riemann tensor which describes the contributions of nonlocal sources to spacetime curvature.
$\hat{R}_{\nu\mu}$	Traceless part of the spatially-projected Ricci tensor, ${P^\alpha}_\mu {P^\beta}_\nu R_{\alpha\beta} - \frac{1}{3}P_{\nu\mu}P^{\alpha\beta}R_{\alpha\beta}$. By virtue of the Einstein equations, $\hat{R}_{\nu\mu}$ is proportional to the trace-free part of the velocity-orthogonal stress tensor $\hat{T}_{\nu\mu}$, such that it vanishes In the absence of anisotropic stress in the fluid rest frame.
$\cdot$	$\mathrm{d}/\mathrm{d}t_F$
∂^F_i	$\partial/\partial x^i_F$.
a_F	Local scale factor, defined to be physically observable via $\dot{a}_F/a_F \equiv \Theta/3$ and Θ a physical quantity. All isotropic large-scale cosmological perturbations are absorbed into it. If $a_F \equiv 1$, we recover FNC.
H_F	Local expansion rate, $\dot{a}_F/a_F$. Reduces to the global H when $\Phi_{\mathrm{cN}} = \Psi_{\mathrm{cN}} = 0$.
δ_{ij}	Kronecker delta, used to raise and lower 3-indices.
v^i	Peculiar fluid velocity $a_F \mathrm{d}x^i_F/\mathrm{d}t_F = \mathcal{O}(x^i_F)$.
$\mathcal{E}^F_{ij}$	A particular component of the Weyl tensor in CFC frame, which is directly related to the perturbation h^F_{00} of the 00-component of the CFC metric, $a_F^{-2}C_{Fi0j0}$.
K_F	Local spatial curvature, conserved as it is an integration constant.
$\Phi_{\mathrm{cN}}, \Psi_{\mathrm{cN}}$	Gravitational potentials in a coarse-grained metric with long-wavelength modes and in the cN gauge, defined in Eq. 7.27

$\mathcal{R}$	Comoving curvature perturbation (on comoving slices, gauge-invariant), is the locally observable curvature, whose conservation that follows from the conservation of K_F, is necessary for SUP. This definition of $\mathcal{R}$ is to be distinguished from the curvature perturbation on uniform density slices appearing in other literature.
$\delta_L^{[1]}$	Linearly-extrapolated overdensity in the fluid's rest frame. It is the small-scale density field that one gets in the absence of long-wavelength modes.
$\delta_F(\mathbf{x}_F, t)$	Small-scale overdensity field (w.r.t. mean cosmic density) in the fluid rest frame at a fixed proper time t expressed in CFC coordinates (a.k.a. synchronous-comoving or fliuid coordinates).
$\delta_F(\mathbf{x}, t)$	$\delta_F(\mathbf{x}_F)$ expressed in Eulerian coordinates (a.k.a. global coordinates), via $\delta_F(\mathbf{x}) = \delta_F(\mathbf{x}_F)\big\|_{\rm G} - \boldsymbol{s}^i\partial_i\delta_F\big\|_{\rm G}$, where $\big\|_{\rm G}$ means evaluate on the geodesic labelled by "G". The physical of the mapping is like this: We take the Lagrangian (coordinate system tied to each fluid trajectory) density fields evaluated on each geodesic, label by G, and stitch them together to get a density field defined across a quasi-local Eulerian coordinate patch as relevant in SPT.
$\bar{a}(t_F)$	Scale factor in the unperturbed FLRW spacetime, $(t_F/t_0)^{2/3}$, where t_0 is some reference time.
$D(t_F)$	Linear matter growth factor. It is the growing mode solution to obeys $\ddot{D} + H\dot{D} - (3/2)\Omega_m HD = 0$, normalized to $a(t_F)$ of the background universe during matter domination.
$\boldsymbol{q}(\boldsymbol{x}, t)$	CFC (synchronous-comoving or fliuid) spatial coordinates $\mathbf{x}_F$, corresponding to the given Eulerian (global) coordinate, $\boldsymbol{x}$, such that for the fluid trajectory , $\boldsymbol{x}(\boldsymbol{q}, t) = \boldsymbol{q} + \boldsymbol{s}(\boldsymbol{q}, t)$. This notation is just to aid mapping to existing literature on the subject.
$\boldsymbol{s}(\boldsymbol{q}, t)$	Displacement field from the CFC (SC/fluid) coordinates to the global (Eulerian) coordinates at a fixed proper time t.
$K_{ij}^{[1]}$	Tidal field, $\frac{1}{4\pi G\bar{\rho}}\left[\partial_i\partial_j - \frac{1}{3}\partial^2\right]\Phi_{\rm cN} = \frac{2}{3}\frac{1}{\bar{a}^2\bar{H}^2}\mathcal{E}_{Fij}^{[1]} = \frac{3}{2}\bar{a}t_0^2\mathcal{E}_{Fij}^{[1]}$ in an Einstein-de Sitter background.

7.3 Nonlinear evolution of density and tidal fields

In this section, we derive a closed system of evolutionary equations for $\{\rho, \Theta, \sigma_{\nu\mu}, E_{\nu\mu}\}$. Importantly, our relations will be derived at fully NL order and fully relativistically, without assuming $v^2 \ll c^2$ or subhorizon scales $k \gg \mathcal{H} := aH$ as usually done in large-scale structure studies. Moreover, by giving expressions in the CFC frame, our results correspond directly to local observables from the point of view of a comoving observer.

We will assume that the cosmological fluid is pressureless (CDM) and perfect. It follows

that there is no anisotropic stress and the stress-energy tensor takes the form $T^{\nu\mu} = \rho U^\mu U^\nu$. However, our results also hold in the presence of pressure, as long as pressure *perturbations* can be neglected. This holds trivially for a cosmological constant. Moreover, it is valid as long as the long-wavelength perturbations considered are outside the sound horizon of all fluid components.

The flow-orthogonal part of the velocity gradient can be decomposed as [52, 45, 44]

$$P^\alpha{}_\mu P^\beta{}_\nu \nabla_\alpha U_\beta = \frac{1}{3}\Theta P_{\nu\mu} + \sigma_{\nu\mu}\,, \tag{7.7}$$

where we have neglected $\omega_{\mu\nu}$, since for a single barotropic fluid, vorticity is not generated, and any initial vorticity decays, we set $\omega_{\mu\nu}$ to zero throughout. Including this decaying mode is a trivial extension.

7.3.1 Covariant equations

Our goal is to generalize the separate universe picture, by finding a closed system of equations for the evolution of a homogeneous ellipsoid. The Friedmann equations governing the background evolution of an FLRW spacetime are a special case of the Raychaudhuri equation,

$$U^\alpha \nabla_\alpha \Theta + \frac{1}{3}\Theta^2 + \sigma_{\nu\mu}\sigma^{\nu\mu} = -4\pi G(\rho + 3p)\,. \tag{7.8}$$

While intrinsically a purely geometric relation derived from the Ricci identity, we have used the Einstein equations to replace the Ricci scalar with the trace of the stress-energy tensor on the r.h.s.. The Ricci identity holds for any Levi-Civita connection $\Gamma^\alpha_{\nu\mu}$ and is given by

$$[\nabla_\mu, \nabla_\nu]\, U^\alpha = R^\alpha{}_{\beta\nu\mu} U^\beta\,. \tag{7.9}$$

It describes the difference between parallel-transporting U^α in the direction ∇_μ then ∇_ν and vice versa. Contracting Eq. (7.9) with $P^\nu{}_\alpha U^\mu$ then yields Eq. (7.8).

We complement this with energy-momentum conservation, projected with U_μ,

$$U_\mu \nabla_\nu T^{\nu\mu} = 0, \tag{7.10}$$

which for our CDM fluid reduces to the evolutionary equation for ρ.

In addition, we need an equation governing the evolution of the velocity shear, which can again be derived from the Ricci idenity Eq. (7.9), namely by contracting with $U^\mu P^{\sigma\nu} P_{\rho\alpha}$ and then $P_{\mu\sigma}$. This yields

$$U^\alpha \nabla_\alpha \sigma_{\nu\mu} = -\frac{2}{3}\Theta\sigma_{\nu\mu} - \sigma_{\mu\alpha}\sigma^\alpha{}_\nu + \frac{1}{3}P_{\nu\mu}\sigma_{\alpha\beta}\sigma^{\alpha\beta} + E_{\mu\nu} + \frac{1}{2}\hat{R}_{\nu\mu}\,. \tag{7.11}$$

As we will see, $E_{\nu\mu}$ can be understood as the invariant definition of the local tidal field.

Eq. (7.11) shows that there are two sources of velocity shear: $E_{\mu\nu}$ and $\hat{R}_{\nu\mu}$. In the absence of anisotropic stress in the fluid rest frame, which is the case for baryons and

CDM, $\hat{R}_{\nu\mu}$ vanishes. Clearly, in the actual universe *velocity shear is sourced by the electric part of the Weyl tensor $E_{\mu\nu}$, which is the relativistic generalization of the Newtonian tidal tensor* $(\partial_i\partial_j - \delta_{ij}/3\nabla^2)\Psi_{\rm N}$.

Now, in order to obtain a closed system of evolutionary equations, we need an equation governing $E_{\nu\mu}$. This can be obtained by combining the Bianchi identity and the Einstein equation,

$$\nabla^\kappa C_{\nu\mu\kappa\lambda} = 8\pi G\left(\nabla_{[\mu}T_{\nu]\lambda} + \frac{1}{3}g_{\lambda[\mu}\nabla_{\nu]}g_{\alpha\beta}T^{\alpha\beta}\right). \tag{7.12}$$

This equation is the only one in the set that involves spatial—more precisely, fluid-orthogonal—derivatives acting on the Riemann tensor (via the Weyl tensor) and the density ρ. Note that fluid-orthogonal derivatives are simply spatial derivatives in the frame comoving with the fluid. We are interested in describing the evolution of a long-wavelength perturbation. In order to obtain a closed system of evolutionary equations, we thus *discard fluid-orthogonal derivatives acting on the density and the Riemann tensor* and neglect them in the following (of course, throughout we retain terms involving any derivatives acting on the velocity). This is the key approximation made in our derivation, and we will discuss its implications in detail below.

7.3.2 Closed system in CFC frame

At this point, it is not obvious that the four relations Eqs. (7.8), (7.10), (7.11), and (7.12) can be rewritten to form a closed local system. However, this becomes clear once expressing all relations in the CFC frame.

It is sufficient to evaluate all quantities on the geodesic $x^i_F = 0$. This is because we are free to choose a geodesic through any given point. Thus, all terms that scale, after taking all spatial derivatives, as $(x^i_F)^n$, $n \geq 1$, vanish. This applies in particular to v^i_F. Then, without making any further approximations, the NL tensor equations simplify greatly. On the geodesic, we have $U^\mu = a_F^{-1}(1,0,0,0)$, and the projection tensor simply becomes

$$P^F_{\nu\mu} = a_F^2\ \mathrm{diag}\,\{0,1,1,1\} \quad \text{and} \quad P_F^{\nu\mu} = \frac{1}{a_F^2}\,\mathrm{diag}\,\{0,1,1,1\}\,. \tag{7.13}$$

Firstly, Eq. (7.8) becomes

$$\dot{H}_F + H_F^2 + \frac{1}{3{a_F}^2}\sigma_{Fij}\sigma_F^{ij} + \frac{4\pi G}{3}\rho_F = 0\,, \tag{7.14}$$

We have pulled out a factor of a_F^{-1} in the definition of the velocity shear. Further, recall that in CFC, we define $\Theta := 3H_F$ on the geodesic, such that the spatial velocity divergence, $\nabla_{k,F}v^k_F$, is absorbed into the definition of a_F. Thus, σ_{Fij} is trace-free.

Secondly, Eq. (7.10) becomes

$$\dot{\rho}_F + 3H_F\rho_F = 0, \tag{7.15}$$

which is unsurprisingly the familiar continuity equation. Thirdly, Eq. (7.11) becomes

$$\dot{\sigma}_{Fij} + H_F \sigma_{Fij} + \frac{1}{a_F}\left(\sigma_{Fil}\sigma^{l}_{Fj} - \frac{1}{3}\delta_{ij}\sigma_{Flm}\sigma_F^{lm}\right) + \frac{\mathcal{E}^F_{ij}}{a_F} = 0\,, \tag{7.16}$$

Further, we have used the fact that

$$(P_F)^{\mu}{}_{i}\,(P_F)^{\nu}{}_{j}\,\hat{R}_{F\nu\mu} = \hat{R}_{Fij} = R_{Fij} - \frac{1}{3}\delta_{ij}\delta^{kl}(R_F)_{kl} = 0\,. \tag{7.17}$$

This vanishes on the geodesic when we evaluate $R_{F\nu\mu}$ using the trace-reversed Einstein equation because the CFC frame is defined to be the fluid rest frame, and we assume no anisotropic stress as discussed above.

Finally, in order to evaluate Eq. (7.12), note that the Weyl tensor is trace-free over any two indices and has the same symmetry properties as the Riemann tensor. Moreover, $\partial^F_k C_{Flij0} = \mathcal{O}\left(\partial^F_k R_{Flij0}\right)$ is a fluid-orthogonal derivative of the Riemann tensor and thus neglected as explained after Eq. (7.12). Moreover, in the CFC construction this term is naturally higher order, as for the leading expression given in Eq. (7.2), $\partial^F_k C_{Flij0} = \mathcal{O}\left(\vec{x}_F\right)$ vanishes when evaluated on the observer's worldline. It follows then that the $0ij0-$component of the LHS of Eq. (7.12) becomes

$$-a_F\left(\dot{\mathcal{E}}^F_{ij} + H_F\mathcal{E}^F_{ij}\right)\,, \tag{7.18}$$

while all other components of Eq. (7.12) either vanish or are higher order in derivatives, as shown in App. B. Finally, for the RHS of Eq. (7.12), we neglect spatial derivatives (in CFC) acting on the stress energy tensor and apply the continuity equation, Eq. (7.15), to yield on the observer's worldline

$$4\pi G a_F^2 \rho_F \sigma_{Fij}\,. \tag{7.19}$$

Thus, without higher spatial derivatives and on the central geodesic, Eq. (7.12) in CFC reduces to

$$\dot{\mathcal{E}}_{Fij} + H_F\mathcal{E}_{Fij} + 4\pi G a_F \rho_F \sigma_{Fij} = 0\,. \tag{7.20}$$

Note that Eqs. (7.18)–(7.20) would look different if we had inserted the covariant definition $E_{\nu\mu}(U) := C_{\mu\alpha\nu\beta}U^\alpha U^\beta$ into Eq. (7.12), as the spatial derivatives acting on U^μ yield non-negligible terms. Since our goal is to derive a closed system in terms of *local* gravitational observables in the framework of the CFC, we choose Eq. (7.18) as the local approximation to Eq. (7.12). In order to emphasize the subtle distinction between $E_{\nu\mu}(U)$ and C^F_{i0j0} in the context of our local approximation, we have introduced the new symbol $\mathcal{E}^F_{ij}$ in Eq. (7.1).

The physical interpretation of $\mathcal{E}^F_{ij}$ becomes clear when deriving its relation to the perturbation h^F_{00} of the 00-component of the metric in CFC Eq. (7.2). Using the transformation law of the Riemann tensor under a conformal rescaling of the metric, one obtains

$$\begin{aligned}\tilde{R}^F_{0l0m} &= \frac{1}{{a_F}^2}R^F{}_{0l0m} + \delta_{lm}{a_F}^2\left(\dot{H}_F + H_F^2\right)\\ &= \frac{1}{{a_F}^2}R^F{}_{0l0m} - \delta_{lm}\left(\frac{1}{3}\sigma_{Fij}\sigma_F^{ij} + \frac{4\pi G}{3}{a_F}^2\rho_F\right)\,,\end{aligned} \tag{7.21}$$

where we have used Eq. (7.14) in the second line. Using the definition of the Weyl tensor as trace-subtracted version of the Riemann tensor $\tilde{R}^F$, we then obtain [see also Eq. (3.31) in [39]]

$$h^F_{00} = \left(-\mathcal{E}^F_{lm} + \frac{1}{3}\delta_{lm}\sigma_{Fij}\sigma^{ij}_F\right)_{\mathbf{0}} x^l_F x^m_F \,, \tag{7.22}$$

where we have used Eq. (7.1). Note that since the Weyl tensor is invariant under conformal rescaling, we have $\tilde{C}^F = C^F$. We see that $\mathcal{E}^F_{lm}$ is exactly the trace-free part of $-\partial_l\partial_m h^F_{00}$, which is the local tidal field acting on non-relativistic bodies in the CFC frame. Any other Ricci-contribution to the local tidal field would have to be due to anisotropic stress.

The four equations Eqs. (7.14)–(7.20) now clearly form a closed, local system of ordinary differential equations governing the evolution of the four unknowns ρ_F, H_F, σ_F, and $\mathcal{E}_F$ along the fluid geodesic:

$$\begin{aligned}
&\dot{H}_F + H_F^2 + \frac{1}{3{a_F}^2}\sigma_{Fij}\sigma^{ij}_F + \frac{4\pi G}{3}\rho_F = 0 \\
&\dot{\sigma}_{Fij} + H_F\sigma_{Fij} + \frac{1}{a_F}\left(\sigma_{Fil}\sigma^l_{Fj} - \frac{1}{3}\delta_{ij}\sigma_{Flm}\sigma^{lm}_F\right) + \frac{\mathcal{E}_{Fij}}{a_F} = 0 \\
&\dot{\rho}_F + 3H_F\rho_F = 0 \\
&\dot{\mathcal{E}}_{Fij} + H_F\mathcal{E}_{Fij} + 4\pi G a_F\rho_F\sigma_{Fij} = 0 \,.
\end{aligned} \tag{7.23}$$

Note that $\mathcal{E}_F$ has dimensions $1/\text{length}^2$, while σ_F has dimensions $1/\text{length}$. Given initial conditions for ρ_F, H_F (or equivalently, K_F), σ^F_{ij}, and $\mathcal{E}_{Fij}$, Eq. (7.23) can be integrated numerically without any further approximations. Since we have used the Einstein equations through Eq. (7.8) and Eq. (7.12) (with all components of the latter derived in App. B), all constraints are self-consistently fulfilled at leading order in derivatives. In the next section, we will consider the general perturbative solution around a flat matter-dominated (Einstein-de Sitter) universe.

The fully relativistic system Eq. (7.23) clarifies the physical meaning of the locally observable impact of tidal fields. That is, tides are a manifestation of the Weyl tensor, which encodes the nonlocal part of gravitational interactions, and thus of the large-scale *inhomogeneities* in the matter distribution. This is to be contrasted with *homogeneous and anisotropic* Bianchi I spacetimes, where the anisotropy is sourced by the trace-free part of the Ricci tensor $\hat{R}_{ij}$. As we argued above, this in fact vanishes everywhere for a pressureless (and indeed any ideal) fluid. Thus, the construction leading to Eq. (7.23), rather than a Bianchi I solution, are the proper relativistic model of long-wavelength density and tidal perturbations.

Note that the system simplifies further when setting $\sigma_F = 0 = \mathcal{E}_F$ initially, corresponding to a spherically symmetric system. The symmetry is preserved so that σ_F and $\mathcal{E}_F$ remain zero. We then obtain

$$\begin{aligned}
&\dot{H}_F + H_F^2 + \frac{4\pi G}{3}\rho_F = 0 \\
&\dot{\rho}_F + 3H_F\rho_F = 0 \,.
\end{aligned} \tag{7.24}$$

These are just the second Friedmann equation and continuity equation of the FLRW spacetime. One can then show (again, assuming scales much larger than the sound horizon of the fluid) that the first Friedmann equation is satisfied as well [39]. This proceeds in the usual way by multiplying Eq. (7.24) with $\dot{a}_F$, integrating once, and using the continuity equation to yield

$$H_F^2 = \frac{8\pi G}{3}\rho_F - \frac{K_F}{{a_F}^2}. \tag{7.25}$$

This is the well-known *SUP* in Section 7.1 Eq. (7.24) is also equivalent to the spherical collapse equation [115]. Note that Eq. (7.24) is exact given the said assumptions, while in the anisotropic case Eq. (7.23) is an approximation whose accuracy we will discuss further below. First, however, we will proceed to solve the general, anisotropic case.

7.4 Perturbative solution in EdS Spacetime

We now consider a perturbed Einstein-de Sitter universe, where in the background the Hubble rate satisfies $\bar{H}^2 = 8\pi G\bar{\rho}/3 \propto \bar{a}^{-3}$. We expand all quantities into orders of perturbation, denoted by $^{[n]}, n = 1, 2, \cdots$. Quantities with an overbar are evaluated in the background Einstein-de Sitter universe. Correspondingly, we write the density as

$$\rho = \bar{\rho}(t)\left[1 + \delta_F\left(t, x^i\right)\right] . \tag{7.26}$$

Throughout, we assume that initial conditions are set at sufficiently early times (see Sec. 7.4.1 below), so that we can restrict to the fastest growing modes throughout. This is merely for calculational convenience; it is straightforward to keep the subleading modes when solving Eq. (7.23).

7.4.1 Initial conditions

We briefly describe how the growing-mode initial conditions for Eq. (7.23) can be determined. For this, we assume they are set at sufficiently early times, so that linear perturbation theory is accurate. We can then relate the CFC-frame quantities to those in a given global coordinate system at linear order in perturbations. Specifically, we consider two frequently used gauge choices: conformal-Newtonian gauge, defined through

$$ds^2 = a^2(\tau)\left[-(1 + 2\Phi_{\text{cN}})d\tau^2 + (1 - 2\Psi_{\text{cN}})\delta_{ij}dx^i dx^j\right] , \tag{7.27}$$

and comoving gauge, which is frequently used for calculations during inflation:

$$ds^2 = a^2(\tau)\left[-(1 + 2N_1)d\tau^2 + 2N_i d\tau dx^i + (1 + 2\mathcal{R})\delta_{ij}dx^i dx^j\right] . \tag{7.28}$$

Here, spatial slices are chosen such that $T^0_i = 0$, hence the designation "comoving". In both cases, we have only included scalar perturbations. The reason is that vector perturbations

are pure decaying modes in both cases, so that they are irrelevant for the fastest growing modes. Tensor modes on the other hand are propagating modes whose NL evolution we do not expect to be described correctly by the local approximation employed in Eq. (7.23). The linear evolution of a tensor-mode-induced $\mathcal{E}^F_{ij}$ and its effect on small-scale perturbations was derived in [103, 38]. We stress again that this simplification is merely for convenience and not required within the CFC formalism; one can straightforwardly include vector and tensor modes and their associated decaying modes.

Let us first consider the simpler, isotropic case, where the initial conditions can be either specified through δ_F or K_F. As shown in [39], one has

$$K_F = \frac{2}{3}\left(\partial^2\Psi_{\rm cN} - \mathcal{H}\partial_i v^i\right) = \frac{2}{3}\partial^2\mathcal{R}\,. \tag{7.29}$$

Note that $K_F = \text{const}$ at all times (not only during matter domination), as long as it is outside the sound horizon of all fluid components. During matter domination and at linear order, one further has

$$K_F = \frac{5}{3}\Omega_{m0}H_0^2 a^{-1}(t)\delta_F(t)\,, \tag{7.30}$$

where Ω_{m0} is the matter density parameter today.

Next, consider the anisotropic case. Restricting to the growing mode, it is sufficient to provide initial conditions for $\mathcal{E}^F_{ij}$. In conformal-Newtonian gauge, we have at linear order in perturbations

$$\mathcal{E}^F_{ij}\Big|_{\rm linear} = \left(\partial_i\partial_j - \frac{1}{3}\delta_{ij}\partial^2\right)\Phi_{\rm cN}\,, \tag{7.31}$$

where we have used the CFC metric constructed at linear order by [39], and Eq. (7.22).[3] Moreover, using that the two spacetime potentials in conformal-Newtonian gauge are equal in the absence of anisotropic stress, and setting vorticity to zero, it is easy to show that Eq. (7.20) yields the correct evolution of $\mathcal{E}^F_{ij}$ *at linear order* [cf. Eq. (4.50) in [17]].

Note that unlike the K_F, $\mathcal{E}^F_{ij}$ is in general not conserved during cosmic evolution even outside the sound horizon of all fluid components. This is a qualitative difference to the isotropic case, where the effect of the long-wavelength perturbation is described by K_F which is constant at all orders on large scales. However, in the particular case of matter domination, $\mathcal{E}^F_{ij}$ is conserved at linear order (see below). In this case, initial conditions can be simply specified by using the well-known relation for growing-mode adiabatic perturbations during matter domination, $\mathcal{R} = (5/3)\Phi_{\rm cN}$, so that

$$\mathcal{E}^F_{ij}\Big|_{\text{linear, mat. dom.}} = \frac{3}{5}\left(\partial_i\partial_j - \frac{1}{3}\delta_{ij}\partial^2\right)\mathcal{R}\,. \tag{7.32}$$

This relation can be used immediately to initialize a calculation for the NL evolution of the tidal field $\mathcal{E}^F_{ij}$ for modes that enter the horizon during matter domination. In general, one should follow the *linear* evolution of $\mathcal{E}^F_{ij}$ via Eq. (7.31) until matter domination (for example, using a Boltzmann code), at which point $\mathcal{E}^F_{ij}$ approaches a constant and can be matched to the *NL* calculation in matter domination which we describe next.

[3] Note that $g^F_{00} = a_F^2[-1 + h^F_{00}] = -a_F^2[1 - h^F_{00}]$.

7.4.2 Perturbative solution up to second order

We begin with the linear evolution in CFC, which matches that of standard (subhorizon) perturbation theory [15], and was derived in [39]. In terms of the matter density perturbation and electric Weyl tensor, we obtain

$$\delta_F^{[1]} = \bar{a}(t_F)\delta_L^{[1]}(\boldsymbol{x}_F) \tag{7.33}$$

$$\mathcal{E}_{Fij}^{[1]} = \mathcal{E}_{Fij}^{[1]}(\boldsymbol{x}_F)\,. \tag{7.34}$$

Here, we have introduced the linearly-extrapolated initial overdensity $\delta_L^{[1]}(\boldsymbol{x}_F) := \delta_F^{[1]}(\boldsymbol{x}_F, t_0)$ and the local tidal field, $\mathcal{E}_{Fij}^{[1]}(\boldsymbol{x}_F)$, for later convenience. Note that $\delta_F^{[1]} \propto \bar{a}$, while $\mathcal{E}_{Fij}^{[1]} = \text{const}$ at linear order. One could thus think of $\mathcal{E}_{Fij}$ as the analog for anisotropic perturbations of the spatial curvature K. Unlike the latter however, we will see that $\mathcal{E}_{Fij}$ is not conserved at NL order. Moreover, even at linear order the conservation of $\mathcal{E}_{Fij}$ only holds in a flat matter-dominated universe.

The local scale factor and velocity shear are at linear order given by

$$a_F{}^{[1]} = \bar{a}(t_F) - \frac{1}{3}\bar{a}^2(t_F)\delta_L^{[1]}(\boldsymbol{x}_F) \tag{7.35}$$

$$\sigma_{Fij}^{[1]} = -\,\bar{a}^{1/2}(t_F)t_0\mathcal{E}_{Fij}^{[1]}(\boldsymbol{x}_F)\,. \tag{7.36}$$

Continuing to solve the equations Eq. (7.23) perturbatively, and keeping only the fastest growing mode (i.e. the term with the highest power of t_F), gives, at second order in perturbations,

$$a_F = \bar{a} - \frac{1}{3}\bar{a}^2\delta_L^{[1]} - \frac{1}{21}\bar{a}^3\left(\delta_L^{[1]}\right)^2 - \frac{3}{14}\bar{a}^3 t_0^4\left(\mathcal{E}_{Fij}^{[1]}\right)^2 + \cdots \tag{7.37}$$

$$\delta_F = \bar{a}\delta_L^{[1]} + \frac{17}{21}\bar{a}^2\delta_L^{[1]2} + \frac{9}{14}\bar{a}^2 t_0^4\left(\mathcal{E}_{Fij}^{[1]}\right)^2 + \cdots \tag{7.38}$$

$$\mathcal{E}_{Fij} = \mathcal{E}_{Fij}^{[1]} + \frac{20}{21}\bar{a}\delta_L^{[1]}\mathcal{E}_{Fij}^{[1]} + \frac{3}{7}\bar{a}t_0^2\left(\mathcal{E}_{Fil}^{[1]}\mathcal{E}_{Fj}^{l\;[1]} - \frac{1}{3}\delta_{ij}\mathcal{E}_{Flm}^{[1]}\mathcal{E}_F^{lm[1]}\right) + \cdots \tag{7.39}$$

$$\begin{aligned}\frac{\sigma_{Fij}}{\bar{a}^{1/2}} =& -t_0\mathcal{E}_{Fij}^{[1]} - \frac{19}{21}\bar{a}\delta_L^{[1]}t_0\mathcal{E}_{Fil}^{[1]} \\ &- \frac{18}{21}\bar{a}\,t_0^3\left(\mathcal{E}_{Fil}^{[1]}\mathcal{E}_{Fj}^{l\;[1]} - \frac{1}{3}\delta_{ij}\mathcal{E}_{Flm}^{[1]}\mathcal{E}_F^{lm[1]}\right) + \cdots\,,\end{aligned} \tag{7.40}$$

where the left-hand side is evaluated at t_F and x_F, while on the right-hand side the time dependence is completely encoded in the factors of $\bar{a} = \bar{a}(t_F)$. Instead of writing the solutions in terms of the initial conditions at some early time, we have followed the customary choice in cosmological perturbation theory of phrasing the solution in terms of $\delta_L^{[1]}(\boldsymbol{x}_F)$ and initial electric Weyl contribution $\mathcal{E}_F^{[1]}$ introduced above. The results Eqs. (7.37)–(7.40) can be formally continued straightforwardly to higher order. Further, in order to describe the solution in a ΛCDM background, one can perform the standard very accurate approximation of replacing $\bar{a}^n$ with $[D(t_F)]^n$.

In the next section, we will connect our results to those from other, previously considered local approaches to NL gravitational evolution of non-spherically symmetric systems.

7.4.3 Connection to the local tidal approximation and ellipsoidal collapse

Interestingly, the system Eq. (7.23) has been derived before, in the subhorizon limit, by Ref. [56] who referred to this as the *Local Tidal Approximation* (LTA). This approximation originated in a series of attempts at improving the local approximation to study large-scale structure and at clarifying the relation between general relativity and Newtonian dynamics. The first was the ZelâĂŹdovich approximation (ZA) [123]. Bertschinger and Jain [19] proposed the non-magnetic approximation (NMA). In the NMA, the covariant magnetic part of the Weyl tensor is set to zero, $H_{ij} = 0$. However, Refs. [18, 69] showed that H_{ij} cannot be consistently neglected in the Newtonian limit. That is, H_{ij} has a Newtonian counterpart after all. Later, Hui and Bertschinger proposed the LTA. Here they defined a new quantity M_{ij}, composed of a combination of terms in the tidal evolution equation, and set it to 0. They found that whereas NMA is exact for spherical perturbations but not cylindrical ones; LTA is exact for both and, more generally, for any growing-mode perturbations whose gravitational equipotential surfaces have constant shape with time.

In the LTA approximation, the authors imposed the condition

$$M_{ij} := -\nabla_k \epsilon^{kl}{}_{(i} H_{j)l} + \theta E_{ij} + \delta_{ij}\sigma^{kl}E_{kl} - 3\sigma^k{}_{(i}E_{j)k} - \omega^k{}_{(i}E_{j)k} = 0\,, \tag{7.41}$$

where conformal-Newtonian gauge is adopted and $E_{ij} \equiv (\partial_i\partial_j - (\delta_{ij}/3)\nabla^2)\Phi_{\rm cN}$ is the tidal field in the subhorizon approximation. Note that in the subhorizon limit, the velocity-orthogonal projection is equivalent to simply restricting to spatial coordinates. H_{ij} here is the magnetic component of the Weyl tensor. The tensor M_{ij} can also be written as

$$M_{ij} = -4\pi G a^2 \rho \nabla_{(i} v_{j)} - \frac{\mathrm{d}}{\mathrm{d}t}\left(\nabla_i\nabla_j a\frac{h_{00}}{2}\right). \tag{7.42}$$

Using Eq. (7.22) for h_{00} in CFC, Eq. (7.20) implies immediately that the trace-free part of M_{ij} vanishes. On the other hand, the trace part corresponds to a combination of the Raychaudhuri and continuity equations. Correspondingly, Eq. (7.23) agrees with Eq. (22) of [56]. Thus, the CFC approach offers a simple and fully covariant derivation of the LTA. In addition, it yields an additional interpretation of the nature of the approximation made in the LTA construction, namely through the terms neglected in Eq. (7.12). The resultant E_{ij} in LTA is in fact our local tidal field $\mathcal{E}^F_{ij}$.

Ref. [56] discussed the LTA in the context of the collapse of a homogeneous *isolated* ellipsoid [58, 118]. In this model, one neglects the gravitational effect of the ellipsoid on the surrounding matter. Ref. [117] studied the validity of this approximation by performing an N-body simulation which allows for the backreaction of the ellipsoid on its environment. Specifically, the environment consisted of a small homogeneous negative density perturbation to compensate for the mass contained within the overdense ellipsoid. He found that the above-mentioned approximation is quite accurate until the late stages of collapse. The advantage of neglecting gravitational backreaction on the environment is that a closed, semi-analytical solution can be obtained.

In particular, working in the conformal-Newtonian gauge and taking the subhorizon limit, the evolution of an irrotational, isolated homogeneous ellipsoid embedded in an FLRW background is governed by

$$\frac{\mathrm{d}^2 R_i}{\mathrm{d}t^2} = -2\pi G R_i \left[\frac{2}{3}\bar{\rho} + \alpha_i \delta\right], \quad \text{for } i = 1, 2, 3, \tag{7.43}$$

where R_i are the proper axis lengths of the ellipsoid; $\bar{\rho}$ is the local homogeneous (or, mean) density around the ellipsoid, such that $\rho := \bar{\rho}\,(1+\delta)$; t is the proper time; and α_i are defined by

$$\alpha_i := \left(\prod_{n=1}^{3} R_n\right) \int_0^\infty \frac{\mathrm{d}s}{(R_i^2 + s)\sqrt{\sum_{k=1}^{3}(R_k^2 + s)}}\,. \tag{7.44}$$

The peculiar velocity field inside the ellipsoid is

$$v_i = a\left(\frac{\dot{R}_i}{R_i} - \frac{\dot{a}}{a}\right) x_i, \tag{7.45}$$

where x_i are comoving spatial coordinates. These relations can be used to derive the local Hubble rate, velocity shear, and electric Weyl tensor component [56], which in CFC become

$$H_F = \frac{1}{3}\sum_i \frac{\dot{R}_i}{R_i} \tag{7.46}$$

$$\sigma_{Fij} = a_F\,\mathrm{diag}\left(\frac{\dot{R}_i}{R_i} - H_F\right) \tag{7.47}$$

$$E_{Fij} = 2\pi G a_F^2 \delta_F\ \mathrm{diag}\left(\alpha_i - \frac{2}{3}\right)\,. \tag{7.48}$$

Given this one-to-one mapping to quantities in the system Eq. (7.23), the isolated ellipsoid can be considered as another local approximation to the evolution of non-spherically symmetric perturbations, even though it is not truly local as the α_i, and thus $\mathcal{E}_{Fij}$, obey an integral equation Eq. (7.44). As shown in [56] however, the LTA, and hence the closed system in CFC derived in Sec. 7.3.2, recovers the evolution of Eqs. (7.43)–(7.44) only up to first order. Thus, given the N-body results of [117], the LTA describes the actual evolution of an isolated ellipsoidal perturbation much less accurately than Eqs. (7.43)–(7.44). This difference can be attributed to the perfectly local approximation made in LTA, whereas the isolated ellipsoid does take into account the finite extent of the perturbation.

However, in practice, perturbations in the universe cannot be considered isolated, at least until they have reached sufficient density to dominate the local gravitational potential. As discussed in Sec. 9.2, the correct evolution of tidal fields is fundamentally nonlocal starting at second order. This is qualitatively different from isotropic perturbations, where the LTA reduces to the "separate universe" which provides an exact solution for large-scale adiabatic perturbations.

7.5 Application: the rest-frame matter three-point function

As derived in Sec. 7.4, the matter density perturbation in CFC frame up to second order in perturbations is given by

$$\delta_F(\boldsymbol{q},t) = D(t)\delta_L^{[1]}(\boldsymbol{q}) + \frac{17}{21}[D(t)\delta_L^{[1]}(\boldsymbol{q})]^2 + \frac{2}{7}[D(t)K_{ij}^{[1]}(\boldsymbol{q})]^2\,, \tag{7.49}$$

where $K_{ij}^{[1]}$ is defined through Eq. (7.1). Here, we have only assumed adiabatic Gaussian initial conditions. $\boldsymbol{q}$ is a spatial coordinate which labels the geodesic around which the CFC frame is constructed, while t denotes proper time along the geodesic. We will choose $\boldsymbol{q}$ to denote the spatial position on a constant-proper-time slice at $t = 0$, that is, at the end of inflation.

We now would like to relate this result to the observed, late-time statistics of the matter density field, without resorting to the sub-horizon approximation made in most large-scale structure studies; specifically, we are interested in the leading signature of NL evolution, the three-point function. Unfortunately, the precise prediction for these statistics depends on how the matter density field is measured, for example through gravitational lensing (which strictly measures the deflection of photon geodesics), or tracers such as galaxies (whose relation to matter is complicated by bias, redshift-space distortions, and other effects; see [42] for a review). Since these issues go beyond the scope of this paper, we here assume the idealized case of observers on different geodesics communicating their local rest-frame matter density as well as proper time to a distant observer on their future light cone.

Let us define the displacement $\boldsymbol{s}$ as parametrizing the difference between the spatial position $\boldsymbol{x}$, as observed by the distant observer, of the fluid geodesic relative to the initial position $\boldsymbol{q}$ as a function of proper time:

$$\boldsymbol{x} = \boldsymbol{q} + \boldsymbol{s}(\boldsymbol{q},t)\,. \tag{7.50}$$

Note that $\boldsymbol{s}$ depends on how the distant observer measures the spacetime position of the geodesic. In general, $\boldsymbol{s}$ describes the effect of large-scale gravitational perturbations on the geodesic, which are given by an integral over the gradient of the gravitational potential, as well as the details of the distant observer's measurement. For example, if they use apparent photon arrival directions and redshifts, then $\boldsymbol{s}$ includes Doppler shift, gravitational redshift, and deflection by structures along the line of sight. The explicit expression of $\boldsymbol{s}$ further depends on the coordinate (gauge) choice that is used to calculate the displacement, although the end result is independent of the gauge; see [65] for a brief overview. For this reason, we will not derive $\boldsymbol{s}$ explicitly here. However, independently of the gauge choice, $\boldsymbol{s}$ is first order in cosmological perturbations. Hence, we can expand the CFC-frame density field up to second order as

$$\delta_F(\boldsymbol{x},t) = \delta_F(\boldsymbol{q},t) - s^i(\boldsymbol{q},t)\partial_i\delta_F(\boldsymbol{q},t)\,. \tag{7.51}$$

Moreover, since only the cross-correlation of $\boldsymbol{s}$ with the density field δ_F enters in the leading three-point function, it is sufficient to consider the longitudinal contribution to $\boldsymbol{s}$, which we write as

$$s^i(\boldsymbol{q},t) = \partial^i S(\boldsymbol{q},t)\,, \tag{7.52}$$

where S is a scalar function which, for a fixed Lagrangian position $\boldsymbol{q}$, only depends on proper time t. Note that S has dimension of length^2.

With a slight generalization of the results in App. A of [14], we can then write the three-point function of the CFC-frame matter density as

$$\begin{aligned}\langle\delta_F(\boldsymbol{x}_a,t)\delta_F(\boldsymbol{x}_b,t)\delta_F(\boldsymbol{x}_c,t)\rangle = \Bigg\{ &\frac{34}{21}\xi_0(r_1,t)\xi_0(r_2,t) + \frac{4}{7}\left[\mu_{12}^2 - \frac{1}{3}\right]\xi_2(r_1,t)\xi_2(r_2,t) \\ &- \mu_{12}\left[\frac{\partial\xi_{S\delta}(r_1,t)}{\partial r_1}\frac{\partial\xi_0(r_2,t)}{\partial r_2} + (1\leftrightarrow 2)\right]\Bigg\} \\ &+ 2 \text{ cycl. perm.}\,. \end{aligned} \tag{7.53}$$

Here, $\boldsymbol{r}_1 = \boldsymbol{x}_b - \boldsymbol{x}_a$, $\boldsymbol{r}_2 = \boldsymbol{x}_a - \boldsymbol{x}_c$, $\boldsymbol{r}_1 = \boldsymbol{x}_c - \boldsymbol{x}_b$, while $\mu_{ij} \equiv \boldsymbol{r}_i \cdot \boldsymbol{r}_j / r_i r_j$.

While Eq. (7.53) only represents an idealized case, which does not include the mapping from the local rest-frame matter density to a realistic observable, it clearly illustrates the simplicity of the result obtained, without restriction to subhorizon scales, when using CFC to describe NL gravitational evolution. Given the assumption stated at the beginning of the section, Eq. (7.53) is fully accurate at second order, and not restricted to the squeezed limit.

Chapter 8

Distinction from Bianchi I Spacetime

A Bianchi spacetime is homogeneous (metric components are independent of $\mathbf{x}$) but not necessarily isotropic on spatial slices (the scale factors for each spatial cartesian direction can be different).

$$\mathrm{d}s^2 = -\mathrm{d}t^2 + a^2(t)\left[\delta_{ij} + H_{ij}(t)\right]\mathrm{d}x^i\mathrm{d}x^j\,, \tag{8.1}$$

where $\delta_{ij} + H_{ij}(t)$ is a trace-free symmetric positive-definite matrix. We can rotate the spatial coordinates to the frame where H_{ij} is diagonal, such that

$$\delta_{ij} + H_{ij}(t) = \exp\begin{pmatrix} 2\alpha(t) & 0 & 0 \\ 0 & 2\beta(t) & 0 \\ 0 & 0 & 2\xi(t) \end{pmatrix}\,, \tag{8.2}$$

where

$$\alpha + \beta + \xi = 0 \tag{8.3}$$

for all t. In other words, we write Eq. (8.1) as

$$\mathrm{d}s^2 = -\mathrm{d}t^2 + a^2(t)\left[e^{2\alpha_1(t)}\mathrm{d}x^2 + e^{2\alpha_2(t)}\mathrm{d}y^2 + e^{2\alpha_3(t)}\mathrm{d}z^2\right]\,. \tag{8.4}$$

We see that comoving test particles in 8.4 (i.e. at fixed comoving spatial position, $\mathrm{d}x^i = \mathrm{d}r^i/a_i(t)$, where $a_i(t) \equiv a(t)\mathrm{e}^{2\alpha_i(t)}$) follow geodesics of constant $\mathbf{x}$. However, if we have a set of comoving particles, such as a little ball of them, its volume and shape (ball becomes an ellipsoid) would change over time. In fact, the motion of a NR test particle in such a spacetime is equivalent to that in an FLRW metric perturbed, in conformal-Newtonian gauge, by a tidal potential perturbation that can locally be written as (e.g., Sec. 7 of [38])

$$\Phi_{\mathrm{cN}} \equiv -\frac{1}{2}a^{-2}\delta g_{00} = -\frac{1}{2}a^2\left(\ddot{H}_{ij} + 2H\dot{H}_{ij}\right)x^i x^j\,, \tag{8.5}$$

where dots denote derivatives with respect to time t.

When $\alpha_i \equiv 0$, we recover the familiar isotropic (unperturbed) FLRW spacetime

$$ds^2 = -\mathrm{d}t^2 + a^2(t)q_{ij}\mathrm{d}x^i\mathrm{d}x^j, \tag{8.6}$$

where q_{ij} is the metric of a maximally symmetric three-dimensional space with either positive, negative, or vanishing curvature.

Note however, that the anisotropic Bianchi I spacetime does not describe large-scale perturbations in our Universe.

Jacobs [63] derived the solution of the Einstein equations for the ansatz Eq. (8.4), assuming a perfect-fluid stress tensor (he also considered the case of a uniform magnetic field, which we do not discuss here), and obtained [Eq. (10) there]

$$\begin{aligned} \ddot{\Pi} + 3H\dot{\Pi} = 0\,, \quad \Pi := \alpha + \beta = -\xi \\ \ddot{\Sigma} + 3H\dot{\Sigma} = 0\,, \quad \Sigma := \alpha - \beta\,, \end{aligned} \tag{8.7}$$

where $H = \dot{a}/a$, while Π, Σ are the anisotropy parameters. The isotropic scale factor $a(t)$ satisfies the standard Friedmann equation. Thus, apart from an unobservable constant mode, which can be removed by a trivial redefinition of spatial coordinates, the anisotropy always decays as $\dot{\Pi}$, $\dot{\Sigma} \propto a^{-3}$. The tidal field experienced by a local comoving observer in this spacetime [Eq. (8.5)] then scales as

$$\partial_i \partial_j \Phi_{\rm cN} \propto a^2 \left[\ddot{\Pi} + 2H\dot{\Pi}\right] = -a^2 H\dot{\Pi} \propto H(t)/a\,, \tag{8.8}$$

and analogously for Σ. That is, in a universe whose stress energy content is given by a perfect fluid (more specifically, in the absence of significant anisotropic stress, applicable to our dust-filled universe), any initial tidal field/anisotropy described by a Bianchi I spacetime decays rapidly, $\propto H/a$. In case of initial conditions from inflation, which are set when a given mode exits the horizon, this contribution disappears exponentially fast after horizon exit, as expected for a decaying mode. This is clearly very different from actual tidal fields, which do not decay outside the horizon, but rather grow in conjunction with the perturbations in the matter density, such that it plays an important role in the growth of structure remains relevant up to late times. A Bianchi I spacetime cannot therefore be the correct physical picture. Nonetheless, Eq. 8.5 can be used to in N-body simulations to simulate the effects of large scale tidal fields on non-relativistic matter, since only the $00-$th component of the metric is relevant in this context. [102] The appeal of a Bianchi I spacetime over the truly physically-accurate description is that the former is homogeneous thus permits periodic boundary conditions inherent in conventional N-body simulations.

In fact, we will explicitly show in Section 7.3.2 that the tidal fields in our universe are not sourced by any component of the Ricci tensor, but are instead encoded by the Weyl tensor.

Chapter 9

Connection to (Eulerian) Standard Perturbation Theory (SPT)

9.1 SPT Overview

We are interested in describing the NL gravitational evolution of CDM (approximated by a self-gravitating, pressureless single fluid with only longitudinal-velocity) density contrast $\delta(\boldsymbol{x},\tau)$ and velocity fields $\theta \equiv \boldsymbol{\nabla}_{\boldsymbol{x}} \cdot \boldsymbol{v}(\boldsymbol{x},\tau)$ in the Eulerian frame. These are governed by the Euler and Poisson equations, closed with the continuity equation. The system can be reduced to two coupled equations in Fourier space for $\delta(\boldsymbol{k},\tau)$ and $\theta(\boldsymbol{k},\tau)$, which can then be solved perturbatively in terms of the linear density contrast $\delta^{[1]}(\boldsymbol{k},\tau)$. Note that the e.o.m.s have sources of $\mathcal{O}\left[\left(\delta^{[1]}\right)^2\right]$, of the form

$$\delta' + \theta = \mathcal{O}\left[\left(\delta^{[1]}\right)^2\right]; \tag{9.1}$$

$$\theta' + \mathcal{H}\theta + 3\mathcal{H}^2\Omega_{\rm m}\delta = \mathcal{O}\left[\left(\delta^{[1]}\right)^2\right], \tag{9.2}$$

such that on large scales where $\boldsymbol{k} \to 0$, we have $\delta^{[1]} \ll 1$, and they combine into a single scale-independent ($\boldsymbol{k}-$independent) second-order ODE for the evolution of $\delta^{[1]}$. In other words, all Fourier modes evolve the same way, with

$$\delta^{[1]\prime\prime} + \mathcal{H}\delta^{[1]\prime} - 3\mathcal{H}^2\Omega_{\rm m}\delta^{[1]}/2 = 0; \tag{9.3}$$

$$\theta^{[1]} = -\left(\ln D\right)' \delta^{[1]}, \tag{9.4}$$

$$\left(\ln D\right)'' = \mathcal{H}^2\left[3\Omega_{\rm m}/2 - {\rm d}\ln D/{\rm d}\ln a - \left({\rm d}\ln D/{\rm d}\ln a\right)^2\right]. \tag{9.5}$$

Then the $n-$th order ansatz is

$$\delta^{[n]}(\boldsymbol{k},\tau) = \int_{\boldsymbol{k}_1} \cdots \int_{\boldsymbol{k}_n} (2\pi)^3 \delta_{\text{Dirac}}(\boldsymbol{k} - \sum_{i=1}^{n} \boldsymbol{k}_i) \tag{9.6}$$

$$F_n(\boldsymbol{k}_1, \cdots, \boldsymbol{k}_n, \tau)\delta^{[1]}(\boldsymbol{k}_1,\tau)\cdots\delta^{[1]}(\boldsymbol{k}_n,\tau), \tag{9.7}$$

$$\theta^{[n]}(\boldsymbol{k},\tau) = -\left(\ln D(\tau)\right)' \int_{\boldsymbol{k}_1} \cdots \int_{\boldsymbol{k}_n} (2\pi)^3 \delta_{\text{Dirac}}(\boldsymbol{k} - \sum_{i=1}^{n} \boldsymbol{k}_i) \tag{9.8}$$

$$G_n(\boldsymbol{k}_1, \cdots, \boldsymbol{k}_n, \tau)\delta^{[1]}(\boldsymbol{k}_1,\tau)\cdots\delta^{[1]}(\boldsymbol{k}_n,\tau). \tag{9.9}$$

In EdS spacetime, where F_n and G_n are time-independent, the only time/cosmology-dependence is contained in $D(\tau)$.

9.2 Connection of CFC Results to SPT

Since the initial conditions of LSS are generated from quantum mechanical (non-deterministic) vacuum fluctuations, they must be described statistically as random fields. We shall only concern ourselves with random scalar fields here.

By the cosmological principle, we have that cosmological random fields on a spatial hypersurface at a given proper time are *statistically* homogeneous and isotropic.

Table 9.1:

Term	Definition
$\int_{\boldsymbol{k}}$	Momentum integral, $\int \mathrm{d}^3\boldsymbol{k}/(2\pi)^3$.
$\mathcal{FT}[f(\boldsymbol{x})](\boldsymbol{k})$	Fourier transform of some function $f(\boldsymbol{x})$, $\int \mathrm{d}^3\boldsymbol{x} f(\boldsymbol{x})\mathrm{e}^{-i\boldsymbol{k}\cdot\boldsymbol{x}}$.
L	denotes Lagrangian
$\xi_L(r)$	Linear matter two-point correlation function, $\int_k P_L(k)\mathrm{e}^{i\boldsymbol{k}\cdot\boldsymbol{r}} = \int_k \mathrm{d}^3k P_L(k)\mathrm{e}^{i\boldsymbol{k}\cdot\boldsymbol{r}}/(2\pi)^2$.
$P_{\mathrm{L}}(k,t)$	Linear matter power spectrum (of the linearly extrapolated rest-frame matter density perturbations, equivalent to the density perturbations in SC gauge), $\langle\rangle$
$\langle\cdot\rangle$	Ensemble average, or by the ergodic hypothesis (and cosmological principle for translational invariance), spatial average, provided that the samplings are sufficiently far from each other, consequently are independent and identically distributed (iid).
$\mathbb{P}_n\left(\phi(\boldsymbol{x}_1), ..., \phi(\boldsymbol{x}_n)\right)$	Set of distribution functions associated with the random field, ϕ, sampled at Euclidean coordinates $\boldsymbol{x}_i$, $i = 1, \cdots, n$ on the spatial hypersurface (of a given proper time) concerned.

$\langle\phi(\boldsymbol{x}_1)...\phi(\boldsymbol{x}_n)\rangle$	n-point correlation function, an expectation value, $\int[\mathrm{d}\phi(\boldsymbol{x}_1)]\cdots[\mathrm{d}\phi(\boldsymbol{x}_n)]\,\mathbb{P}_n\left(\phi(\boldsymbol{x}_1),\cdots,\phi(\boldsymbol{x}_n)\right)\,\phi(\boldsymbol{x}_1)\cdots\phi(\boldsymbol{x}_n)$. Then if the samplings are far enough away from each other that they are iid, the expression reduces to $\langle\phi\rangle^n$.
$\xi_{2l}(k,t)$	Correlation function multipole, $\int_{\boldsymbol{k}} P_L(k,t)j_{2l}(kr)$, where $j_{2l}(kr)$ is the spherical Bessel function of order $2l$ for $l=0,1,\cdots$.
$P_{S\delta}(k,t)$	Cross-power spectrum between S and δ at linear order, $\langle S_L(\boldsymbol{q}_1,t)\delta_L(\boldsymbol{q}_2)\rangle$
$S(\boldsymbol{q},t)$	Scalar function with dimension of length, such that the longitudinal component of the displacement $s^i(\boldsymbol{q},t)\vert_{\text{long.}}\equiv\partial^i S(\boldsymbol{q},t)$ at the Lagrangian position $\boldsymbol{q}$.
$\langle\phi(\boldsymbol{x}_1)...\phi(\boldsymbol{x}_n)\rangle_{\text{w/o}}$	n-point correlator without momentum conservation, such that $\langle\phi(\boldsymbol{x}_1)\cdots\phi(\boldsymbol{x}_n)\rangle\equiv(2\pi)^3\delta_{\text{Dirac}}(\boldsymbol{k}_1+\cdots+\boldsymbol{k}_n)$.
$F_n(\boldsymbol{k}_1,\cdots,\boldsymbol{k}_n,\tau)$	Symmetrized density kernel in the integral for the $\delta^{[n]}$ ansatz. $F_1=1$ and for an EdS universe, where $\Omega_{\text{m}}=\mathrm{d}\ln D/\mathrm{d}\ln a=1$, F_n becomes time-independent and $F_2=5/7+(2/7)(\boldsymbol{k}_1\cdot\boldsymbol{k}_2)^2/(k_1k_2)^2+(\boldsymbol{k}_1\cdot\boldsymbol{k}_2/2k_1k_2)(k_1/k_2+k_2/k_1)$, giving real space density field $\delta^{[n]}(\boldsymbol{x},\tau)=(17/21)(\delta^{[1]})^2+(2/7)(K^{[1]}_{ij})^2-s^i_{[1]}\partial_i\delta^{[1]}$. G_n is the analogous kernel for θ.
K_{ij}	Tidal field (dimensionless), $(\partial_i\partial_j/\boldsymbol{\nabla}^2-\delta_{ij}/3)\,\delta = 2\partial_i\partial_j\Phi_{\text{cN}}/(3\Omega_{\text{m}}\mathcal{H}^2)-\delta_{ij}\delta/3$.

It is instructive to compare our result Eq. (7.38) to the second order density perturbation in standard (subhorizon) perturbation theory [15, 104], which yields

$$\delta_F(\boldsymbol{x},t)=\delta_F^{[1]}(\boldsymbol{q}[\boldsymbol{x},t],t)+\frac{17}{21}(\delta_F^{[1]})^2+\frac{2}{7}(K_{ij}^{[1]})^2\,. \tag{9.10}$$

Recall the definition of δ_F in Table 9.1. The subscript $_F$ is a reminder that this is the overdensity w.r.t. the mean cosmic density defined in the fluid's rest frame.

The second term in Eq. (9.10) describes the second order growth of density perturbations in the absence of tidal fields; its coefficient is exactly what is obtained from the second order expansion of the spherical collapse solution. The third term encodes the tidal effects on the density perturbations. In standard Eulerian perturbation theory, the first, linear term is expanded around the Eulerian position yielding a displacement term

$$\delta_F^{[1]}(\boldsymbol{q}[\boldsymbol{x},t],t)=\delta_F^{[1]}(\boldsymbol{x},t)-\boldsymbol{s}^{[1]}(\boldsymbol{x},t)\cdot\boldsymbol{\nabla}\delta_F^{[1]}(\boldsymbol{x},t). \tag{9.11}$$

Since the CFC calculation corresponds to working in Lagrangian coordinates (as the origin of the coordinate system comoves with the fluid, evidenced by the fact that $\boldsymbol{v}_F=0$ on the geodesic), this displacement does not appear in Eq. (7.38); that is, the CFC formalism

automatically resums all the displacement terms appearing in Eulerian perturbation theory. Using that

$$\frac{9t_0^4}{14}\bar{a}^2\left(\mathcal{E}^{[1]}_{Fij}\right)^2 = \frac{9}{14}\cdot\frac{4}{9}(K^{[1]}_{ij})^2 = \frac{2}{7}(K^{[1]}_{ij})^2\,, \tag{9.12}$$

we immediately see that Eq. (7.38) matches the standard perturbative calculation Eq. (9.10). However, in the derivation of Eq. (7.38) we have not assumed that the scale of the perturbation is much smaller than the Hubble horizon. This shows that, when measured in the proper rest frame, the second order evolution of the matter density in the presence of tidal fields is *exactly* as given by the standard result which is seemingly only valid on subhorizon scales. This fact was already known for isotropic perturbations, in which case the evolution is determined by a local Friedmann equation [39]. Eq. (7.38) generalizes this result to the anisotropic case, i.e. the inclusion of tidal fields.

However, the agreement between the evolution predicted by the closed system Eq. (7.23) and standard perturbation theory no longer holds at higher order. This can already be seen in the result for σ_{Fij} at second order, Eq. (7.40). The SPT prediction for σ_{ij}, which corresponds to the derivative with respect to Lagrangian coordinates of the fluid velocity $\boldsymbol{v}$, can be derived by using that $\boldsymbol{v}$ is equal to the convective (or Lagrangian) time derivative w.r.t. τ of the Lagrangian displacement $\boldsymbol{s}$. This yields (e.g. App. B of [85])

$$\begin{aligned}\frac{\sigma_{ij}}{\bar{a}^{1/2}} &= -t_0\mathcal{E}^{[1]}_{Fij} + \bar{a}^{1/2}\left[\frac{\partial_i\partial_j}{\nabla^2} - \frac{1}{3}\delta_{ij}\right]\frac{\partial}{\partial\tau}\left[-\frac{2}{14}(\delta^{[1]})^2 + \frac{3}{14}(K^{[1]}_{ij})^2\right] \\ &= -t_0\mathcal{E}^{[1]}_{Fij} + \bar{a}\left[\frac{\partial_i\partial_j}{\nabla^2} - \frac{1}{3}\delta_{ij}\right]\left[-\frac{4}{21}t_0^{-1}(\delta^{[1]}_L)^2 + \frac{9}{14}t_0^3\,\mathcal{E}^{[1]}_{Flm}\mathcal{E}^{lm[1]}_F\right]\,. \end{aligned}\tag{9.13}$$

Clearly, this differs from Eq. (7.40). In particular, the SPT result is *spatially nonlocal* (the same holds when deriving the SPT result for the NL evolution of $\mathcal{E}_{Fij}$). The differences go back to the terms neglected when evaluating the evolution equation Eq. (7.12) for the electric Weyl tensor component. When neglecting these terms, we were able to obtain a closed system that is local in space around the fluid geodesic. However, the gravitational evolution of density and tidal fields within a region, when followed over a finite duration of time, is not completely described by the local tidal and density field. This is encoded in the nonlocal terms appearing at second order in σ_{ij} in standard perturbation theory, which, apart from dropping post-Newtonian terms, does not make approximations in Eq. (7.12). Note that the nonlocal term appears in the density perturbation δ_F only at third order (see also [87, 57]); in fact the nonlocal contributions to $\delta_F^{[3]}$ are proportional to $\sigma^{[1]lm}\sigma^{[2]}_{lm}$ [85]. Finally, we see that the nonlocal terms disappear in the case of spherical symmetry, in which case Eq. (7.23) recovers the exact separate universe result which matches perturbation theory to all orders.

Chapter 10

Summary of Part II

The conformal Fermi coordinates (CFC) are a convenient construction designed to explicitly isolate the leading locally observable gravitational effects of long-wavelength perturbations in the cosmological context. We show that using this construction, there is a natural way to derive a closed system of ordinary differential equations [Eq. (7.23)] describing the evolution of a long-wavelength perturbation. Here, long-wavelength means that the scale of the perturbation is much larger than the sound horizon of all fluid components (note that the sound horizon for pressureless matter is the NL scale, $r_s \sim 1/k_{\rm NL}$ [12]). This system is exactly equivalent to the local tidal approximation (LTA). Moreover, the CFC frame provides a fully relativistic realization of this closed system; that is, the results are valid on horizon or super-horizon scales without any post-Newtonian corrections. As shown in [90, 39], the CFC also allows for a direct connection to the initial conditions from inflation at NL order.

This construction clarifies the anisotropic generalization of the separate universe result for spherically symmetric long-wavelength perturbations. That is, while the latter are entirely described locally by a curved FLRW spacetime, anisotropic long-wavelength perturbations contain a nonzero electric component $E_{\nu\mu}$ of the Weyl tensor as well. Physically, this is entirely different from a Bianchi I spacetime, where the anisotropy is encoded in the tracefree part of the spatial *Ricci* tensor. The latter is negligible for ideal fluids. We thus argue that the Bianchi I picture is not the proper local physical representation of long-wavelength perturbations in our Universe.

Solving the system of evolutionary equations up to and including second order, we have found that the solution for the density field is exactly equivalent to the result of standard, sub-horizon perturbation theory. Since our closed system in the CFC frame recovers the exact NL evolution of *isotropic* perturbations, and recovers the correct *linear* evolution of anisotropic perturbations, our result for δ_F represents the proper rest-frame matter density at second order in perturbations, including all relativistic corrections (assuming matter domination holds, and that primordial decaying modes can be neglected). This follows from the fact that anisotropic perturbations only contribute to the density at quadratic or higher order. Note that this statement includes any vector and tensor metric perturbations that are generated by anisotropic perturbations at second order [83, 13, 21]; these can only

contribute to the rest-frame matter density at third order (we did not however include *primordial* vector and tensor modes, which would contribute at second order). A corollary is that, if we interpret the results of standard N-body simulations in this frame, any post-Newtonian corrections to the measured density field have to be third order in perturbation theory. This provides a strong constraint on their numerical relevance. On the other hand, our closed system fails for local tidal fields and velocity shear already at second order. Further, post-Newtonian corrections to non-ideal fluids, such as neutrinos, and on gravitational lensing are in general less suppressed than those for the matter density [32, 1, 2].

In this context, one might wonder whether this approach could be used to study the generation of gravitational waves from large-scale structure. However, for this one needs to define what gravitational wave means. A natural, physical definition is to derive the transverse-traceless component of metric perturbations in the far-field limit [35, 34]. Unfortunately, the local nature of the CFC construction implies that we cannot derive the far-field limit of these metric perturbations in this approach.

As a first, simple application of these results, we have derived the leading three-point function of the CFC-frame matter density field in Sec. 7.5 [Eq. (7.53)]. While this expression is idealized in the sense that it assumes that local observers directly communicate their local density to a distant observer, it is fully valid on arbitrarily large scales, and not restricted to specific configurations such as the squeezed limit. A further interesting possible application of these results is the implementation of N-body simulations with a long-wavelength, non-spherically symmetric perturbation imposed; that is, the anisotropic generalization of the "separate universe simulations" presented in [84, 107, 48, 79, 114, 10]. In principle, the effect of the electric Weyl tensor component $\mathcal{E}_{Fij}$ can be simply included by adding an external force $\propto \mathcal{E}_{Fij}x^j$ to any particle with position $\boldsymbol{x}$. This however breaks the periodic boundary conditions inherent in conventional N-body simulations, and can thus cause numerical problems. Note also that, unlike the the isotropic case, where the superimposed long mode can be made NL [114], this is nontrivial in the anisotropic case, as the correct NL evolution of $\mathcal{E}_{Fij}$ is nonlocal [see discussion after Eq. (9.13)].

This is indeed the main caveat to all local approximations to the NL evolution of (non-spherically symmetric) perturbations. At second order, the gravitational evolution of tidal field and velocity shear is spatially nonlocal. This comes as no surprise, given that we have shown that the tidal forces are due to the Weyl tensor, which captures those parts of the full Riemann tensor that are not locally related to the matter distribution. In case of the density field, this nonlocality only appears at third order. Thus, in all applications restricted to sufficiently low order, local approximations are exact; however, starting at third order in the matter (and galaxy) density field, spatial nonlocality is an unavoidable feature of NL gravitational evolution.

Appendix A

Calculation of PPN Parameters in Chapter 4: General Theory

In this appendix we will generalise our calculation in section 4.1 to the general theory where the Jordan frame metric is

$$\tilde{g}_{\mu\nu} = C^2(\phi)\left(g_{\mu\nu} + \frac{D^2(\phi)}{{\Lambda_{\rm disf}}^2}\partial_\mu\phi\partial_\nu\phi\right). \tag{A.1}$$

Now that we have gained some intuition from the previous calculation, it is possible to greatly simplify this without the need to repeat the entire calculation using brute force. Recall from the previous section that, even though we calculated the field to 2PN, neither the 1PN nor 2PN field contributed to the PPN parameters at leading-order. The reason for this was that $\phi_{1,2} \sim \Sigma$ and their contribution to $\tilde{g}_{00}$ scaled like $\Sigma\phi_{1,2}$ which meant they only contributed terms that were higher-order in Σ. We therefore examine the changes to the calculation that occur in the general case to discern whether there are any new leading-order contributions to the Jordan frame metric. Purely conformal contributions are already constrained by previous analyses of scalar-tensor theories [46] and so we are interested to see if pure disformal and mixed terms will yield new constraints after the calculation.

There are two new parameters that enter in the general case: $\hat{\beta}_\phi \equiv \hat{\beta}_\phi(\phi_{\rm CMB}) = [\ln C(\phi)]_{,\phi}\Big|_{\phi=\phi_{\rm CMB}}$ and $\hat{\Delta}_\phi \equiv \hat{\Delta}_\phi(\phi_{\rm CMB}) = [\ln D(\phi)]_{,\phi}\Big|_{\phi=\phi_{\rm CMB}}$. Expanding in these, one has, to $\mathcal{O}_{\rm PN}(2)$

$$C(\phi) = C^2_{\rm CMB}\left[1 + 2\phi_1\hat{\beta}_\phi + \left(2\phi_1^2\hat{\beta}_\phi^2 + 2\phi_2\hat{\beta}_\phi + \phi_1^2\hat{\beta}'_\phi\right)\right], \quad \text{and} \tag{A.2}$$

$$D(\phi) = 1 + 2\phi_1\hat{\Delta}_\phi + 2\phi_1^2\hat{\Delta}_\phi^2 + 2\phi_2\hat{\Delta}_\phi + \phi_1^2\hat{\Delta}'_\phi, \tag{A.3}$$

where $C^2_{\rm CMB} \equiv C^2(\phi_{\rm CMB})$ and we have set $D(\phi_{\rm CMB}) = 1$ as before since we can absorb it into $\Lambda_{\rm disf}$. In addition to this, the definition of Υ and Σ are modified to include a factor of $D^2(\phi_{\rm CMB})$ so that $\Upsilon \to D^2(\phi_{\rm CMB})\Upsilon$ and $\Sigma \to D^2(\phi_{\rm CMB})\Sigma$. In fact, since we are setting $D(\phi_{\rm CMB}) = 1$ this is not important in what follows but it does have implications for the

LLR constraints derived in section 4.2 where we take time-derivatives of Υ. Using the same Einstein frame coordinates as the previous calculation, the Jordan frame metric is

$$\tilde{g}_{00} = -N^2 C_{\rm CMB}^2 \left[1 - 2\frac{\chi_1}{N^2} - 2\frac{\chi_2}{N^2} - 2\hat{\Delta}_\phi \frac{\Upsilon}{N^2}\phi_1 - \frac{\Upsilon}{N^2}\left(2\hat{\Delta}_\phi\phi_2 + 2\hat{\Delta}_\phi^2\phi_1^2 + \hat{\Delta}'_\phi\phi_1^2\right)\right.$$
$$\left. -2\frac{\dot{\phi}_{\rm CMB}\dot{\phi}_1}{N^2{\Lambda_{\rm disf}}^2} + 2\hat{\beta}_\phi\phi_1 + 2\hat{\beta}_\phi\phi_2 + 2\hat{\beta}_\phi^2\phi_1^2 + \hat{\beta}'_\phi\phi_1^2 - 4\hat{\beta}_\phi\frac{\phi_1\chi_1}{N^2} - 4\hat{\beta}_\phi\hat{\Delta}_\phi\frac{\Upsilon}{N^2}\phi_1^2\right], \quad \text{(A.4)}$$

$$\tilde{g}_{0i} = C_{\rm CMB}^2 B_i + C_{\rm CMB}^2\left[\frac{\dot{\phi}_{\rm CMB}}{{\Lambda_{\rm disf}}^2}\partial_i\phi_1 + \frac{\dot{\phi}_{\rm CMB}}{{\Lambda_{\rm disf}}^2}\partial_i\phi_2 + 2(\hat{\beta}_\phi + \hat{\Delta}_\phi)\frac{\dot{\phi}_{\rm CMB}}{{\Lambda_{\rm disf}}^2}\phi_1\partial_i\phi_1\right] \quad \text{and} \quad \text{(A.5)}$$

$$\tilde{g}_{ij} = C_{\rm CMB}^2\left[1 + 2\hat{\beta}_\phi\phi_1 + 2\Psi_1\right]. \quad \text{(A.6)}$$

If we want to find the field to 1PN we only need the energy-momentum tensor (and its trace) to this order. At zeroth-order, one has $\gamma_{\rm Lorentz} = N^{-1}$, where the Jordan-frame Lorentz factor $\gamma_{\rm Lorentz}$ is defined below equation (4.21), and so one finds

$$T^{00}_{(I)} = -T_{(I)} = \frac{C^4_{\rm CMB}\rho_{(I)}}{N}, \quad \text{(A.7)}$$

where we have used the general relation between the two energy-momentum tensors

$$T^{\mu\nu}_{(I)} = C^6(\phi)\sqrt{1 - \frac{2D^2(\phi)X}{\hat{\beta}_\phi^2}}\tilde{T}^{\mu\nu}_{(I)}. \quad \text{(A.8)}$$

The scalar field equation at 1PN is then

$$\nabla^2\phi_1 = \frac{8\pi G\rho_{\rm m}C^4_{\rm CMB}}{N^3}f(\phi_{\rm CMB}, \dot{\phi}_{\rm CMB}, \ddot{\phi}_{\rm CMB}) \quad \text{with} \quad f(\phi_{\rm CMB}, \dot{\phi}_{\rm CMB}, \ddot{\phi}_{\rm CMB}) \equiv \hat{\beta}_\phi - \Upsilon(\hat{\beta}_\phi - \hat{\Delta}_\phi) + \Sigma, \quad \text{(A.9)}$$

so that the 1PN solution is

$$\phi_1 = -2\frac{C^4_{\rm CMB}f}{N^3}U. \quad \text{(A.10)}$$

The general case differs from the minimal one in that it contains factors of Υ and $\hat{\beta}_\phi$ multiplying U. In the purely conformal case where $\hat{\Delta}_\phi = \Upsilon = \Sigma = 0$ one has $f = \hat{\beta}_\phi$ and the Eddington light bending parameter is [46]

$$|\gamma_{\rm PPN} - 1| = \frac{2\hat{\beta}_\phi^2}{1 + 2\hat{\beta}_\phi^2}. \quad \text{(A.11)}$$

One can see from (A.4)–(A.6) that this contribution is not affected by disformal contributions and so, in the absence of any fine-tuning[1] or screening mechanism, the Cassini bound

[1] By this, we mean that we ignore cases where two or more parameters are fine-tuned against each other. One example of this is a cosmic evolutions such that $\frac{D(\phi_{\rm CMB})\dot{\phi}_{\rm CMB}}{\Lambda_{\rm disf}} \sim \Sigma$. [97] have shown that models where this is the case are unviable since they predict Newtonian limits that are not compatible with SS, tests. The absence of fine-tuned models ensures that our counting scheme is self-consistent.

$|\gamma_{\rm PPN} - 1| < 2.1 \times 10^{-5}$ [16] imposes the constraint $\hat{\beta}_\phi \lesssim 10^{-3}$. The lapse N is unchanged in the general case (this is a consequence of choosing $D(\phi_{\rm CMB}) = 1$) and so, looking at (A.4)–(A.6)[2], the only non-purely conformal leading-order corrections to the PPN parameters found in the minimal theory must be proportional to $\hat{\beta}_\phi \hat{\Delta}_\phi \Upsilon$ or $\hat{\beta}_\phi \Sigma$.[3] Demanding that we do not fine-tune different contributions to the PPN parameters means that Υ is still constrained by the α_2 constraint such that $\Upsilon,\ \Sigma \lesssim 10^{-7}$. Therefore, any additional contributions present in the general theory automatically satisfy the PPN constraints. In particular, there are no new bounds on the conformal parameter $\hat{\beta}_\phi$ and the parameter $\hat{\Delta}_\phi$ is completely unconstrained. The one caveat to this is that we have assumed that $\hat{\Delta}_\phi \sim \mathcal{O}_{\rm PN}(1)$. One can see that there is a very weak requirement that $\hat{\Delta}_\phi \lesssim 10^5$ due to a contribution to $\gamma_{\rm PPN}$ of $\mathcal{O}(\hat{\beta}_\phi \hat{\Delta}_\phi \Upsilon)$ and a similar constraint $\hat{\Delta}_\phi \lesssim 10^{4.5}$ coming from a contribution to $\beta_{\rm PPN}$ of $\mathcal{O}(\hat{\beta}_\phi^2 \hat{\Delta}_\phi^2 \Upsilon)$. Similarly, one can see that there is a contribution to $\beta_{\rm PPN}$ of $\mathcal{O}(\hat{\Delta}'_\phi \Upsilon)$, which imposes the weak constraint $\hat{\Delta}'_\phi \lesssim 10^9$. Note that these bounds apply when $\hat{\beta}_\phi$ and Υ just satisfy their bounds i.e. $\hat{\beta}_\phi^2 \sim 10^{-5}$ and $\Upsilon \sim 10^{-7}$. When $\hat{\beta}_\phi$ and Υ assume values smaller than this, $\hat{\Delta}_\phi$ and $\hat{\Delta}'_\phi$ can assume larger values and still satisfy SS tests.

[2] One should really perform the generalised versions of the gauge transformations used in section 4.1, but it is clear that these just add terms proportional to $\Upsilon\phi_{1,2}$ and $(\hat{\beta}_\phi + \hat{\Delta}_\phi) f^2 U^2$ to $\tilde{g}_{00}$, which do not circumvent our arguments relating to (A.4)–(A.6).

[3] $\hat{\beta}'_\phi \lesssim \mathcal{O}_{\rm PN}(10^2)$ from measurements of the perihelion shift of Mercury, which constrains the PPN parameter $\beta_{\rm PPN} < 3 \times 10^{-3}$ [120]. Even taking the most extreme value does not alter the conclusions presented here.

Appendix B

Completeness of Eq. (7.23)

We now show that the, perhaps surprisingly, simple form of the evolution equation for $\mathcal{E}^F_{ij}$ is the single nontrivial component of Eq. (7.12) in CFC at leading order in derivatives. This implies that Eq. (7.23) consistently contains all constraints from the *full* covariant Einstein system, with no additional constraints at leading order in derivatives. We begin with the full covariant equation for the Weyl tensor, Eq. (7.12) :

$$\nabla^\kappa C_{\nu\mu\kappa\lambda} = 8\pi G \left(\nabla_{[\mu} T_{\nu]\lambda} + \frac{1}{3} g_{\lambda[\mu} \nabla_{\nu]} g_{\alpha\beta} T^{\alpha\beta} \right) , \tag{B.1}$$

evaluated in CFC, and consider all the distinct combinations of space-time indices, up to symmetries of the Weyl tensor (which are the same as those of the Riemann tensor). Henceforth, we shall drop the "F" subscript. CFC shall be assumed throughout. The line element of the CFC metric is given by Eq. (7.1)

$$g_{\nu\mu}(x^\mu) = a^2(\tau) \left[\eta_{\nu\mu} + h_{\nu\mu} \left(\tau, x^i \right) \right] , \tag{B.2}$$

We shall first consider the LHS of the system,

$$\begin{aligned} \nabla^\kappa C_{\nu\mu\kappa\lambda} =& \nabla_\kappa C_{\nu\mu}{}^\kappa{}_\lambda & \text{(B.3)} \\ =& \partial_\kappa C_{\nu\mu}{}^\kappa{}_\lambda - \Gamma^\alpha_{\kappa\mu} C_{\alpha\nu}{}^\kappa{}_\lambda - \Gamma^\alpha_{\kappa\nu} C_{\mu\alpha}{}^\kappa{}_\lambda + \Gamma^\kappa_{\kappa\alpha} C_{\mu\nu}{}^\alpha{}_\lambda - \Gamma^\alpha_{\kappa\lambda} C_{\mu\nu}{}^\kappa{}_\alpha . & \text{(B.4)} \end{aligned}$$

The relevant Christoffel symbols of Eq. (B.2) evaluated on the geodesic are [61],

$$\Gamma^\mu_{0\nu}|_{\text{geo}} = \mathcal{H}|_{\text{geo}} \delta^\mu_\nu , \quad \Gamma^0_{ij}|_{\text{geo}} = \mathcal{H}|_{\text{geo}} \delta_{ij} \tag{B.5}$$

For $\{\mu,\nu,\lambda\} = \{0,0,0\}$, $C_{00\kappa0}$ is automatically zero given the symmetries of the Weyl tensor. For $\{\mu,\nu,\lambda\} = \{0,0,i\}$, the only non-vanishing Weyl component is C_{0ik0}. Since $h_{\nu\mu} = \mathcal{O}(x^2)$ and in leading order CFC we restrict to 2 spatial derivatives, regarding spatial derivatives acting on the metric, only terms of the form $\partial^2_k h_{\nu\mu}$ survive. Also, any spatial derivative of the Weyl tensor is neglected in leading order CFC. We further note that the Weyl tensor is tracefree w.r.t. any 2 indices. It follows that

$$\nabla^\kappa C_{0i\kappa0} = 0. \tag{B.6}$$

For $\{\mu,\nu,\lambda\} = \{0,i,j\}$, we retrieve the LHS of the evolution equation for $\mathcal{E}_{ij}$ in Eq. (7.23). For $\{\mu,\nu,\lambda\} = \{i,j,k\}$, we have

$$\partial_\tau C_{ij}{}^0{}_k \,. \tag{B.7}$$

We shall now consider the RHS of Eq. (7.12) for the components with non-trivial LHS, adopting an ideal pressureless fluid stress-energy tensor (again, we really only require the absence of pressure perturbations). For $\{\mu,\nu,\lambda\} = \{0,i,j\}$, we retrieve the RHS of the evolution equation for $\mathcal{E}_{ij}$ in Eq. (7.23). For $\{\mu,\nu,\lambda\} = \{i,j,k\}$, noting that $U_i|_{\text{geo}} = 0$ (when not acted on by a spatial derivative),

$$8\pi G\left(\nabla_{[i}T_{j]k} + \frac{1}{3}g_{k[i}\nabla_{j]}g_{\alpha\beta}T^{\alpha\beta}\right) = -\frac{8\pi G a^2}{3}\delta_{k[i}\partial_{j]}\rho = 0 \quad \text{(higher derivative)}\,. \tag{B.8}$$

This is a higher-derivative contribution, as it involves a spatial (fluid-orthogonal) derivative on the stress-energy tensor and is thus equivalent to a third spatial derivative acting on the metric. Consequently, the only apparently non-trivial component of the system, besides our equation for $\mathcal{E}_{ij}$, is

$$\dot{C}_{ij}{}^0{}_k = 0\,. \tag{B.9}$$

At this order in derivatives, this component is entirely decoupled from the other quantities in Eq. (7.23) and corresponds to a constant that can be set to zero.

Bibliography

[1] J. Adamek, D. Daverio, R. Durrer und M. Kunz, *Phys. Rev. D* **88** (2013), 103527.

[2] J. Adamek, D. Daverio, R. Durrer und M. Kunz, *JCAP* **1607** (2016), 053.

[3] P.A.R. Ade et al. , *Astron. Astrophys.* **571** (2014), A1.

[4] P.A.R. Ade et al. , *Astron. Astrophys.* **571** (2014), A16.

[5] P.A.R. Ade et al. , *Astron. Astrophys.* **594** (2016), A13.

[6] L. Amendola et al. , *Living Rev. Rel.* **16** (2013), 6.

[7] C. Armendariz-Picon, V.F. Mukhanov und P.J. Steinhardt, *Phys. Rev.* **D63** (2001), 103510.

[8] E. Babichev, C. Deffayet und R. Ziour, *Int. J. Mod. Phys.* **D18** (2009), 2147.

[9] T. Baldauf, U. Seljak, L. Senatore und M. Zaldarriaga, *JCAP* **1110** (2011), 031.

[10] T. Baldauf, U. Seljak, L. Senatore und M. Zaldarriaga, *JCAP* **1609** (2016), 007.

[11] J.D. Barrow und P. Saich, *Mon. Not. Roy. Astron. Soc.* **262** (1993), 717.

[12] D. Baumann, A. Nicolis, L. Senatore und M. Zaldarriaga, *JCAP* **7** (2012), 051.

[13] D. Baumann, P. Steinhardt, K. Takahashi und K. Ichiki, *Phys. Rev. D* **76** (2007), 084019.

[14] J. Bel, K. Hoffmann und E. GaztaÃśaga, *Mon. Not. Roy. Astron. Soc.* **453** (2015), 259.

[15] F. Bernardeau, S. Colombi, E. Gaztanaga und R. Scoccimarro, *Phys.Rept.* **367** (2002), 1.

[16] B. Bertotti, L. Iess und P. Tortora, *Nature* **425** (2003), 374.

[17] E. Bertschinger: *Cosmological dynamics: Course 1. Cosmological dynamics: Course 1*, In *Summer School on Cosmology and Large Scale Structure (Session 60) Les Houches, France, August 1-28, 1993.* (1993).

[18] E. Bertschinger und A.J.S. Hamilton, *Astrophys. J.* **435** (1994), 1.

[19] E. Bertschinger und B. Jain, *Astrophys. J.* **431** (1994), 486.

[20] D. Bettoni und S. Liberati, *Phys.Rev.* **D88** (2013), 084020.

[21] L. Boubekeur, P. Creminelli, J. Norena und F. Vernizzi, *JCAP* **0808** (2008), 028.

[22] P. Brax, C. van de Bruck, A.C. Davis, J. Khoury und A. Weltman, *Phys. Rev.* **D70** (2004), 123518.

[23] P. Brax und C. Burrage, *Phys. Rev.* **D90** (2014), 104009.

[24] P. Brax und C. Burrage, *Phys. Rev.* **D91** (2015), 043515.

[25] P. Brax, C. Burrage, A.C. Davis und G. Gubitosi, *JCAP* **1311** (2013), 001.

[26] P. Brax, A.C. Davis, B. Li, H.A. Winther und G.B. Zhao, *JCAP* **1304** (2013), 029.

[27] P. Brax, A.C. Davis und J. Sakstein, *Class.Quant.Grav.* **31** (2014), 225001.

[28] C. van de Bruck und J. Morrice, *JCAP* **1504** (2015), 036.

[29] C. van de Bruck, J. Morrice und S. Vu, *Phys.Rev.Lett.* **111** (2013), 161302.

[30] C. van de Bruck und G. Sculthorpe, *Phys.Rev.* **D87** (2013), 044004.

[31] M. Bruni, S. Matarrese, S. Mollerach und S. Sonego, *Class.Quant.Grav.* **14** (1997), 2585.

[32] M. Bruni, D.B. Thomas und D. Wands, *Phys. Rev. D* **89** (2014), 044010.

[33] C. Burrage und J. Sakstein, *Journal of Cosmology and Astroparticle Physics* **2016** (2016), 045.

[34] C. Carbone, C. Baccigalupi und S. Matarrese, *Phys. Rev. D* **73** (2006), 063503.

[35] C. Carbone und S. Matarrese, *Phys. Rev. D* **71** (2005), 043508.

[36] S.M. Carroll, V. Duvvuri, M. Trodden und M.S. Turner, *Phys. Rev. D* **70** (2004), 043528.

[37] S. Cole, *Mon. Not. Roy. Astron. Soc.* **286** (1997), 38.

[38] L. Dai, E. Pajer und F. Schmidt, *JCAP* **11** (2015), 043.

[39] L. Dai, E. Pajer und F. Schmidt, *JCAP* **1510** (2015), 059.

[40] T. Damour und G. Esposito-Farese, *Class.Quant.Grav.* **9** (1992), 2093.

[41] A.C. Davis, E.A. Lim, J. Sakstein und D. Shaw, *Phys.Rev.* **D85** (2012), 123006.

[42] V. Desjacques, D. Jeong und F. Schmidt, *Phys. Rept.* **733** (2018), 1.

[43] G. DomÃĺnech, A. Naruko und M. Sasaki, *JCAP* **1510** (2015), 067.

[44] J. Ehlers: *General relativity and kinetic theory. General relativity and kinetic theory.*, In *General Relativity and Cosmology*, herausgegeben von R. K. Sachs. (1971) Seiten 1–70.

[45] G.F.R. Ellis: *Relativistic cosmology. Relativistic cosmology.*, In *General Relativity and Cosmology*, herausgegeben von R. K. Sachs. (1971) Seiten 104–182.

[46] G. Esposito-Farese, *AIP Conf.Proc.* **736** (2004), 35.

[47] J. Gleyzes, D. Langlois, F. Piazza und F. Vernizzi, *JCAP* **1502** (2015), 018.

[48] N.Y. Gnedin, A.V. Kravtsov und D.H. Rudd, *Astrophys. J. Suppl.* **194** (2011), 46.

[49] R. Hagala, C. Llinares und D.F. Mota, *Astronomy & Astrophysics* **585** (2015), A37.

[50] R. Hagala, C. Llinares und D.F. Mota, *Astron. Astrophys.* **585** (2016), A37.

[51] R. Hagala, C. Llinares und D.F. Mota, *Phys. Rev. Lett.* **118** (2017), 101301.

[52] S.W. Hawking, *Astrophys. J.* **145** (1966), 544.

[53] K. Hinterbichler, J. Khoury, A. Levy und A. Matas, *Physical Review D* **84** (2011).

[54] T. Hiramatsu, W. Hu, K. Koyama und F. Schmidt, *Phys. Rev.* **D87** (2013), 063525.

[55] G.W. Horndeski, *Int.J.Theor.Phys.* **10** (1974), 363.

[56] L. Hui und E. Bertschinger, *Astrophys. J.* **471** (1996), 1.

[57] J.c. Hwang, D. Jeong und H. Noh, *Mon. Not. Roy. Astron. Soc.* **459** (2016), 1124.

[58] V. Icke, *Astron. Astrophys.* **27** (1973), 1.

[59] L. Iorio, *Int. J. Mod. Phys.* **D23** (2014), 1450006.

[60] H.Y. Ip, J. Sakstein und F. Schmidt, *JCAP* **1510** (2015), 051.

[61] H.Y. Ip und F. Schmidt, *JCAP* **1702** (2017), 025.

[62] H.Y.S. Ip und F. Schmidt, *JCAP (accepted)* (2018).

[63] K.C. Jacobs, *Astrophys. J.* **153** (1968), 661.

[64] B. Jain, V. Vikram und J. Sakstein, *Astrophys.J.* **779** (2013), 39.

[65] D. Jeong und F. Schmidt, *Class. Quant. Grav.* **32** (2015), 044001.

[66] A. Joyce, B. Jain, J. Khoury und M. Trodden, *Phys. Rept.* **568** (2015), 1.

[67] A. Joyce, L. Lombriser und F. Schmidt, *Ann. Rev. Nucl. Part. Sci.* **66** (2016), 95.

[68] N. Kaloper, *Phys.Lett.* **B583** (2004), 1.

[69] L. Kofman und D. Pogosyan, *Astrophys. J.* **442** (1995), 30.

[70] T. Koivisto und H.J. Nyrhinen, *Phys. Scripta* **92** (2017), 105301.

[71] T.S. Koivisto, (2008).

[72] T.S. Koivisto, D.F. Mota und M. Zumalacarregui, *Phys.Rev.Lett.* **109** (2012), 241102.

[73] K. Koyama und J. Sakstein, *Phys. Rev.* **D91** (2015), 124066.

[74] M. Kramer, I.H. Stairs, R. Manchester, M. McLaughlin, A. Lyne et al. , *Science* **314** (2006), 97.

[75] A. Laforgia, *Journal of Computational and Applied Mathematics* **34** (1991), 263.

[76] L.J. Landau, *Journal of the London Mathematical Society* **61** (2000), 197.

[77] D. Lee, A. Lightman und W. Ni, *Phys.Rev.* **D10** (1974), 1685.

[78] G. Lemaître, *Annales de la Societe Scietifique de Bruxelles* **53** (1933), 51.

[79] Y. Li, W. Hu und M. Takada, *Phys. Rev. D* **89** (2014), 083519.

[80] J.. Lindroos, C. Llinares und D.F. Mota, *Phys. Rev.* **D93** (2016), 044050.

[81] C. Llinares und D.F. Mota, *Phys. Rev.* **D89** (2014), 084023.

[82] K.A. Malik und D. Wands, *Phys.Rept.* **475** (2009), 1.

[83] S. Matarrese, S. Mollerach und M. Bruni, *Phys. Rev.* **D58** (1998), 043504.

[84] P. McDonald, *Astrophys. J.* **585** (2003), 34.

[85] M. Mirbabayi, F. Schmidt und M. Zaldarriaga, *JCAP* **7** (2015), 030.

[86] J.F. Navarro, C.S. Frenk und S.D.M. White, *Astrophys. J.* **490** (1997), 493.

[87] H. Noh und J.c. Hwang, (2003).

[88] J. Noller, *JCAP* **1207** (2012), 013.

[89] K. Nordtvedt, *Astrophys. J.* **320** (1987), 871.

[90] E. Pajer, F. Schmidt und M. Zaldarriaga, *Phys. Rev. D* **88** (2013), 083502.

[91] L. Perivolaropoulos, *Phys. Rev.* **D81** (2010), 047501.

[92] R. Pourhasan, N. Afshordi, R.B. Mann und A.C. Davis, *JCAP* **1112** (2011), 005.

[93] C. de Rham, A. Matas und A.J. Tolley, *Phys.Rev.* **D87** (2013), 064024.

[94] J. Sakstein, *Phys.Rev.* **D88** (2013), 124013.

[95] J. Sakstein: *Astrophysical Tests of Modified Gravity.* Cambridge U., DAMTP, Dissertation, 2014.

[96] J. Sakstein, *JCAP* **1412** (2014), 012.

[97] J. Sakstein, *Phys.Rev.* **D91** (2015), 024036.

[98] J. Sakstein, B. Jain und V. Vikram, *Int. J. Mod. Phys.* **D23** (2014), 1442002.

[99] J. Sakstein und S. Verner, *Phys. Rev.* **D92** (2015), 123005.

[100] L. Sampson, N. Yunes und N. Cornish, *Phys.Rev.* **D88** (2013), 064056.

[101] K. Schleich und D.M. Witt, *J. Math. Phys.* **51** (2010), 112502.

[102] A.S. Schmidt, S.D.M. White, F. Schmidt und J. StÃijcker, (2018).

[103] F. Schmidt, E. Pajer und M. Zaldarriaga, *Phys. Rev. D* **89** (2014), 083507.

[104] B.D. Sherwin und M. Zaldarriaga, *Phys. Rev. D* **85** (2012), 103523.

[105] A. Silvestri, L. Pogosian und R.V. Buniy, *Phys. Rev.* **D87** (2013), 104015.

[106] A. Silvestri, L. Pogosian und R.V. Buniy, *Phys. Rev.* **D87** (2013), 104015.

[107] E. Sirko, *Astrophys.J.* **634** (2005), 728.

[108] A.A. Starobinsky, *JETP Lett.* **86** (2007), 157.

[109] F. Taddia, M.D. Stritzinger, J. Sollerman, M.M. Phillips, J.P. Anderson, M. Ergon, G. Folatelli, C. Fransson, W. Freedman, M. Hamuy, N. Morrell, A. Pastorello, S.E. Persson und S. Gonzalez, *Astronomy & Astrophysics* **537** (2012), A140.

[110] S.G. Turyshev und J.G. Williams, *Int.J.Mod.Phys.* **D16** (2007), 2165.

[111] V. Vikram, A. CabrÃĺ, B. Jain und J.T. VanderPlas, *JCAP* **1308** (2013), 020.

[112] V. Vikram, J. Sakstein, C. Davis und A. Neil, *Phys. Rev.* **D97** (2018), 104055.

[113] E. Villa und C. Rampf, *JCAP* **1601** (2016), 030. [Erratum: JCAP1805,no.05,E01(2018)].

[114] C. Wagner, F. Schmidt, C.T. Chiang und E. Komatsu, *Mon.Not.Roy.Astron.Soc.* **448** (2015), 11.

[115] C. Wagner, F. Schmidt, C.T. Chiang und E. Komatsu, *Mon. Not. Roy. Astron. Soc.* **448** (2015), L11.

[116] T.A. Wagner, S. Schlamminger, J.H. Gundlach und E.G. Adelberger, *Class. Quant. Grav.* **29** (2012), 184002.

[117] S.D.M. White: *Formation and evolution of galaxies: Lectures given at Les Houches, August 1993. Formation and evolution of galaxies: Lectures given at Les Houches, August 1993*, In *Summer School on Cosmology and Large Scale Structure (Session 60) Les Houches, France, August 1-28, 1993*. (1994) Seiten 349–430.

[118] S.D.M. White und J. Silk, *Astrophys. J.* **231** (1979), 1.

[119] C. Will: *Theory and Experiment in Gravitational Physics*. Cambridge University Press, 1993.

[120] C.M. Will, *Living Rev.Rel.* **9** (2006), 3.

[121] C.M. Will, *Living Reviews in Relativity* **17** (2014).

[122] C.M. Will und J. Nordtvedt, Kenneth, *Astrophys.J.* **177** (1972), 757.

[123] Y.B. Zel'dovich, *Astron. Astrophys.* **5** (1970), 84.

[124] M. Zumalacarregui, T. Koivisto, D. Mota und P. Ruiz-Lapuente, *JCAP* **1005** (2010), 038.

[125] M. Zumalacarregui, T.S. Koivisto und D.F. Mota, *Phys.Rev.* **D87** (2013), 083010.

[126] M. ZumalacÃąrregui und J. GarcÃŋa-Bellido, *Phys.Rev.* **D89** (2014), 064046.

Acknowledgments

While I'm not sure that this thesis merits an acceptance speech, I hope at least that those tagged would not be too embarrassed by the association. I am incredibly fortunate to have crossed paths with some lovely people and they deserve a heartfelt thank you.

Of course, there is my supervisor Fabian Schmidt. A man arbitrarily close to omniscience that a physicist would declare him so[1]. He also happens to be patient and understanding and has never thrown objects at me, quietly burying any disappointment deep inside.[2]

Then there is my official supervisor Eiichiro Komatsu, a powerhouse of enthusiasm and one who has the curious superpower of squeezing a million things into a day. He probably also fights crime in a cape after-hours.

Thank you both very much for taking a chance on me. It's been an honour!

A massive thank you to Jeremy Sakstein, anyone's dream collaborator, always on the ball (and not just Earth)! On top of that, his encouraging kind messages have provided much needed reanimation – Shelley is huddled up in shame for messing up the name.

I must also thank all my influencers along the way. To name a few: Feynman (self-explanatory), Dave Williams (Mr Williams indulged my after-school physics chats and conned me into believing in myself), Vicky Neale (an exceptional mathematician, who is also compassionate and nurturing. I've personally not attained any of these qualities but it is apparently possible), Jörn Dunkel (who was incredibly kind, a wonderful mentor who went the extra mile to encourage me to reach for more). The list goes on and my gratitude extends to all who have charitably spared me their time.

Many thanks to my parents Samuel and Joanne, who while supportive of my academic pursuits never forced them.

Every now and then one sees only futility, disappointment and assumes the ways of a soggy bog roll. I have been lucky enough to have some lovely people in my life who would present me with a different gauge choice at such times. Occasionally I get to reciprocate, which also brings remarkable joy. Needless to say, their company outside such times is a delight, rivalling Wodehouse with a cuppa. So a wholehearted thank you to the amazing T.F., Elisa, Robin, Irene, Ben, Aniket and Lily!

Then there is Simon, who is responsible for much of my homesickness and to whom

[1] We discuss taking limits carefully in this thesis, for our purposes here let's assume everything is well-behaved.

[2] Just to clarify, while I jest, Fabian is really rather lovely!

this thesis is dedicated. If there is ever proof of injustice in the world, it is this, as I have done nothing to deserve someone so dear and sweet, for whom I am heartily grateful. But soft! It is a truth universally acknowledged that "le fromage c'est dommage"[3], I should stop before this grows into a balcony soliloquy that sends eyeballs rolling in their sockets.

In short, I am profoundly grateful to have you all in my life and while I don't express it enough, you hold my warmest wishes and highest esteem.

[3]There is a back-story to this madness but "hanc marginis exiguitas non caperet".